

PHYSICAL LIMITATIONS ON FREE-FIELD MICROPHONE CALIBRATION

by

JEROME R. COX, JR.

S.B., Massachusetts Institute of Technology  
(1947)

S.M., Massachusetts Institute of Technology  
(1949)

SUBMITTED IN PARTIAL FULFILLMENT OF THE

REQUIREMENTS FOR THE DEGREE OF

DOCTOR OF SCIENCE

at the

MASSACHUSETTS INSTITUTE OF TECHNOLOGY  
January, 1954

Signature of Author Signature redacted  
 Department of Electrical Engineering, January 11, 1954

Certified by Signature redacted  
 Thesis Supervisor

Accepted by Signature redacted  
 Chairman, Departmental Committee on Graduate Students



PHYSICAL LIMITATIONS ON FREE-FIELD  
MICROPHONE CALIBRATION

by

Jerome R. Cox, Jr.

Submitted to the Department of Electrical Engineering on  
11 January 1954 in partial fulfillment of the require-  
ments for the degree of Doctor of Science.

ABSTRACT

The basis for reciprocity has been studied in some detail. It is shown that all linear Lagrangian systems are reciprocal whether formulated on a lumped or distributed parameter basis. Some non-reciprocal systems are discussed and a general statement of electroacoustic reciprocity including viscous losses is presented.

Method for describing the near field of a transducer in terms of its far field are described. The acoustic center and limit of the far field are defined. A graphical method is described for computing this limit directly from the directivity gain plot. The technique is of great use in estimating the error introduced by the close spacing of transducers. All of these results are shown to have meaning, whether the transducer is acting as a source or a receiver. Some calculations are made for idealized transducers, a point source and a piston source on a hard sphere.

Measurements were made of the acoustic center and the directivity patterns of a number of commercial microphones. A free-field calibration was performed in a non-anechoic space utilizing an approximation to a point source on a hard sphere. A discussion of experimental techniques includes the following topics: the measurement of reciprocity and linearity, effects of standing waves, effect of the size of the enclosure, measurement of the microphone polarizing voltage, pulse techniques applied to detection of reflecting surfaces and to calibration, transducer stability, point-by-point and automatic data-taking techniques, and factors governing the selection of a sound source.

Thesis Supervisor: Leo L. Beranek

Title: Associate Professor of Electrical Engineering

*Handwritten note:*  
See appendix 2, 3, 4, 5, 6, 7, 8, 9, 10, 11, 12, 13, 14, 15, 16, 17, 18, 19, 20, 21, 22, 23, 24, 25, 26, 27, 28, 29, 30, 31, 32, 33, 34, 35, 36, 37, 38, 39, 40, 41, 42, 43, 44, 45, 46, 47, 48, 49, 50, 51, 52, 53, 54, 55, 56, 57, 58, 59, 60, 61, 62, 63, 64, 65, 66, 67, 68, 69, 70, 71, 72, 73, 74, 75, 76, 77, 78, 79, 80, 81, 82, 83, 84, 85, 86, 87, 88, 89, 90, 91, 92, 93, 94, 95, 96, 97, 98, 99, 100

## ACKNOWLEDGMENTS

The author wishes to acknowledge the help and guidance of Professor L. L. Beranek, the supervisor of this thesis. In addition, he would like to thank Professors R. H. Bolt, R. D. Fay, S. J. Mason, and O. K. Mawardi for many helpful suggestions and criticisms. The experimental work of this thesis could not have been carried through successfully without the assistance and encouragement of Mr. B. G. Watters.

## TABLE OF CONTENTS

	Page
CHAPTER I. INTRODUCTION	
1.1 Purpose . . . . .	1
1.2 Results . . . . .	1
1.3 History of Primary Means for the Measurement of Sound. . . . .	2
1.4 Need for the Investigation. . . . .	6
1.5 Free-field Calibrations . . . . .	7
1.6 Units and Conventions. . . . .	9
CHAPTER II: RECIPROCITY IN LINEAR SYSTEMS	
2.1 History . . . . .	11
2.2 Lumped Constant Systems . . . . .	12
2.3 Distributed Systems . . . . .	43
2.4 Summary . . . . .	47
CHAPTER III. TRANSDUCER THEORY	
3.1 Introduction . . . . .	50
3.2 Source of Finite Dimensions in a Free Field . . . . .	50
3.3 Reciprocal Transducers. . . . .	66
3.4 The Field of a Spherical Source . . . . .	75
3.5 Summary . . . . .	83
CHAPTER IV: MEASUREMENTS AND MEASUREMENT TECHNIQUES	
4.1 Introduction . . . . .	84
4.2 Measurements. . . . .	85
4.3 Measurement Techniques. . . . .	125
4.4 Summary . . . . .	144
APPENDIX I. . . . .	146
APPENDIX II . . . . .	185
BIOGRAPHICAL SKETCH.. . . .	199
BIBLIOGRAPHY. . . . .	200

# CHAPTER I

## INTRODUCTION

### 1.1 Purpose

The fundamental tool of acoustic measurements is the microphone. However, existing methods for the accurate calibration of microphones are of sufficient complexity to restrict their use to the well-equipped acoustical laboratory. The errors introduced by simplifications in technique cannot be predicted until the physical limitations on microphone calibration are understood. It is the purpose of the work described below to investigate these limitations and to describe some resultant practical considerations for free-field calibrations.

### 1.2 Results

The reciprocity technique is the most accurate and convenient of the absolute calibration methods, and for this reason other methods were not investigated. The basis for reciprocity, however, has been studied in some detail. It is shown that all linear Lagrangian systems are reciprocal whether formulated on a lumped or distributed parameter basis. Some non-reciprocal systems are discussed and a general statement of electroacoustic reciprocity including viscous losses is presented. This material is useful in the design of experiments whose purpose is to discover whether a transducer is reciprocal.

Methods for describing the near field of a transducer in terms of its far field are described. The acoustic center and limit of the far field are defined. A graphical method is described for computing this limit directly from the directivity gain plot. The technique is of great use in estimating the error introduced by the close spacing of transducers. All of these results are shown to have meaning whether the transducer is acting as a source or a receiver. Some calculations are made for idealized transducers, a point source and a piston source on a hard sphere.

Measurements were made of the acoustic center and the directivity patterns of a number of commercial microphones. A free-field calibration was performed in a non-anechoic space utilizing an approximation to a point source on a hard sphere. A discussion of experimental techniques includes the following topics: measurement of reciprocity and linearity, effects of standing waves, effect of the size of the enclosure, measurement of the microphone polarizing voltage, pulse techniques applied to detection of reflecting surfaces and to calibration, transducer stability, point-by-point and automatic data-taking techniques, and factors governing the selection of a sound source.

### 1.3 History of Primary Means for the Measurement of Sound

The first important method of making an absolute measurement of the sound pressure (actually velocity) of a sound wave was suggested by Rayleigh.<sup>1</sup> A small circular

<sup>1</sup>Rayleigh, "On an Instrument Capable of Measuring the Intensity of Aerial Vibrations," Phil. Mag., v. 14, p. 186, 1882.

disk suspended in a stream of air by a thin fiber tends to rotate against the restoring torque of the fiber so that the particle motion of the air is normal to its surface. The position of the disk is unchanged by reversing the direction of the stream of air. Thus a steady angular displacement of the disk is observed in an alternating sound field.

The thermophone method, first discussed quantitatively by Arnold and Crandall<sup>1</sup> consists of a small cavity acoustically excited by passing a pulsating direct current through strips inside the cavity. If one knows the current and the thermal properties of the components, it is possible to calculate the sound pressure at the diaphragm of a microphone located in the cavity.

The pistonphone method, perfected by Wente<sup>2</sup>, is similar to the thermophone in that the microphone is placed in a cavity in which the pressure can be computed. In this method the actual amplitude of motion of a piston located in a wall of the cavity is observed. If one knows the impedance of the cavity, the pressure acting on the diaphragm of the microphone may be computed.

The difference between the pressure calibration and the free-field calibration was first discovered experimentally

-----  
<sup>1</sup>Arnold, H. D. and Crandall, I. B., "The Thermophone as a Precision Source of Sound", Phys. Rev., v. 10, p. 22, 1917.

<sup>2</sup>Wente, "The Thermophone", Phys. Rev., v. 19, p. 333, 1922.

by Ballantine<sup>1</sup> when trying to check a thermophone calibration with a Rayleigh disk calibration. The difference is caused by the diffracted wave introduced by the microphone itself. For certain simplified microphones this diffraction effect may be predicted.<sup>2,3,4,5,6,7</sup>

A method of calibration utilizing a perforated grille located adjacent to the microphone diaphragm was suggested by Ballantine.<sup>7</sup> To this grille is applied a pulsating d-c voltage which exerts an electrostatic force on the diaphragm. If one knows the dimensions of the grille, it is possible to calculate the force acting on the diaphragm.

-----  
<sup>1</sup>Ballantine, S., "Effect of Diffraction Around the Microphone in Sound Measurement", Phys. Rev., v. 32, p. 988, 1928.

<sup>2</sup>Ballantine, S., "Effect of Cavity Resonance on the Frequency Response Characteristic of the Condenser Microphone", Proc. Inst. Radio Eng. v. 18, p. 1206, 1930.

<sup>3</sup>Aldridge, A. J., "Calibration of Wente Condenser Transmitter", Jour. Post Office Elec. Eng., v. 21, p. 223, 1928.

<sup>4</sup>Barnes, E. J., "Discussion of a Paper by R. S. Cohen," Proc. Inst. Elec. Eng., v. 66, p. 195, 1928.

<sup>5</sup>West, W., "Pressure on the Diaphragm of a Condenser Transmitter," Proc. Inst. Elec. Eng., v. 5, p. 145, 1930.

<sup>6</sup>Oliver, D. A., "An Improved Condenser Microphone for Sound Pressure Measurements," Jour. Scientific Inst., v. 7, p. 113, 1930.

<sup>7</sup>Ballantine, S., "Technique of Microphone Calibration", Jour. Acous. Soc. Am., v. 3, p. 319, 1932.



Schottky<sup>1</sup> and later Ballantine<sup>2</sup> described the reciprocity principle for electroacoustic transducers. However, MacLean<sup>3</sup> and Cook<sup>4</sup> were the first to show how this principle could be applied to microphone calibration. No solid foundation for the reciprocity calibration technique was established until the treatment by Foldy and Primakoff.<sup>5</sup> Essentially the method requires that a microphone be put in its own sound field. The overall transfer impedance is proportional to the square of the microphone calibration. The only other quantities that need be known are: the frequency, the separation between the two locations of the acoustic center of the microphone, and the density of the medium. The method has proven to be the most accurate of all, and yet the experimental techniques are comparatively simple.

-----

<sup>1</sup>Schottky, W., "Tiefenpfangagesetz", Zeits. f. Physik, v. 36, p. 689, 1926.

<sup>2</sup>Ballantine, S., "Reciprocity in Electromagnetic, Mechanical, Acoustical, and Interconnected Systems", Proc. Inst. Radio Eng., v. 17, p. 929, 1929.

<sup>3</sup>MacLean, W. R., "Absolute Measurement of Sound without a Primary Standard", Jour. Acous. Soc. Am., v. 12, p. 140, 1940.

<sup>4</sup>Cook, R. K., "Absolute Pressure Calibration of Microphones", Jour. Acous. Soc. Am., v. 12, p. 415, 1941.

<sup>5</sup>Foldy, L.L. and Primakoff, H., "General Theory of Passive Linear Electroacoustic Transducers and the Electroacoustic Reciprocity Theorem I and II", Jour. Acous. Soc. Am., v. 17, p. 109, 1945.

#### 1.4 Need for the Investigation

Accurate calibration of microphones is of primary importance in most acoustic measurements. The accuracy of final data can never be superior to the accuracy of the calibration of the microphone with which the data were taken. Ideally, each element of a measurement chain should be capable of yielding results with an accuracy of the same order of magnitude as any other element of the chain. At present the microphone is almost invariably the weakest link of any acoustic measurement chain. Errors of the order of 20 per cent are taken for granted, and errors of ten or twenty times this size are not uncommon. The errors in the remainder of the measurement chain (the electrical components, the indicating device, and the observer) can, with moderate care, be kept less than 5 per cent.

Any methods yielding reasonable accuracy that would not require large or costly facilities would aid almost all branches of acoustic measurements. Several of these branches have become extremely important recently and probably will be even more important in the future. The evaluation and quieting of industrial noise and the establishment of damage risk criteria for the ear are two such branches of acoustic measurements. The development of better microphones and loudspeakers is greatly hampered by the inability of the manufacturer to measure the performance of a new

device with precision.

The present state of affairs is not a result of any basic theoretical trouble with classical methods of calibration but rather an economic trouble. Only a half-dozen laboratories in the nation have the expensive facilities necessary for accurate calibration and, in general, these laboratories find it difficult to spend the time required to set up and perform accurate calibration. In addition it is extremely difficult by existing methods to estimate the errors introduced into a calibration performed under less than ideal conditions. It is therefore of considerable interest to investigate the physical limitations on the calibration of microphones.

### 1.5 Free-Field Calibrations

In the vast majority of measurement problems, one needs to know either the free-field response of the microphone or a response derivable from it. The thermophone, the pistonphone, the electrostatic actuator, and coupler reciprocity are all methods yielding the pressure response of a microphone. It is not possible to derive the free-field response from the pressure response except in cases of extremely simple geometry. For this reason no pressure methods are discussed. Other than reciprocity, the only

free-field method in use is the Rayleigh disk, and it is limited by a serious vulnerability to winds. In addition the method fails when the dimensions of the disk are comparable to a wavelength.

The reciprocity method, on the other hand, may be applied in either free-field or pressure calibrations. There is no fundamental limitation on the method at either low or high frequencies, providing the transducers involved are reciprocal and have reasonable sensitivity.

Most of the experimental techniques discussed will have particular reference to calibrations above about one kilocycle. Below this frequency the wavelength of sound is long enough that diffraction effects are of secondary importance for most microphones. For this reason it is probably easier to make a pressure calibration of a standard microphone and apply a free-field correction. Secondary comparison calibrations carried out with such a standard and in a moderately anechoic space can be quite accurate.

Above one kilocycle, however, almost all measurements become more difficult. At some frequency dependent on the size of the microphone and the gas used, all the coupler methods will fail. The electrostatic actuator method may still be used for condenser microphones and other types with conductive diaphragms.<sup>1</sup> But the free-field correction to  
<sup>1</sup>"Application de la Methode Electrostatique d'Etalonnage Absolu a Certains Types de Microphones," Note - 152, Centre de Recherches Scientifiques Industrielles and Maritimes, Marseille, 1947.

the pressure calibration becomes larger and more difficult to evaluate with accuracy. Free-field comparison calibrations must be carried out with great care in order to maintain the accuracy obtained with ease below one kilocycle.

In practice one finds that the precautions necessary to the performance of an accurate comparison calibration at high frequencies are only slightly less stringent than those necessary to the performance of an accurate reciprocity calibration. Therefore, if accurate high-frequency comparison calibrations are to be carried out, the most practical method of primary calibration is probably the free-field reciprocity technique.

#### 1.6 Unit and Conventions

The units used throughout will be the rationalized MKS system<sup>1</sup>. This choice simplifies the form of the electroacoustic reciprocity theorem considerably.

In general capital Roman letters without other markings will represent matrices. In some cases subscripts on Roman letters will indicate an element of a matrix. In any case capital Roman letters with subscripts will be scalars except for the subscripts *d* and *t*. These notations will indicate the dual matrix and the transposed matrix, respectively.

---

<sup>1</sup>see for instance: Skilling, H.H., Fundamentals of Electric John Wiley, New York, 1948.

The term 'electrostatic transducer' will describe all those electroacoustic devices employing coupling by means of piezoelectric mechanisms and/or static charge. The term 'electromagnetic transducer' will describe those devices employing coupling by means of magnetostrictive mechanisms or a steady magnetic field. Those transducers that employ coupling of both the electrostatic and electromagnetic type are ruled out of both classifications.

The words 'level' and 'gain' and 'response' will always be used in connection with logarithmic quantities such as 'sound pressure level'. When these quantities are contained in equations, it will always be stated whether the units are decibels or nepers.

## CHAPTER II

### RECIPROCITY IN LINEAR SYSTEMS

#### 2.1 History

One of the first references to the phenomenon of reciprocity is by von Helmholtz<sup>1</sup> in 1859. He describes an experiment with a simple source first located at A and then at B. The proof that the intensity of the sound at B in the first experiment is the same as that at A in the second utilizes Green's theorem in the manner now well known. In 1873 Rayleigh<sup>2</sup> described a general statement of the principle of reciprocity which sets down, probably for the first time, several of the simple ways by which the principle may manifest itself. A great unifying step was taken by Lamb<sup>3</sup> five years later. He showed that many systems satisfying the Lagrange equations will obey reciprocity.

Apparently Schottky<sup>4</sup> was the first to realize that the principle of reciprocity could be applied to an electro-acoustic system such as a microphone located in a free field.

This subject was again studied by Ballantine<sup>5</sup> who attempted

<sup>1</sup>Helmholtz, H. von, "Theorie der Luftschwingungen in Röhren mit offenen Enden," Crelles Journal, v. 57, p. 1, 1859.

<sup>2</sup>Rayleigh, Lord, "Some General Theorems Relating to Vibrations", Proc. London Math. Soc., v. 4, 1873.

<sup>3</sup>Lamb, H., "On Reciprocal Theorems in Dynamics," Proc. London Math. Soc., v. 19, 1888.

<sup>4</sup>Schottky, W., "Das Gesetz des Tiefempfangs in der Akustik und Elektroakustik", Zeits. f. Physik, v. 36, p. 689, 1926.

<sup>5</sup>Ballantine, S., "Reciprocity in Electromagnetic, Mechanical, Acoustical and Interconnected Systems", Proc. Inst. Radio Eng., v. 17, p. 929, 1929.

the first proof of the reciprocity of electroacoustic and electromagnetic transducers. His proof rested on the assumption that the transducer could be represented by an analogous network of inductances, capacitances and resistances. It was then a simple matter to complete the proof. This step certainly made electroacoustic reciprocity plausible, but the necessity to assume that the system can be represented by an electrical network seriously limited the application of the proof. The question remained, "Which physical systems are representable by this type of analog?"

Further light on the fundamental basis of the electroacoustic reciprocity theorem was not shed until after several writers had shown how the principle could be applied successfully to the calibration of microphones.<sup>1,2</sup> It was Foldy and Primakoff<sup>3</sup> who finally laid the theoretical foundation on which this reciprocity calibration is based.

## 2.2 Lumped Constant Systems

Some of the results in this section are not new. The methods presented here are believed to be novel and useful, however. In addition, the material provides the necessary

<sup>1</sup> MacLean, W.R., "Absolute Measurement of Sound without a Primary Standard", Jour. Acous. Soc. Am., v. 12, p. 140, 1940.

<sup>2</sup> Cook, R.K., "Absolute Pressure Calibration of Microphones", Jour. Acous. Soc. Am., v. 12, p. 415, 1941.

<sup>3</sup> Foldy, L.L. and Primakoff, H., "General Theory of Passive Linear Electroacoustic Transducers and the Electroacoustic Reciprocity Theorem I and II", Jour. Acous. Soc. Am., v. 17, p. 109, 1945, and v. 19, p. 50, 1947.



foundation for the new results in this and later sections.

The phrase "linear, lumped-constant, passive system" quite often implies that the system is representable by network equations or a schematic diagram employing resistances, inductances, capacitances and ideal transformers. Either one of these two devices is sufficient to specify completely, or at least for normal purposes, the behavior of the system once the boundary and initial conditions are known. If any system is completely described by electrical network equations, it must be linear, reciprocal, and have a finite number of normal frequencies.

For the purposes of this section it will be convenient to generalize slightly the meaning of "linear, lumped-constant system." Let us include within this category any linear system that is completely represented for the purpose at hand by a finite number of variables, all a function of time or frequency only. Under these conditions the system need neither satisfy reciprocity nor have a finite number of normal frequencies. For instance, a transistor is not reciprocal, and over a portion of its operating characteristic it may be described by linear equations. Similarly, the behavior at the terminals of a length of transmission line may be described by linear equations even though the line itself is a distributed system.

## 2.21 Conditions for Reciprocity

This generalized characterization of a lumped system may be expressed mathematically by the matrix equations

$$E = Z I \quad (2.1)$$

or

$$I = Y E \quad (2.2)$$

Here  $E$  and  $I$  are column matrices with the same number of elements of the form  $E_1, E_2 \dots$  and  $I_1, I_2 \dots$ . Throughout this chapter Roman letters without subscripts will represent matrices. The addition of a subscript usually indicates an element of the matrix. The impedance and admittance matrices  $Z$  and  $Y$  are square and the number of elements per side is equal to  $E$  or  $I$ . The symbols  $E$ ,  $I$ ,  $Z$  and  $Y$  are all complex functions of radian frequency and do not involve time.

The generalized condition for reciprocity utilizes the results of two experiments on the same system. The variables pertaining to the two different experiments will be identified by the superscripts (1) and (2). These superscripts will be applied to  $E$  and  $I$ , but not to  $Z$  or  $Y$ , since the impedance or admittance matrices are invariant as long as only one system is studied. The generalized condition for reciprocity is

$$I^{(1)} E^{(2)} - I^{(2)} E^{(1)} = 0 \quad (2.3)$$

In this case  $I$  must become a row matrix. The statement that the matrix product  $I^{(1)}E^{(2)}$  is invariant under the interchange of superscripts is a necessary and sufficient condition for reciprocity. This statement can be placed in a more recognizable form by the substitution of the system equations (2.1) or (2.2).

$$I^{(1)} Z I^{(2)} - I^{(2)} Z I^{(1)} = I^{(1)} [Z - Z_t] I^{(2)} = 0 \quad (2.4)$$

The subscript  $t$  indicates that the impedance matrix has been transposed. Assuming that neither of the  $I$  matrices vanish

$$Z - Z_t = [0] \quad (\text{i.e. } Z_{jk} = Z_{kj}) \quad (2.5)$$

where  $[0]$  is the null matrix. Similar manipulations involving the admittance matrix yield

$$Y - Y_t = [0] \quad (\text{i.e. } Y_{jk} = Y_{kj}) \quad (2.6)$$

These two equations describe the equality of the transfer impedances and admittances connecting any two ports (terminal pairs) of the system.

Some familiar aspects of reciprocity appear when the behavior of any two ports of an electrical system are examined separately. The condition for reciprocity now reads

$$E_1^{(1)} I_1^{(2)} - E_1^{(2)} I_1^{(1)} + E_2^{(1)} I_2^{(2)} - E_2^{(2)} I_2^{(1)} = 0 \quad (2.7)$$

Let experiment (1) be the measurement of the open-circuit transfer impedance from port 1 to 2,  $z_{21}$ . Similarly, let experiment (2) be the measurement of the open-circuit transfer impedance from port 2 to 1,  $z_{12}$ . These two experiments are illustrated in Fig. 2.1a. Since the resulting output voltages are measured under open-circuit conditions,  $I_1^{(2)}$  and  $I_2^{(1)}$  must vanish. Thus the first and last terms of (2.7) become zero and the resultant equation may be rewritten to show that the transfer impedances are equal,

$$z_{21} = \frac{E_2^{(1)}}{I_1^{(1)}} = \frac{E_1^{(2)}}{I_2^{(2)}} = z_{12} \quad (2.8)$$

A second pair of experiments is shown schematically in Fig. 2.1. These experiments yield a measurement of the short-circuit transfer admittances,  $y_{21}$  and  $y_{12}$  and require that  $E_2^{(1)}$  and  $E_1^{(2)}$  vanish. Dropping the second and third terms of (2.7), the result may be rewritten,

$$y_{21} = \frac{I_2^{(1)}}{E_1^{(1)}} = \frac{I_1^{(2)}}{E_2^{(2)}} = y_{12} \quad (2.9)$$

The third pair of experiments (Fig. 2.1c) is a measurement of the transfer ratios of the system,  $h_{21}$  and  $h_{12}$ . These quantities are analogous to the turns ratio of a transformer (see Guillemin<sup>1</sup>). In this case  $E_2^{(1)}$  and  $I_1^{(2)}$

<sup>1</sup>Guillemin, E.A., Communication Networks, Vol. II, John Wiley and Sons, Inc., New York, (1935), p. 137.

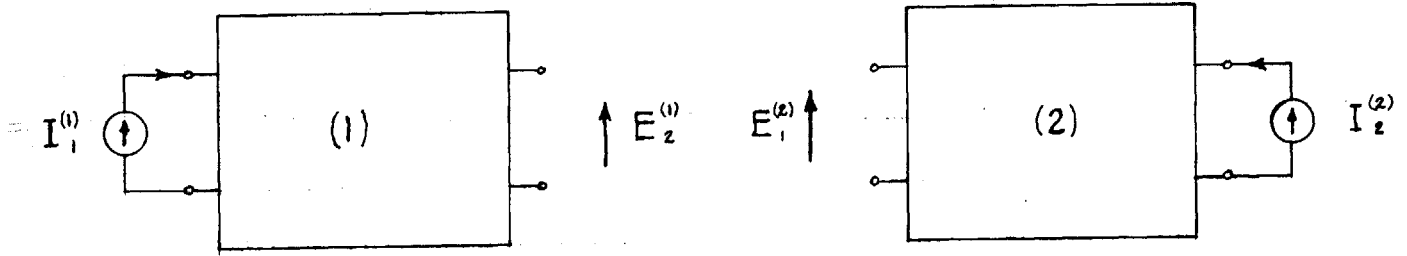


Fig. 2.1a Measurement of Open-circuit Transfer Impedances,  $z_{21}$  and  $z_{12}$ .

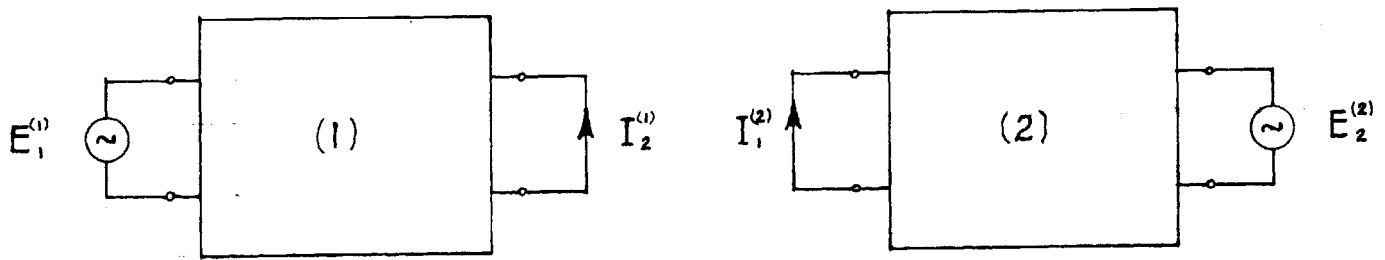


Fig. 2.1b Measurement of Short-circuit Transfer Admittances,  $y_{21}$  and  $y_{12}$ .

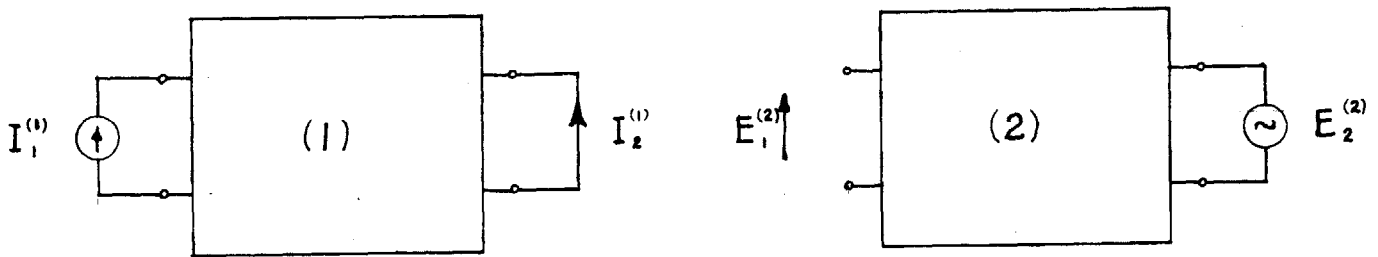


Fig. 2.1c Measurement of Transfer Ratios,  $h_{21}$  and  $h_{12}$ .

Fig. 2.1 Pertaining to the Definition of the Transfer Parameters of an Electrical Network

in (2.7) vanish and one finds that

$$h_{21} = \frac{I_2^{(1)}}{I_1^{(1)}} = - \frac{E_1^{(2)}}{E_2^{(2)}} = - h_{12} \quad (2.10)$$

which is the same result that one would expect for the turns ratio of a transformer. The current  $I_2$  is defined flowing into the network rather than out, accounting for the negative sign.

Let us consider an interesting hypothetical situation in which two engineers set out to measure the transfer impedance of a rather large network. Unfortunately they are from two different countries and occasionally misunderstand each other. They plan to perform the experiment shown in Fig. 2.1a, but the man at the second port confuses the words for voltage and current. He therefore measures the short-circuit current instead of the open-circuit voltage in experiment (1). Similarly, he measures the voltage supplied to the network rather than the current as he should have in experiment (2). When the data are reduced they are surprised to find that the transfer impedances are apparently equal, but opposite in sign. This result could have been predicted from Fig. 2.1c, since this illustrates that the experiment actually performed was the measurement of the transfer ratio.

The above example serves to emphasize that confusion of the quantity to be called voltage and that to be called current can result in a device that apparently violates reciprocity. This rather improbable experiment becomes more significant when one investigates the reciprocity of an electroacoustic transducer.

It has been shown that the reciprocity condition leads directly to reciprocity as expressed by the three pairs of experiments shown in Fig. 2.1. Likewise, equations like (2.4) show that reciprocity from any one of the three pairs of experiments will lead to the general condition for reciprocity (2.3).

## 2.22 Conservation of Energy

If the system described by (2.1) is lossless, it is possible to show an interesting relation involving the transfer impedances. The average power consumed by the system  $\mathcal{P}_{av}$  must vanish. Therefore,

$$\mathcal{P}_{av} = \frac{1}{2} \operatorname{Re} \{ I^* E \} = \frac{1}{4} [ I^* Z I + I Z^* I^* ] = 0 \quad (2.11)$$

Here the star indicates that the complex conjugate has been taken. Script capitals like  $\mathcal{P}_{av}$  will in general be scalars. Note that the factor  $1/2$  appears in front of the product  $I^* E$  indicating that variables are peak rather than root mean square quantities.

If the term  $IZ^*I^*$  in (2.11) is transposed, it is possible to factor an  $I$  in front of and after the brackets. For an arbitrary  $I$  this manipulation yields

$$Z + Z_t^* = [0] \tag{2.12}$$

The above equation shows that any corresponding pair of transfer impedances of a lossless and not necessarily reciprocal system are equal in magnitude. The driving point impedances must be imaginary, but the transfer impedances may have any angle. It is only necessary that a corresponding pair be images of each other in the imaginary axis.

An equation similar to (2.12) may be obtained for the admittance matrix. Thus any lossless system satisfies reciprocity in magnitude, but not in angle. This proves to be a tremendous weakening of true reciprocity. The addition of a reciprocal, but lossy system to a system satisfying reciprocity in magnitude only, in general, will yield a completely non-reciprocal result.<sup>1</sup>

### 2.23 Combination of Reciprocal Systems

By the methods of matrix algebra it is fairly difficult to prove that any combination of two reciprocal systems with many ports will give a new system that is reciprocal between all pairs of ports. A novel and relatively simple proof of this theorem that avoids the use of matrices is described below.

---

<sup>1</sup>McMillan, E.M., "Violation of the Reciprocity Theorem in Linear Passive Electromechanical Systems," J.A.S.A. v. 18, p. 344, 1946.



Consider the three-port system and the load impedance  $Z_L$  shown in Fig. 2.2a. This load impedance may be zero if one wishes to connect two terminal pairs together. If the current  $I_1$  is applied at the port 1, the current flowing in the load impedance can be calculated as shown in Fig. 2.2b. The open-circuit voltage at port 2,  $E_2$ , is a result of the currents flowing at ports 1 and 3 times the proper transfer impedance and is given by

$$E_2 = Z_{21} I_1 - \frac{Z_{23} Z_{31} I_1}{Z_{33} + Z_L} \quad (2.13)$$

Note that this expression would have been the same if the current had been input at port 2 and the voltage measured at port 1 and if the original device was reciprocal. Therefore, the addition of a load impedance leaves a reciprocal system reciprocal. This proof is perfectly general, since the ports 1 and 2 may be taken anywhere in the system.

It is now necessary to show that the replacement of the load impedance  $Z_L$  by a reciprocal system with many ports will leave the resultant system reciprocal. The tandem connection of systems shown in Fig. 2.2c can be treated in a fashion like that above to obtain  $E_4$  in terms of  $I_1$ . The result is

$$E_4 = \frac{Z_{23} Z_{43} I_1}{Z_{22} + Z_{33}} \quad (2.14)$$

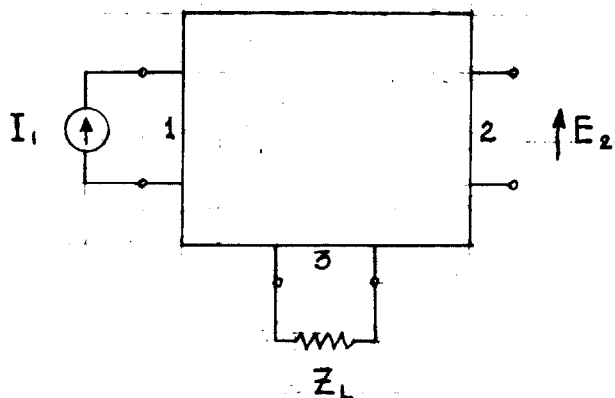


Fig. 2.2a

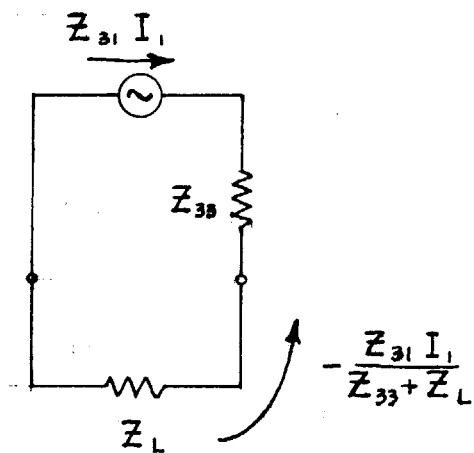


Fig. 2.2b

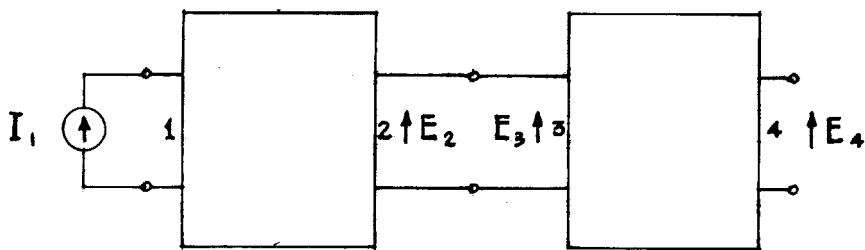


Fig. 2.2c

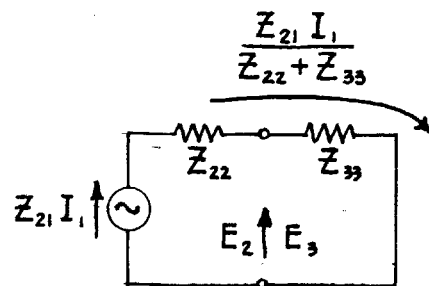


Fig. 2.2d

Fig. 2.2 Diagrams Useful in Proving that the Combination of Reciprocal Systems is Reciprocal.

Again interchanging the current generator and the voltmeter will not alter the resultant transfer impedance provided the original systems were reciprocal.

These two steps constitute a general proof that any combination of reciprocal systems is reciprocal, since parallel, series and other interconnections may be handled one wire at a time. This concept is useful in the analysis of a complex system. For instance, a complicated electrical network can be resolved into the combination of many T or  $\pi$  networks. The components are reciprocal by inspection and, therefore, the combination is reciprocal. Likewise, acoustic reciprocity may be proved by demonstrating reciprocity for an infinitesimal volume of air. This, in turn, is trivial because the infinitesimal volume must be symmetrical.

#### 2.24 Systems Described by the Lagrange Equations

The Lagrange equations can be used to describe the behavior of a vast number of lumped systems. It is important, therefore, to investigate the conditions under which these equations display reciprocity.

Let us assume from the outset that the Lagrangian is not an explicit function of time. This restriction is probably of little importance, since a system with time-varying parameters could hardly be reciprocal. The introduction of such an element into an otherwise reciprocal system would make the results of any significant experiment

different at different times. Even if the element varied sinusoidally at the driving frequency, the output would depend upon the phase relation between the input signal and the driven element.

Thus for the purposes of this section, the general Lagrangian  $\mathcal{L}$  may be written as a function of a set of generalized coordinates  $q_1, q_2, \dots$ , and their time derivatives  $\dot{q}_1, \dot{q}_2, \dots$ , but not as an explicit function of time. Throughout this and several of the following sections the matrix operations are not always as clear as in the above. For this reason a single bracket will denote a row or column matrix and double brackets will denote a rectangular matrix. Under these circumstances the Lagrange equations<sup>1</sup> are given by the matrix equation

$$\left[ \frac{d}{dt} \left( \frac{\partial \mathcal{L}}{\partial \dot{q}} \right) \right] - \left[ \frac{\partial \mathcal{L}}{\partial q} \right] = e] \tag{2.15}$$

in which the elements of the second matrix are derivatives of the Lagrangian with respect to each of the generalized coordinates  $q_1, q_2, \dots$ . The first matrix is constructed in a similar fashion from the time derivative of the Lagrangian with respect to the generalized velocities. The final

-----  
<sup>1</sup> See for instance: Slater and Frank, Mechanics, McGraw-Hill, New York, p. 74, 1947.

matrix contains any additional generalized forces  $e_1, e_2, \dots$  acting on the system. The unusual notation for these forces has been introduced so that the results may be applied to electrical circuits and to avoid notational confusion later.

The instantaneous power input to the system may be evaluated by multiplying the Lagrange equations by their respective velocities and summing. This may be written

$$\underline{\dot{q}} \left[ \frac{d}{dt} \left( \frac{\partial \mathcal{L}}{\partial \dot{q}} \right) \right] - \underline{\dot{q}} \left[ \frac{\partial \mathcal{L}}{\partial q} \right] = \underline{\dot{q}} e] \quad (2.16)$$

Expanding the first term this becomes

$$\frac{d}{dt} \left( \underline{\dot{q}} \left[ \frac{\partial \mathcal{L}}{\partial \dot{q}} \right] \right) - \underline{\ddot{q}} \left[ \frac{\partial \mathcal{L}}{\partial \dot{q}} \right] - \underline{\dot{q}} \left[ \frac{\partial \mathcal{L}}{\partial q} \right] = \underline{\dot{q}} e] \quad (2.17)$$

but the second and third terms are the negative of the total derivative of the Lagrangian with respect to time.

Thus

$$\frac{d}{dt} \left( \underline{\dot{q}} \left[ \frac{\partial \mathcal{L}}{\partial \dot{q}} \right] - \mathcal{L} \right) = \underline{\dot{q}} e] \quad (2.18)$$

Since the righthand side of this equation is the total power input to the system, the quantity within the parentheses must be identified with the energy of the system  $\mathcal{H}$ . When  $\mathcal{H}$  is expressed in terms of generalized momenta  $p_1, p_2, \dots$  and coordinates  $q_1, q_2, \dots$  it may be called the Hamiltonian of the system. The relationship between the

Hamiltonian and the Lagrangian is given by the equations

$$\mathcal{H}(p, q) - p \left[ \frac{\partial \mathcal{H}(p, q)}{\partial p} \right] + \mathcal{L}(\dot{q}, q) = 0 \quad (2.19)$$

$$\mathcal{H}(p, q) - \dot{q} \left[ \frac{\partial \mathcal{L}(\dot{q}, q)}{\partial \dot{q}} \right] + \mathcal{L}(\dot{q}, q) = 0 \quad (2.20)$$

### 2.25 Reciprocity of the Lagrange Equations

The review material of the preceding section has laid the groundwork for an investigation of the requirements on the Lagrange equations in order that they exhibit reciprocity. In this investigation it is again necessary to perform two different experiments, (1) and (2), on the same system. In addition, the time coordinate of one of the experiments will be reversed and the origin shifted. The transformation is accomplished by replacing  $t$  by  $\hat{T} - t$  in all variables pertaining to experiment (2). This change in the time coordinate does not mean that the results of experiment (2) are changed. On the contrary, it is simply a device that allows us to combine in one equation the results of experiment (1) at time  $t$  and the results of experiment (2) at a different time  $\hat{T} - t$ .

With these changes the Lagrange equations for the two experiments are

$$\left[ \frac{d}{dt} \left( \frac{\partial \mathcal{L}^{(1)}(t)}{\partial \dot{q}^{(1)}(t)} \right) \right] - \left[ \frac{\partial \mathcal{L}^{(1)}(t)}{\partial q^{(1)}(t)} \right] = e^{(1)}(t) \quad (2.21)$$

$$- \left[ \frac{d}{dt} \left( \frac{\partial \mathcal{L}^{(2)}(\Gamma-t)}{\partial \dot{q}^{(2)}(\Gamma-t)} \right) \right] - \left[ \frac{\partial \mathcal{L}^{(2)}(\Gamma-t)}{\partial q^{(2)}(\Gamma-t)} \right] = e(\Gamma-t) \quad (2.22)$$

Note that the dot represents differentiation with respect to the argument and not with respect to  $t$ . Multiplying (2.21) by  $q^{(2)}(\Gamma-t)$  and (2.22) by  $q^{(1)}(t)$  and expanding the first term of each will result in

$$\left[ \frac{d}{dt} \left( q^{(2)} \frac{\partial \mathcal{L}^{(1)}}{\partial \dot{q}^{(1)}} \right) \right] + \left[ \dot{q}^{(2)} \frac{\partial \mathcal{L}^{(1)}}{\partial \dot{q}^{(1)}} \right] - \left[ q^{(2)} \frac{\partial \mathcal{L}^{(1)}}{\partial q^{(1)}} \right] = q^{(2)} e^{(1)} \quad (2.23)$$

$$- \left[ \frac{d}{dt} \left( q^{(1)} \frac{\partial \mathcal{L}^{(2)}}{\partial \dot{q}^{(2)}} \right) \right] + \left[ \dot{q}^{(1)} \frac{\partial \mathcal{L}^{(2)}}{\partial \dot{q}^{(2)}} \right] - \left[ q^{(1)} \frac{\partial \mathcal{L}^{(2)}}{\partial q^{(2)}} \right] = q^{(1)} e^{(2)} \quad (2.24)$$

Here the notation that  $q^{(1)}$  and  $q^{(2)}$  are functions of  $t$  and  $\Gamma-t$  has been dropped for brevity. Integrate both of these equations with respect to time from negative infinity to positive infinity. The total derivative terms will vanish

because one or the other of the factors making up these terms will be zero at the limits of the integral. At a very large negative value of  $t$  experiment (1) has not begun, and therefore, the system must be at rest. Since the time coordinate has been reversed for the variables of experiment (2), the system is at rest for very large positive values of  $t$ .

After eliminating the total derivative terms, the difference of the two equations is

$$\int_{-\infty}^{+\infty} \left( \dot{q}^{(2)} \frac{\partial \mathcal{L}^{(1)}}{\partial \dot{q}^{(1)}} - \dot{q}^{(1)} \frac{\partial \mathcal{L}^{(2)}}{\partial \dot{q}^{(2)}} - q^{(2)} \frac{\partial \mathcal{L}^{(1)}}{\partial q^{(1)}} + q^{(1)} \frac{\partial \mathcal{L}^{(2)}}{\partial q^{(2)}} \right) dt \quad (2.25)$$

$$= \int_{-\infty}^{+\infty} \left( q^{(2)} e^{(1)} - q^{(1)} e^{(2)} \right) dt$$

The righthand side is a convolution integral, and therefore, may be rewritten in terms of the transform of the reciprocity condition in the frequency domain (2.3),

$$\int_{-\infty}^{+\infty} \left( \underline{q}^{(2)}(\tau-t) e^{(1)}(t) - \underline{q}^{(1)}(t) e^{(2)}(\tau-t) \right) dt \quad (2.26)$$

$$= \int_{-\infty}^{+\infty} \left( I^{(2)} E^{(1)} - I^{(1)} E^{(2)} \right) \frac{e^{j\omega t}}{j\omega} d\omega$$

where  $I$  and  $E$  are the Fourier transforms of  $\dot{q}$  and  $e$ , respectively. Thus in order that reciprocity hold for the Lagrange equations (2.15), it is necessary that the lefthand side of (2.25) vanish for arbitrary values of  $I^{(1)}$  and  $I^{(2)}$ . This is equivalent to stating that the



integral

$$\mathcal{Q} = \int_{-\infty}^{+\infty} \left( \dot{q}^{(2)} \frac{\partial \mathcal{L}^{(1)}}{\partial \dot{q}^{(1)}} - q^{(2)} \frac{\partial \mathcal{L}^{(1)}}{\partial q^{(1)}} \right) dt \quad (2.27)$$

be unchanged when evaluated with the superscripts interchanged and with arbitrary values of  $q^{(1)}$  and  $q^{(2)}$ .

Examination of the necessary conditions for reciprocity can be accomplished by assuming that all the  $q$ 's are zero except for one in each experiment. Therefore, the only variables will be  $q^{(1)}$ ,  $q^{(2)}$ ,  $\dot{q}^{(1)}$  and  $\dot{q}^{(2)}$ . A general term of the power series expansion of the Lagrangian could be  $q^n \dot{q}^m$ . This gives

$$\mathcal{Q} = \int_{-\infty}^{+\infty} \left\{ m \dot{q}^{(2)} (q^{(1)})^n (\dot{q}^{(1)})^{m-1} - n \dot{q}^{(2)} (q^{(1)})^{n-1} (\dot{q}^{(1)})^m \right\} dt \quad (2.28)$$

Interchanging (1) and (2) will, in general, change the value of the integral unless the Lagrangian is a quadratic form in the  $q$ 's and  $\dot{q}$ 's. It is also possible to have a Lagrangian that will contain a constant and linear terms in the  $\dot{q}$ 's. The constant will vanish by differentiation. The  $\dot{q}$  terms can be integrated with respect to time and will vanish for large positive and negative times if the driving forces are not maintained for an infinite time and if any of the external forces are dissipative. It is interesting to speculate on the fact that a purely lossless system may not show reciprocal behavior because of a current that has been circulating forever.

These conditions on the Lagrangian represent the anticipated restriction that the Lagrange equations be linear. With this restriction the Lagrangian may be written in the following more explicit form:

$$\mathcal{L} = \frac{1}{2} \underline{\dot{q}} \left[ \frac{\partial^2 \mathcal{L}}{\partial \dot{q} \partial \dot{q}} \right] \dot{q} + \underline{\dot{q}} \left[ \frac{\partial^2 \mathcal{L}}{\partial \dot{q} \partial q} \right] q + \frac{1}{2} \underline{q} \left[ \frac{\partial^2 \mathcal{L}}{\partial q \partial q} \right] q \quad (2.29)$$

The square matrices contain the mixed partials with respect to all the q's and q-dot's. These mixed partials must be constants of the system. The result of substituting this expression into the integral (2.27) is

$$\mathcal{Q} = \int_{-\infty}^{+\infty} \left( \underline{\dot{q}}^{(2)} \left[ \frac{\partial^2 \mathcal{L}}{\partial \dot{q} \partial \dot{q}} \right] \dot{q}^{(1)} + \underline{\dot{q}}^{(2)} \left[ \frac{\partial^2 \mathcal{L}}{\partial \dot{q} \partial q} \right] q^{(1)} - \underline{q}^{(2)} \left[ \frac{\partial^2 \mathcal{L}}{\partial \dot{q} \partial q} \right] \dot{q}^{(1)} - \underline{q}^{(2)} \left[ \frac{\partial^2 \mathcal{L}}{\partial q \partial q} \right] q^{(1)} \right) dt \quad (2.30)$$

The corresponding evaluation starting with the Lagrangian for experiment (2) is just the transpose of the original integral (2.30). Of course, the square matrices are unchanged when transposed because their elements are mixed partials and the order of differentiation is immaterial. It can be concluded, therefore, that linear and only linear Lagrange equations exhibit reciprocity.

The general condition for reciprocity expressed in the time domain is not as simple as the equivalent statement in

the frequency domain (2.26). However, for a displacement impulse  $\delta(t)$  at the time origin

$$q^{(1)} = \begin{bmatrix} q_1^{(1)} \\ \vdots \\ \vdots \\ \vdots \end{bmatrix} = \begin{bmatrix} \delta(t) \\ \vdots \\ \vdots \\ \vdots \end{bmatrix} ; \quad q^{(2)} = \begin{bmatrix} q_1^{(2)} \\ \vdots \\ \vdots \\ \vdots \end{bmatrix} = \begin{bmatrix} \delta(t) \\ \vdots \\ \vdots \\ \vdots \end{bmatrix} \quad (2.31)$$

for both experiments, the general reciprocity condition becomes

$$\int_{-\infty}^{+\infty} (\delta(\tau-t) e_2^{(1)}(t) - \delta(t) e_1^{(2)}(\tau-t)) dt \quad (2.32)$$

$$= e_2^{(1)}(\tau) - e_1^{(2)}(\tau)$$

This equation states that if a displacement impulse set off at port 1 results in a certain force at port-2 at a time  $\tau$  later, then an equivalent impulse set off at port 2 will result in an equivalent voltage at port 1 at a time  $\tau$  later.

## 2.26 Dissipative Systems

So far the system under consideration has been conservative. All dissipative elements were removed from the system by including the resultant forces in the list of those acting on the system externally. Dissipation can be included in the system itself by subdividing the force matrix into those forces resulting from lossy elements  $e_{r1}, e_{r2}, \dots$  and those applied externally  $e_{s1}, e_{s2}, \dots$ . If only viscous elements are included, it is possible to write

$$\underline{e}] = \underline{e}_s] - \underline{e}_r] = \underline{e}_s] - R \dot{q}] \quad (2.33)$$

where  $R$  is a square resistance matrix relating the  $\dot{q}$ 's to the  $\underline{e}_r$ 's. As a matter of convenience all the matrices in (2.33) have been defined with a number of zero elements so that each is conformable with  $\underline{q}$ . Thus  $\underline{e}_s]$  may have zeros corresponding to the dissipative forces and  $\underline{e}_r]$  may have zeros corresponding to the external forces. Substitution of this modified expression for the forces into the left-hand side of (2.26) yields

$$\int_{-\infty}^{+\infty} \left( \underline{q}^{(2)} \underline{e}_s^{(1)}] - \underline{q}^{(1)} \underline{e}_s^{(2)}] - \underline{q}^{(2)} R \dot{q}^{(1)}] + \dot{q}^{(1)} R \dot{q}^{(2)}] \right) dt = 0 \quad (2.34)$$

when the result is equated to zero. Noting that

$$\int_{-\infty}^{+\infty} \left( \underline{q}^{(2)} R \dot{q}^{(1)}] - \dot{q}^{(2)} R \dot{q}^{(1)}] \right) dt = \underline{q}^{(2)} R \dot{q}^{(1)}] \Big|_{-\infty}^{+\infty} = 0 \quad (2.35)$$

it is again possible to write

$$\int_{-\infty}^{+\infty} \left( \underline{q}^{(2)} \underline{e}_s^{(1)}] - \dot{q}^{(1)} \underline{e}_s^{(2)}] \right) dt = 0 \quad (2.36)$$

providing that the matrix  $R$  is symmetrical.

The system to which (2.36) applies has been generalized to include viscous forces  $\underline{e}_{r1}$ ,  $\underline{e}_{r2}$ , ... that are related to

the  $\dot{q}$ 's by a set of linear equations. Since  $R$  must be symmetrical, it is possible to derive the viscous forces from a quadratic form. This is called the Rayleigh dissipation function and is defined by

$$\mathcal{F} = \frac{1}{2} \dot{q} \underline{R} \dot{q} \quad (2.37)$$

The viscous forces in terms of the dissipation function may be written

$$e_r] = \frac{\partial \mathcal{F}}{\partial \dot{q}} ] = R \dot{q} ] \quad (2.38)$$

Therefore, the most general matrix equation describing a realizable lumped system that displays reciprocity is

$$\frac{d}{dt} \left( \frac{\partial \mathcal{L}}{\partial \dot{q}} \right) ] + \frac{\partial \mathcal{F}}{\partial \dot{q}} ] - \frac{\partial \mathcal{L}}{\partial q} ] = e_s ] \quad (2.39)$$

where both  $\mathcal{L}$  and  $\mathcal{F}$  are quadratic forms with  $\mathcal{L}$  a function of the  $q$ 's and  $\dot{q}$ 's and  $\mathcal{F}$  a function of the  $\dot{q}$ 's only. The function  $\mathcal{L}$  may include a constant and linear terms in the  $\dot{q}$ 's.

## 2.27 Conditions on the Energy of the System

The relationship between the Lagrangian and the Hamiltonian of the system was given in (2.19) and (2.20). If the Lagrangian is a quadratic form, it is clear that the Hamiltonian must also be. Under these circumstances

one can identify

$$\underline{p} \left[ \frac{\partial^2 \mathcal{H}}{\partial p \partial p} \right] p] = \underline{\dot{q}} \left[ \frac{\partial^2 \mathcal{L}}{\partial \dot{q} \partial \dot{q}} \right] \dot{q}] \quad (2.40)$$

$$\underline{q} \left[ \frac{\partial^2 \mathcal{H}}{\partial q \partial q} \right] q] = - \underline{q} \left[ \frac{\partial^2 \mathcal{L}}{\partial q \partial q} \right] q] \quad (2.41)$$

However, the cross term

$$\underline{\dot{q}} \left[ \frac{\partial^2 \mathcal{L}}{\partial \dot{q} \partial q} \right] q]$$

will drop out in the calculation of  $\mathcal{H}$  from  $\mathcal{L}$ . Similarly the cross term in  $\mathcal{H}$

$$\underline{p} \left[ \frac{\partial^2 \mathcal{H}}{\partial p \partial q} \right] q]$$

will drop out in the calculation of  $\mathcal{L}$ . Therefore, if such cross terms are allowed, there will be no unique relationship between the Lagrangian and the total energy of the system. Furthermore, a Lagrangian defined by (2.19) cannot be a valid representation of a linear system containing such a cross term in the energy because a computation of the energy from the Lagrange equations would omit this term.

Let us examine a few systems in which terms involving  $q$  and  $p$  appear in the energy. Stated in another manner, let us examine systems in which a given displacement will do work that is proportional to one of the momenta.

Perhaps the first system of this type that would come to mind is the rotating top or gyroscope. The significant aspects of the top can be illustrated by a much simpler example, the rotation of a particle in central field of constant magnitude. A physical realization of such a system is a spherical mass,  $m$ , rotating in a conical bowl. Under quiescent conditions the sphere rolls around the bowl at radius  $r_0$  with constant angular velocity  $\omega_0$ . The equations describing incremental motion of the particle about the quiescent conditions are

$$m\ddot{r} - m\omega_0^2 r - (2mr_0\omega_0)\dot{\theta} = f \quad (2.42)$$

$$mr_0^2\ddot{\theta} + (2mr_0\omega_0)\dot{r} = \tau \quad (2.43)$$

where  $f$  is the external force acting on the mass in a radial direction exclusive of the steady force caused by gravity. The quantity  $\tau$  is the incremental torque acting on the mass.

The equations (2.42) and (2.43) do not obey reciprocity in the usual sense because the coefficient of  $\dot{\theta}$  in (2.42) is equal to the negative of the coefficient of  $\dot{r}$  in (2.43). The kinetic energy  $\mathcal{T}$  of the sphere is

$$T = \frac{1}{2} m (r_0 + r)^2 (\omega_0 + \dot{\theta})^2 + \frac{1}{2} m \dot{r}^2 \quad (2.44)$$

The total energy  $\mathcal{H}$  of the system is obtained by adding the potential energy of the sphere resulting from the elevation above the apex of the cone.

$$\mathcal{H} = \frac{1}{2} m \dot{r}^2 + \frac{1}{2} m \omega_0^2 r^2 + \frac{1}{2} m r_0^2 \dot{\theta}^2 + 2 m r_0 \omega_0 r \dot{\theta} + \mathcal{H}' \quad (2.45)$$

where  $\mathcal{H}'$  contains terms not necessary for the derivation of the equations of motion and cubic and quartic terms in the incremental variables. If the total energy had been evaluated directly from the equations of motion, the next to last term of (2.45) would not have appeared. (Incidentally,  $\mathcal{H}'$  would not have appeared either.) Thus, the sphere rolling in a bowl is a simple example of the kind of confusion that can be expected when the total energy of the system contains both  $q$  and  $p$  in a single term.

The equations of motion (2.42) and (2.43) are like the equations that would have been obtained experimentally by the two engineers who set out to measure  $z_{12}$  and  $z_{21}$ , but actually measured  $h_{12}$  and  $h_{21}$ . This suggests that interchanging one pair of quantities analogous to current and voltage in the equations of motion would yield a reciprocal system. For instance, if the incremental angular momentum  $p$  which, in terms of the steady momentum  $p_0$ , is



given by

$$\begin{aligned} p_0 + p &= m (r_0 + r)^2 (\omega_0 + \dot{\theta}) \\ &\cong m r_0^2 \omega_0 + m r_0^2 \dot{\theta} + 2 m r_0 \omega_0 r \end{aligned} \quad (2.46)$$

is substituted into the equations of motion, they may be rewritten in the form

$$m \ddot{r} + 3 \frac{p_0^2}{m r_0^4} r - \left( 2 \frac{p_0}{m r_0^3} \right) p = f \quad (2.47)$$

$$\frac{p}{m r_0^2} - \left( 2 \frac{p_0}{m r_0^3} \right) r = \dot{\theta} \quad (2.48)$$

Thus by recasting the equations in terms of the angular momentum rather than the angular displacement, they become reciprocal. Transposing the angular variables in this fashion was apparently first discussed by Rayleigh<sup>1</sup>.

The total energy of the system expressed in terms of the incremental angular momentum  $p$  is

$$\mathcal{H} = \frac{1}{2} m \dot{r}^2 + \frac{1}{2} \frac{p^2}{m r_0^2} + \frac{3}{2} \frac{p_0^2}{m r_0^4} r^2 - 2 \frac{p_0}{m r_0^3} p r + \mathcal{H}' \quad (2.49)$$

Except for the term  $\mathcal{H}'$  the new equations of motion yield the same expression.

The essential change that has been made in the expression for the energy is that  $p$  has been substituted for  $\theta$  as a generalized coordinate. Under these circumstances  $\dot{p}$  corresponds to a generalized velocity,  $\theta$  to a generalized

<sup>1</sup>Lord Rayleigh, Theory of Sound, v. I, p. 154, Dover, New York, 1945.

momentum and  $\dot{\theta}$  to a generalized force.

In order to understand the general application of the manipulations discussed above, let us investigate the conditions for the reciprocity of systems described by Hamilton's equations

$$\dot{q}] = \frac{\partial \mathcal{H}}{\partial p} ] \quad (2.50)$$

$$\dot{p}] = \frac{\partial \mathcal{H}}{\partial q} ] = e] \quad (2.51)$$

Again consider two experiments (1) and (2) and again assume that the argument of the (2) variables is  $\mathcal{T}$ -t. Multiplication of (2.50) for experiment (1) by (2.51) for experiment (2) will result in

$$\dot{q}^{(1)} e^{(2)}] = \dot{q}^{(1)} \left[ \frac{\partial \mathcal{H}^{(2)}}{\partial q} \right] + \dot{p}^{(2)} \left[ \frac{\partial \mathcal{H}^{(1)}}{\partial p} \right] \quad (2.52)$$

The integral

$$\int_{-\infty}^{+\infty} \dot{q}^{(1)} e^{(2)}] dt = \int_{-\infty}^{+\infty} \left( \dot{q}^{(1)} \left[ \frac{\partial^2 \mathcal{H}}{\partial q \partial q} \right] q^{(2)}] + \dot{p}^{(2)} \left[ \frac{\partial^2 \mathcal{H}}{\partial p \partial p} \right] p^{(1)}] + \dot{q}^{(1)} \left[ \frac{\partial^2 \mathcal{H}}{\partial q \partial p} \right] p^{(2)}] + \dot{p}^{(2)} \left[ \frac{\partial^2 \mathcal{H}}{\partial p \partial q} \right] q^{(1)}] \right) dt \quad (2.53)$$

should be unchanged by interchanging (1) and (2) in order that reciprocity hold. With the aid of integral relations similar to (2.35), it is possible to switch the differentiation with respect to time from the front to the rear of the

terms. However, when the integral

$$\int_{-\infty}^{+\infty} (\dot{\underline{q}}^{(1)} e^{(2)} - \dot{\underline{q}}^{(2)} e^{(1)}) dt \quad (2.54)$$

$$= 2 \int_{-\infty}^{+\infty} (\dot{\underline{p}}^{(2)} \left[ \frac{\partial^2 \mathcal{H}}{\partial p \partial q} \right] q^{(1)} - \dot{\underline{p}}^{(1)} \left[ \frac{\partial^2 \mathcal{H}}{\partial p \partial q} \right] q^{(2)}) dt$$

is evaluated, the mixed terms in the p's and q's evidently remain. Therefore, systems described by Hamilton's equations are reciprocal only when all mixed terms such as those in (2.54) are absent.

For the example of the rolling sphere discussed above, it was possible to transpose momentum and angular displacement coordinates in a manner that yielded a reciprocal system. That this technique is possible in general can be demonstrated by considering a system whose energy contains only mixed terms of the form

$$\mathcal{H} = \underline{q}_a \left[ \frac{\partial^2 \mathcal{H}}{\partial q \partial p} \right] p_b \quad (2.55)$$

where the q and p matrices have been subdivided into two groups, a and b. It has been assumed that no terms coupling a displacement with a momentum of the same group exist. With the momenta and displacements in the b group interchanged, the reciprocity condition is

$$\int_{-\infty}^{+\infty} (\dot{\underline{q}}_a^{(1)} e_a^{(2)} + \dot{\underline{q}}_b^{(2)} e_b^{(1)} - \dot{\underline{q}}_a^{(2)} e_a^{(1)} - \dot{\underline{q}}_b^{(1)} e_b^{(2)}) dt = 0 \quad (2.56)$$

The evaluation of the first two terms of this integral for the system whose energy is given by (2.55) yields

$$\int_{-\infty}^{+\infty} \left( \dot{q}_a^{(1)} e_a^{(2)} + \dot{q}_b^{(2)} e_b^{(1)} \right) dt \quad (2.57)$$

$$= \int_{-\infty}^{+\infty} \left( \dot{q}_a^{(1)} \left[ \frac{\partial^2 \mathcal{H}}{\partial q \partial p} \right] p_b^{(2)} + q_a^{(1)} \left[ \frac{\partial^2 \mathcal{H}}{\partial q \partial p} \right] \dot{p}_b^{(1)} \right) dt$$

By means of (2.35) it is possible to see that it makes no difference whether the differentiation with respect to time is applied to the (1) or (2) experiment variables. Thus the lefthand side of (2.56) vanishes and the system obeys reciprocity.

The fact that it is possible to interchange momenta and displacements for a portion of a system should not be surprising. The symmetry of these variables is well known in quantum mechanics. The electrical principle of duality is another expression of this symmetry. If the dual representation is possible, the potential energy may be written in terms of the derivatives of a new set of coordinates composed of linear combinations of the original momenta. For lumped systems where the kinetic and potential energies are separate quadratic forms, this new set of coordinates can always be found.

The total energy as a function of time must of course be the same in both coordinate systems. The new Lagrangian, however, will be the negative of the old, since formally the kinetic and potential energies have changed places.

This change of sign does not alter the fact that the integral of the Lagrangian will be stationary. Therefore, the form of the Lagrange equations will be the same whether they are in terms of the old or the new coordinates. The formulation of the Lagrangian on this dual basis for electrical networks is given by Guillemin<sup>1</sup>.

Since transformations of this sort leave the Lagrange equations and, therefore, Hamilton's equations unchanged in form, one should expect that they are a type of canonical transformation<sup>2</sup>. The condition satisfied by a canonical transformation is that the integral with respect to time of the difference between the Lagrangians expressed in the two coordinate systems be a function of the end points only. The dual formulation for the Lagrangian satisfies this condition, since the difference between the old and new Lagrangian is just twice the old. The integral of this difference is stationary and therefore dependent on the end points only.

Returning to the total energy of the rolling sphere, let us review the ways in which the coupling can be expressed. If the notation is revised so that  $p$ ,  $r$  and  $\theta$  are no longer incremental quantities, but now represent the quiescent plus

<sup>1</sup>Guillemin, E. A., op. cit. p. 250.

<sup>2</sup> Morse, P. M. and Feshbach, H., Methods of Theoretical Physics, McGraw-Hill Co., New York, p. 287, 1953.

the incremental values, the energy involved in the coupling of the rotational and rectangular systems is

$$\frac{1}{2} p \dot{\theta} = \frac{1}{2} m r^2 \dot{\theta}^2 = \frac{1}{2} \frac{p^2}{m r^2} \quad (2.58)$$

It is now clear that the second form must be used and that an angular momentum is analogous to a rectangular displacement.

Another example of the same problem is the condenser microphone. The energy stored is half the voltage  $e$  times the charge  $q$ .

$$\frac{1}{2} e q = \frac{1}{2} c_0 \delta_0 \frac{\lambda^2}{\delta} = \frac{1}{2} \frac{q^2 \delta}{c_0 \delta_0} \quad (2.59)$$

where  $C_0$  is the quiescent capacitance of the microphone with quiescent spacing  $\delta_0$  and instantaneous spacing  $\delta$ . The integral with respect to time of the voltage  $e$  is the total flux  $\lambda$ . Here the second form is again chosen and charge is chosen as the quantity analogous to displacement. This choice will also set current analogous to velocity and is called the classical analogy.

One final example is the moving iron telephone receiver. The energy stored is half the flux  $\lambda$  times the current  $i$ .

$$\frac{1}{2} \lambda i = \frac{1}{2} L_0 \delta_0 \frac{\dot{\lambda}^2}{\delta} = \frac{1}{2} \frac{\lambda^2 \delta}{L_0 \delta_0} \quad (2.60)$$

where  $L_0$  is the quiescent inductance of the receiver with a quiescent spacing  $\delta_0$  and an instantaneous spacing  $\delta$ . In this case the flux  $\lambda$  is analogous to the displacement, and therefore, the voltage is analogous to velocity, the mobility analogy.

Thus, by examining the energy involved in the coupling between two systems, it is possible to determine the coordinates that will make the system reciprocal. Of course, in systems involving more than one kind of coupling, it may not be possible to choose coordinates that would make the whole system reciprocal at one time.

The treatment of the material in this and several of the preceding sections has been carried out in the time domain. It seemed that these sections would be less ambiguous done in this fashion rather than in the frequency domain. In general, however, the manipulations encountered in the study of reciprocity are easier to handle in the frequency domain. Appendix I contains a section devoted to the evaluation of the kinetic energy, potential energy, and dissipation function for the sinusoidal case. Also included is an evaluation of driving point and transfer impedance in terms of these energy functions.

### 2.3 Distributed Systems

Our intuition might tell us that any distributed linear system can be approximated to any desired tolerance by a lumped system. One would expect, therefore, that a distributed

system will be reciprocal if it is linear, is passive, contains only viscous losses, has a kinetic energy that is a function of the velocities only, has a potential energy that is a function of the coordinates only, and has no explicit dependence on time. With the aid of the groundwork laid in past sections, it is not difficult to prove that this is indeed the case.

From an intuitive point of view one can examine a differential volume of a linear distributed system. In many cases the volume will be homogeneous and therefore reciprocal. Since the combination of reciprocal systems is reciprocal, it can be concluded that the whole system is reciprocal. This point of view indicates that violations of reciprocity are likely to occur at a boundary or as a result of coupling between two systems. As shown in Section 2.27, this is actually the case when the coordinates of the two systems are associated incorrectly.

Though the steps are straightforward, the details of the proof of reciprocity for distributed systems is rather involved and is therefore contained in Appendix I. The basic techniques involved are identical with those used in the lumped system case. The general distributed system that obeys reciprocity can be described by a Lagrangian density that is made up of two separate quadratic forms: the kinetic energy density, a function of the generalized velocities only and the potential energy density, a function of the coordinates themselves plus all possible combinations



of the coordinates and their spatial derivatives.

It is shown that a dual representation of the system is always possible if the potential energy contains no terms in the generalized coordinates themselves. In the case of a large steady component of charge or magnetic field, the dual representation is not possible. It turns out that it is necessary to avoid combinations of such systems if one expects reciprocity because both systems cannot be described by the same generalized coordinates.

The general description of the viscous forces that can be included in a distributed system without destroying reciprocity is much the same as the general description of the conservative forces. Another way of expressing this conclusion is to allow the constants in the Lagrange equations to become complex for sinusoidal variations of the coordinates. This modification of these equations will include the most general form of viscous forces obeying reciprocity.

Also included in Appendix I is a demonstration of the relationship between the general reciprocity condition and the symmetry of the Green's function. A generalized impedance has been defined so that the distributed systems may be connected to lumped systems. This impedance for distributed systems takes the form of a matrix of mode impedances<sup>1</sup> in the general case. If one of the coordinates is constant over the area under consideration, the formulation may be simplified so that only one impedance is necessary for a

-----  
<sup>1</sup>Crout, P. D., "An Extension of Lagrange's Equations to Electromagnetic Field Problems," Jour. of App. Phys., v. 19, p. 1007, 1948.

particular coordinate.

The general description of the Lagrangian is shown to include the special cases of heterogeneous, anisotropic elastic and electromagnetic media. Viscous forces caused by expansive friction and shearing losses will be included as will losses caused by electrical conductivity if the conductivity matrix is symmetric.

Systems with steady rotational motion are not in general reciprocal. If the motion is in an incompressible fluid, it is possible to utilize the dual rotational coordinates as in section 2.27 and obtain reciprocity. Similarly the proper set of coordinates must be chosen in order that an electrostatic or an electromagnetic transducer be reciprocal. Let us include within the classification "electrostatic transducer" all those employing coupling by static charge or piezoelectric mechanisms. Likewise, "electromagnetic transducers" include those coupled by magnetostriction or a static magnetic field. For electrostatic coupling the magnetic field strength becomes a generalized velocity and for electromagnetic coupling the electric field strength is the generalized velocity.

The electroacoustic reciprocity theorem may be expressed in terms of the complex current and voltage at the electrical terminals  $i$  and  $e$  and the complex pressure and volume velocity at an ideal acoustic point transducer,  $p^o$  and  $u^o$ . Utilizing (55), (92), (118), (122), and (123) from Appendix I, the reciprocity condition for electrostatic transducers becomes

$$\begin{aligned}
p^{(1)} u^{(2)} - p^{(2)} u^{(1)} &= \int_{a_a} (p^{(1)} \vec{v}^{(2)} - p^{(2)} \vec{v}^{(1)}) \cdot d\vec{a}_a \\
&= - \int_{a_e} (\vec{E}^{(1)} \times \vec{H}^{(2)} - \vec{E}^{(2)} \times \vec{H}^{(1)}) \cdot d\vec{a}_e = -e^{(1)} i^{(2)} + e^{(2)} i^{(1)}
\end{aligned} \tag{2.61}$$

where  $\vec{v}^{\circ}$  is the complex velocity vector,  $a_a$  is the area of a small sphere surrounding the acoustic point transducer,  $\vec{E}^{\circ}$  is the complex electric field vector,  $\vec{H}^{\circ}$  is the complex magnetic field vector and  $a_e$  is the area surrounding the electrical terminals. With the same notation the reciprocity condition for an electromagnetic transducer is

$$\begin{aligned}
p^{(1)} u^{(2)} - p^{(2)} u^{(1)} &= \int_{a_a} (p^{(1)} \vec{v}^{(2)} - p^{(2)} \vec{v}^{(1)}) \cdot d\vec{a}_a \\
&= \int_{a_e} (\vec{E}^{(1)} \times \vec{H}^{(2)} - \vec{E}^{(2)} \times \vec{H}^{(1)}) \cdot d\vec{a}_e = e^{(1)} i^{(2)} - e^{(2)} i^{(1)}
\end{aligned} \tag{2.62}$$

These relations will hold if the transducer is linear, passive and has no time-varying parameters. In addition it is necessary that no electrostatic coupling exist in an electromagnetic transducer and vice-versa. Outside of these restrictions the characterization of the transducer is quite general.

#### 2.4 Summary

It has been shown that certain systems described by the Lagrange equations are reciprocal. Included in this

group are all linear, passive, lumped and distributed systems. Also if a linear passive system is not reciprocal, it cannot be described by linear Lagrange equations.

In some non-reciprocal cases it may be possible to choose new coordinates for part of the system that will restore reciprocity. In these cases the relationship between the energy and the Lagrangian will not be unique for the original coordinates.

A simple example may demonstrate this condition more clearly. Consider a two-port, lossless network. A perfectly general representation of such a network consists of a shunt admittance, a transformer, and a series impedance. Suppose that it is necessary to evaluate the impedances and the transformer turns ratio by energy measurements only. There is a unit current generator and a unit voltage generator available. If the current generator is applied to the series impedance side of the network, the energy stored in this element will be equal to the value of the impedance. This result will be completely independent of the power input at the other port. Conversely, if the shunt admittance is measured with the voltage source attached to its terminals, changes on the series impedance side cannot be detected. The experimenter might erroneously conclude that there was no coupling between the two halves of the system. With the experiments described there is no possible way to evaluate the transformer turns ratio.

Therefore, if one expects to be able to describe the system in terms of its energy, it is necessary that the same coordinates be used on both sides of the transformer; i.e., current generators on both sides. By turning the generators off and on it would be possible to devise enough experiments to evaluate the impedance, admittance, turns ratio, and in addition prove that the device was reciprocal.

The major result of the chapter is given by equations (2.61) and (2.62). Here the results of Foldy and Primakoff<sup>1</sup> have been duplicated, and in addition viscous terms have been included. The proof was based on energy considerations, and the equations of motion were derived instead of serving as the starting point. These results are specialized statements arising from the fact that any linear Lagrangian system is reciprocal.

---

<sup>1</sup>Foldy, L. L. and Primakoff, H., op. cit., Part II, Jour. Acous. Soc. Am., v. 19, p. 50, 1947.

## CHAPTER III

### TRANSDUCER THEORY

#### 3.1 Introduction

An electroacoustic transducer is a device that converts electrical energy into acoustic energy or vice-versa. The complete behavior of a transducer is extremely difficult to formulate in terms of the general electromechanical equations developed in the last chapter. Measurement of all the parameters involved throughout the volume of the transducer is almost an impossible task for a relatively simple device. Even if all the parameters were known, the computation of, for instance, the input impedance of the device, would in general be impractical.

It would then seem wise to attack the problem from the point of view of the information desired about the transducer rather than from the equations describing the device. If the transducer is a sound source, one is usually interested in the relationship between the sound pressure at some point and the electrical input. If the transducer is a microphone, one is usually interested in the relationship of the electrical output to the sound pressure that would have been detected by an ideal point pressure detector.

In general these relationships will not be a function of the transducer alone, but will include the effects of the enclosure within which the system is located. One

method of eliminating the effect of the enclosure is to make it so small that wave motion can be neglected. This method fails for large transducers and for high frequencies. Another method of reducing the effect of the enclosure is to place the transducer in or cause it to generate a random field. As long as the field is uniformly random in the neighborhood of the measurements, the boundary surfaces of the enclosure will have an effect that is easily calculated.

A third method of eliminating the effect of the enclosure is to place the transducer in a free field. This is the obvious method and also yields the most general results. The behavior of the transducer in many environments can be predicted from certain properties measured in a free field. For instance the random field response of a microphone can be found from its free field response. The converse, however, is not true.

### 3.2 Source of Finite Dimensions in a Free Field

Consider a source of finite dimensions surrounded by a homogeneous and unbounded acoustic medium. Henceforth, this environment will be called a free field. No matter how complicated the structure of the source may be, the complex amplitude of the pressure  $p$  in the free field outside an hypothetical sphere enclosing the source will satisfy the wave equation

$$\frac{1}{r^2} \frac{\partial}{\partial r} \left( r^2 \frac{\partial p}{\partial r} \right) + \frac{1}{r^2 \sin \theta} \frac{\partial}{\partial \theta} \left( \sin \theta \frac{\partial p}{\partial \theta} \right) + \frac{1}{r^2 \sin^2 \theta} \frac{\partial^2 p}{\partial \phi^2} + k^2 p = 0 \quad (3.1)$$

where  $r$ ,  $\theta$ ,  $\phi$  and  $k$  are the radius, polar angle, azimuth angle, and the wave number. The spherical wave functions that satisfy this equation form a complete set, and therefore, the radiation from any source may be expressed by an infinite series of these functions.

The radial part of the wave functions are spherical Hankel functions  $h_n^{(2)}(kr)$  if only outgoing waves are considered. The behavior of all the spherical Hankel functions for a sufficiently large radius will be proportional to  $1/r(\exp-jkr)$ . Therefore, at some large distance it is possible to factor out the radial dependence of the series expression for the pressure. The remaining terms, dependent on  $\theta$  and  $\phi$  only, describe the directivity pattern of the source.

If one were given the directivity pattern of a source and it was possible to expand this pattern in a series whose terms would be the angular part of a spherical wave function, one could then compute the pressure throughout the remainder of the field. This is true because the process of expanding the directivity pattern in terms of the angular functions will automatically evaluate the coefficients of the series



representation of the field for any radius. Since the angular parts of the wave functions form a complete set themselves, it will be possible to expand any directivity pattern in this fashion.

One may conclude that the directivity pattern of a source is sufficient to specify the field completely except for points within a sphere that just encloses the source. This is an extremely useful concept, since it makes it possible to specify the source performance quite completely in terms of three parameters: the directivity pattern, the electrical input impedance, and the source response. The input impedance is defined for the transducer immersed in a free field and the source response gives the pressure at some large distance from the source for a unit current input to the electrical terminals.

### 3.21 The Field of a Source in Terms of the Directivity Pattern

Although any given directivity pattern can be expanded in a series of angular functions by graphical or numerical methods if analytical techniques fail, a direct approach to the partial differential equation will yield some interesting relationships between the directivity pattern and the remainder of the field. Let us investigate the solutions  $\psi$  of a new partial differential equation which is formed from (3.1) by means of the transformation

$$\frac{p}{p_0} = \frac{z_0}{z} e^{-j(z-z_0)} \psi \quad (3.2)$$

where  $z = kr$  and  $p_0$  is a reference pressure measured at  $z_0 = kr_0$  and  $\theta = 0$ . This new equation will have solutions whose radial dependence vanishes for large values of  $kr$ . The region in which the  $r$  dependence of  $p$  is  $1/r(\exp(-jkr))$  and in which that of  $\psi$  is constant will be called the far field of the source. The modified partial differential equation is

$$\frac{\partial^2 \psi}{\partial z^2} - 2jz \frac{\partial \psi}{\partial z} + \frac{1}{z^2} L_{\theta\phi}(\psi) = 0 \quad (3.3)$$

where  $L_{\theta\phi}$  is the differential operator

$$L_{\theta\phi}(\ ) = \frac{1}{\sin \theta} \frac{\partial}{\partial \theta} \left( \sin \theta \frac{\partial (\ )}{\partial \theta} \right) + \frac{1}{\sin^2 \theta} \frac{\partial^2 (\ )}{\partial \phi^2} \quad (3.4)$$

The original differential equation (3.1) had a regular singularity at  $r = 0$  and an irregular singularity at  $r = \infty$ . The modified equation still has the same singular points. One would like to expand  $\psi$  in inverse powers of  $z$ , since the field from a finite source must vanish at an infinite distance from the source. Since the irregular singularity is present at infinity, it should be expected that such an expansion will be of the asymptotic type. The series

$$\psi(z, \theta, \phi) = \sum_{n=0}^{\infty} \frac{\Psi_n(\theta, \phi)}{z^n} \quad (3.5)$$

substituted into the differential equation (3.3) will lead to the recurrence relation

$$2n \Psi_n + (n-1)n \Psi_{n-1} + L_{\theta\phi}(\Psi_{n-1}) = 0 \quad (3.6)$$

Note that for  $n = 0$  both sides vanish automatically, since there can be no coefficient for terms in positive powers of  $z$ . Therefore, it is possible to begin with any  $\Psi_0$ , a function of the angular variables, and compute all the  $\Psi_n$  from this relation, (3.6). These functions  $\Psi_n$  together with (3.5) and (3.2) provide us with a formal solution for the pressure anywhere in the field of a sound source whose directivity  $\Psi_0$  is known. Practically, however, the computation becomes enormously complicated after the first few terms.

### 3.22 The Field of an Axially Symmetrical Source

Some of the complexity involved in evaluating the  $\Psi_n$  is eliminated by considering only sources that are symmetrical about the polar axis. The field produced by such sources will also have axial symmetry, and the angular differential operator  $L_{\theta\phi}$  in (3.6) therefore becomes

$$L_{\theta}(\ ) = \frac{1}{\sin \theta} \frac{\partial}{\partial \theta} \left( \sin \theta \frac{\partial(\ )}{\partial \theta} \right) \quad (3.7)$$

Appendix II shows that with the aid of the Legendre polynomials it is possible to compute the  $\Psi_n$  in terms of a summation of the derivatives of  $\Psi_0$  with respect to  $\cos \theta$ . The coefficients of the first few terms of the series have been evaluated for arbitrary  $\theta$ . For  $\theta = 0$ ,  $\theta = \pi$ , and  $\theta = \frac{\pi}{2}$  the coefficients can be expressed in closed form. The resulting expression for  $\cos \theta = \pm 1$  is simply

$$\Psi_n \Big|_{\cos \theta = \pm 1} = (\pm 1)^n \Psi_0^{(n)} \Big|_{\cos \theta = \pm 1} \quad (3.8)$$

where the superscript (n) indicates differentiation with respect to  $\cos \theta$  n times. This same result may be obtained directly by comparison of the  $n^{\text{th}}$  derivatives of  $h_m^{(2)}(\frac{2}{3})$  and  $P_m(\cos \theta)$ , the spherical Hankel function and the Legendre polynomial of the order m.

For  $\theta = \frac{\pi}{2}$  the expression for  $\Psi_n$  in terms of the derivatives of  $\Psi_0$  is slightly more complicated

$$\Psi_n \Big|_{\theta = \frac{\pi}{2}} = \sum_{\nu=0}^{\nu=2n} \frac{(-1)^{\nu/2} n! \Psi_0^{(\nu)} \Big|_{\theta = \frac{\pi}{2}}}{2^n \frac{\nu!}{2!} (n - \frac{\nu}{2})! (\nu - n)!} \quad (3.9)$$

where all the odd derivatives vanish because their coefficients always contain the factor  $\cos \theta$ .

These results agree with what one would expect intuitively for the relationship between the directivity pattern and the near field. If the directivity pattern is a rapid function of angle, the series in inverse powers of the radius will have increasingly large coefficients. It is therefore necessary to get a large distance away from the source before the far field is reached. At a discontinuity in the directivity pattern the coefficients of the inverse powers of radius blow up. In this case it is never possible to get far enough away from the source to reach the far field. For instance, in the plane of symmetry of a dipole one would expect to find large tangential velocities even at great distances from the source. Thus the limit of the far field will be much farther from the source in the vicinity of the plane of symmetry than along the axis of the dipole.

The results described by (3.8) and (3.9) have been used to investigate the near field of a piston in an infinite baffle (Appendix II). The field on the polar axis ( $\theta = 0$ ) may be calculated directly from the integral of the source distribution for a pulsating pill box. The expansion of this result in a series of inverse powers of radius checks the calculation based on the directivity pattern and (3.8).

A series expression for the pressure in the plane  $\theta = \frac{\pi}{2}$  has been calculated in Appendix II. This result is apparently new and converges rapidly for low frequencies or large  $r$ . At

high frequencies the series oscillates and converges rather poorly unless  $r$  is quite large.

### 3.23 The Acoustic Center of a Source

In the far field of any sound source, the dependence on the radius is the same as that for a simple source; i.e.,  $1/r(\exp-jkr)$ . Thus, in the far field, for a given angle it is possible to replace an arbitrary source by a simple source of the proper strength. As a point receiver is brought closer to the origin, the difference between the source and its equivalent simple source will be detected.

At very great distances from the source, the exact positioning of the equivalent source is of little consequence. The distance at which differences between the source and its equivalent appear will, however, be determined by this positioning.

Consider a simple source displaced a distance  $a$  away from the origin along the polar axis ( $\theta = 0$ ). The directivity pattern of the displaced source will be altered in phase only

$$\psi_0(\theta) = e^{+jka(\cos\theta - 1)} \quad (3.10)$$

The derivatives of  $\psi_0$  with respect to  $\cos\theta$  evaluated at  $\theta = 0$  may be substituted into (3.5) to obtain the field of the displaced point source on the polar axis

$$\Psi(r, \theta) = 1 + \frac{a}{r} + \left(\frac{a}{r}\right)^2 + \dots \quad (3.11)$$

The general expression for  $\Psi(r, \theta)$  is given by

$$\Psi(r, \theta) = 1 + \Psi_0^{(1)}(0) \left(\frac{1}{j\beta}\right) + \Psi_0^{(2)}(0) \left(\frac{1}{j\beta}\right)^2 + \dots \quad (3.12)$$

In both cases the reference point  $z_0$  in (3.2) has been chosen so that  $\Psi_0(0) = 1$ . Thus if the equivalent source is adjusted so that

$$z_a = ka = \text{Im}[\Psi_0^{(1)}] \quad (3.13)$$

the difference in the magnitude of the two expressions for  $\Psi(r, \theta)$  will have a leading term of the order  $(1/r)^2$ . In most practical cases one is interested in the magnitude of the pressure only. The value of  $a$  given in (3.15) is therefore the best possible adjustment of the equivalent source in order that it will duplicate the magnitude of the original field as close as possible to the origin. Let us define this position  $z_a = ka$  as the acoustic center of the source.

For  $\theta = \pi$  the acoustic center is given by an identical relation evaluated at the new angle. A source that is symmetrical about the equatorial plane will have its acoustic centers for  $\theta = 0$  and  $\theta = \pi$  located equidistant from the equatorial plane as one might expect. This fact makes it

clear that the location of the acoustic center is a function of angle. For other angles the best location is difficult to evaluate and may not even be on the polar axis. Fortunately, most practical interest in this topic will be for measurements made along the polar axis.

If the directivity pattern is expressed in terms of its phase  $\beta$  and the natural logarithm of its magnitude  $\alpha$  which shall be called the directivity gain

$$\psi_0(\theta) = e^{[\alpha(\theta) + j\beta(\theta)]} \quad (3.14)$$

some of the implications of the definition of the acoustic center become more apparent

$$z_a = ka = \left. \frac{\partial \beta(\theta)}{\partial \cos \theta} \right|_{\theta=0} = \beta''(0) \quad (3.15)$$

Thus the derivative of the phase of the directivity pattern with respect to  $\cos \theta$  is proportional to the location of the acoustic center. If the differentiation is with respect to  $\theta$  itself, the righthand side becomes the negative of the second derivative. Note that the first derivatives of  $\psi_0$ ,  $\alpha$ , or  $\beta$  with respect to  $\theta$  must vanish at the polar axis in order that the field have the assumed symmetry.

Therefore, changes in the magnitude of the directivity pattern do not influence the location of the acoustic center. A good illustration of this point is a source that is



contained in the equatorial plane. If the elements of such a source all radiate in phase, the directivity pattern will be real for all angles. Thus, even though the magnitude of  $\psi_0$  may change rapidly with angle, the derivative of the phase will always be zero. The acoustic center must then be at the origin, as one should have guessed.

The concept of an acoustic center is extremely useful in the calibration of transducers because the far field may be specified by a measurement at distances much closer to the origin than would be otherwise possible. This is a great practical advantage because large free field spaces are expensive and difficult to construct. Before the acoustic center can be used with confidence, it is necessary to evaluate the error involved in replacing a source by its equivalent simple source. This error will increase as the distance to the origin is decreased. At some point the error will become too great to tolerate in any given experiment. This point will be called the limit of the far field.

### 3.24 Limit of the Far Field

Let us assume for the purposes of this section that the source has been adjusted so that its acoustic center is at the origin. Any deviation of  $\psi$  from the far field value  $\psi_0$  will be indicative of an error that will appear when the source is replaced by its equivalent simple source.

Measurements will in general be made of the magnitude of the pressure only. The error  $\epsilon$  resulting from the introduction of the equivalent source is then

$$\epsilon(r, \theta) = \left| \frac{\Psi(r, \theta)}{\Psi_0(\theta)} \right| - 1 = \left| 1 + \frac{\Psi_0^{(1)}(\theta)}{\Psi_0(\theta)} \left( \frac{1}{j\lambda} \right) + \frac{\Psi_0^{(2)}(\theta)}{\Psi_0(\theta)} \left( \frac{1}{j\lambda} \right)^2 + \dots \right| - 1 \quad (3.16)$$

where the real part of the second term within the magnitude signs must vanish, since the source is located so that its acoustic center is at the origin.

On the polar axis the leading term for the error becomes

$$\epsilon(r, 0) = -\left( \frac{1}{2} [\alpha^{(1)}(0)]^2 + \alpha^{(2)}(0) \right) \frac{1}{\lambda^2} + O\left(\frac{1}{\lambda^3}\right) \quad (3.17)$$

where  $\alpha$  is the directivity gain as defined in (3.14). Here the superscripts indicate differentiation with respect to  $\cos \theta$  as usual. If the differentiation had been carried out with respect to  $\theta$ , the result would be

$$\epsilon(r, 0) = -\left( \frac{1}{2} \left( \frac{\partial^2 \alpha}{\partial \theta^2} \right)^2 + \frac{\partial^4 \alpha}{\partial \theta^4} \right) \bigg|_{\theta=0} \frac{1}{\lambda^2} + O\left(\frac{1}{\lambda^3}\right) \quad (3.18)$$

Thus the error is determined largely by the shape of the directivity gain pattern. The leading term of the error can be expressed in terms of the slope and curvature of a plot of the directivity gain  $\alpha$  against the  $\cos \theta$ . If the

directivity gain is plotted against  $\theta$  itself, the error will be determined by the curvature and the fourth derivative.

Unless the directivity pattern is very irregular in the vicinity of the polar axis, the leading term given in (3.17) or (3.18) will give a good indication of the limit of the far field. Usually one is interested in evaluating small errors, and under most circumstances the  $\frac{1}{3^2}$  term will appear well before the higher order terms.

### 3.25 A Construction Approximating the Limit of the Far Field

At some frequencies for sources with smooth directivity patterns, it is often possible to neglect the second term on the righthand side of (3.17) and (3.18). If the source is an efficient radiator, most of the power will be in the lower modes of radiation. Higher order sources can never radiate well at low frequencies and tend to produce irregular directivity patterns at high frequencies. Thus for many practical sources the term  $\alpha^{(2)}(\theta)$  may be small.

It would be convenient to be able to compute the limit of the far field by means of a construction on the directivity gain pattern which is usually plotted in decibels. Patterns of this sort may be obtained automatically with the aid of a rotating microphone and a synchronized polar plotter.

Since by symmetry the slope of the directivity gain pattern will always be zero on the polar axis, the radius

of curvature  $\rho$  of the pattern at this point becomes

$$\rho = \frac{\alpha''(\alpha)}{\alpha(\alpha) - \alpha'(\alpha)} \quad (3.19)$$

if  $\alpha(\alpha)$  is the distance in nepers from the origin to the pattern (Fig. 3.1). Eliminating  $\alpha'(\alpha)$  in (3.17) with the aid of the radius of curvature, the error may now be approximated by

$$\epsilon(r, \alpha) \cong -\frac{1}{2} \left[ \frac{\alpha(\alpha)}{3} \frac{\alpha(\alpha) - \rho}{\rho} \right]^2 \quad (3.20)$$

when  $\epsilon$  is expressed in nepers or

$$\epsilon(r, \alpha) \cong -\frac{1}{2} \left[ \frac{\alpha(\alpha)}{8.693} \left( \frac{\alpha(\alpha) - \rho}{\rho} \right) \right]^2 \quad (3.21)$$

when  $\alpha(\alpha)$  is expressed in decibels.

For a given  $\alpha(\alpha)$ , note that the error is proportional to the distance between the center of the plot and the center of curvature divided by the radius of curvature. Thus for patterns that are very little different from that of a simple source, the center of curvature approaches the center of the plot. This causes the numerator of (3.20) and (3.21) to become quite small and will therefore yield a small value for the error  $\epsilon$ . On the other hand, if  $\rho$  becomes small, as it would for a directional source, the error will become large unless the radius  $r$  is increased

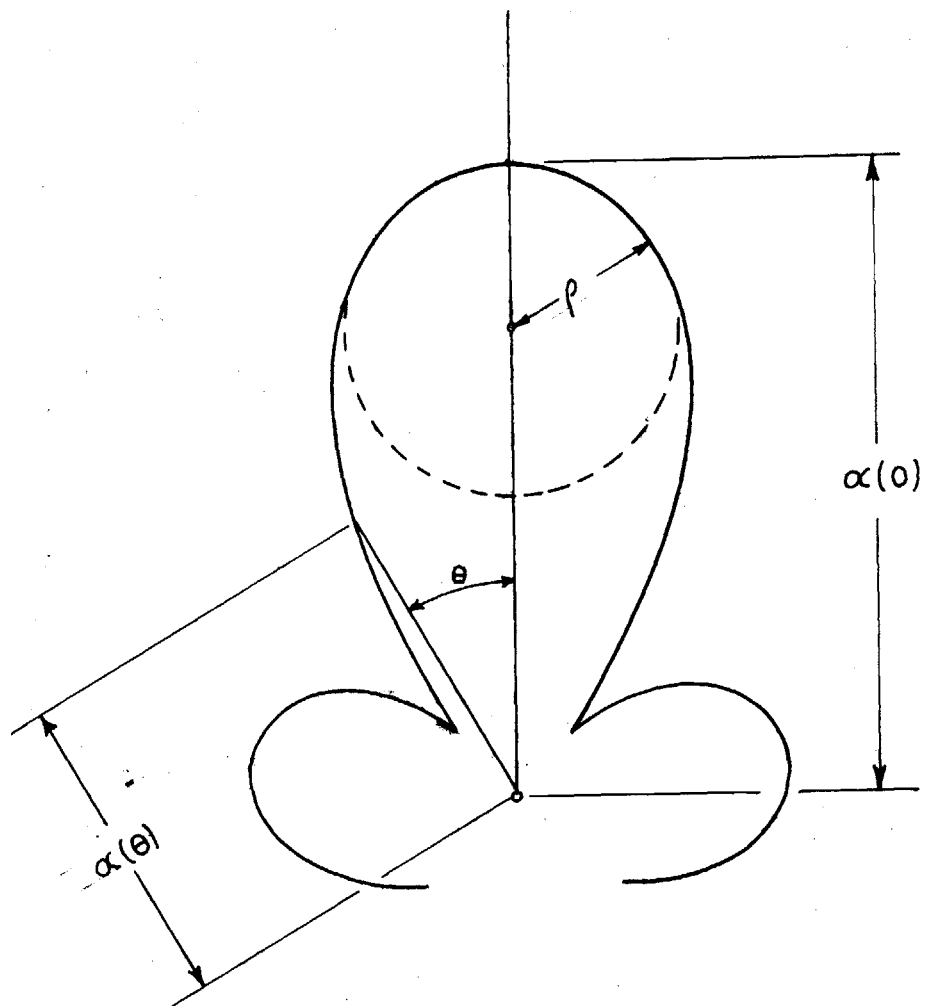


Fig. 3.1 Relative to the Computation of the Limit of the Far Field of a Sound Source.

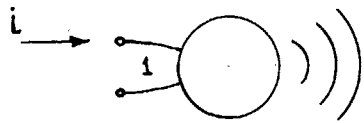
accordingly. Thus the limit of the far field for the directional source is at a much greater distance than that for the omnidirectional source.

This construction is extremely simple, and use has been made of it in the calculation of the limit of the far field for a number of commercial transducers. In practical microphone calibration it provides a method whereby the distance between source and receiver may be minimized for a given error.

### 3.3 Reciprocal Transducers

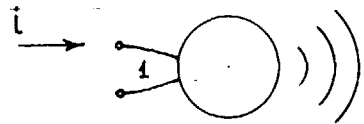
By virtue of the electroacoustic reciprocity theorem of Chapter II, it is possible to demonstrate that a reciprocal transducer has properties that are especially useful in calibration work. Let us first evaluate the transfer impedance between the terminals of a transducer and some point in the free field surrounding the transducer. If the device is reciprocal, the transfer impedance will be the same whether measured from the electrical to the acoustical side or vice-versa.

In Fig. 3.2a, a current  $i$  is input into the electrical terminals and a pressure  $p$  observed at the point  $r$  and  $\theta$ . This measurement defines either the transfer impedance  $z_{21}(r, \theta)$  or the transfer ratio  $h_{21}(r, \theta)$ . The reverse experiment (Fig. 3.2b) involves a simple source of volume velocity  $u$  placed at  $r$  and  $\theta$ . The open-circuit voltage  $e$  is proportional either to the transfer impedance  $z_{12}$



$$p = z_{21}(r, \theta) i$$

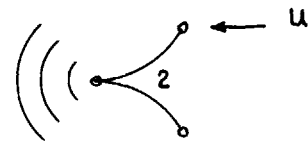
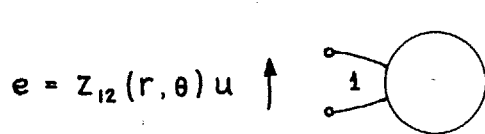
Electrostatic Transducer



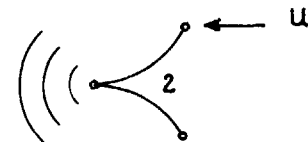
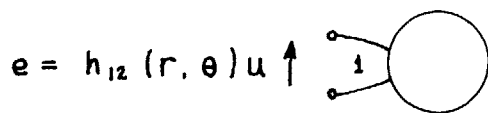
$$p = h_{21}(r, \theta) i$$

Electromagnetic Transducer

Fig. 3.2a



Electrostatic Transducer



Electromagnetic Transducer

Fig. 3.2b

Fig. 3.2 Pertaining to the Reciprocity of Electromagnetic and Electrostatic Transducers

or to the transfer ratio  $h_{12}$ . By the electroacoustic reciprocity theorem (2.61)

$$\begin{aligned} z_{21} &= \frac{P^{(1)}}{I^{(1)}} = \frac{1}{u^{(2)} l^{(1)}} \int_{a_a} p^{(1)} \vec{v}^{(2)} \cdot d\vec{a}_a \\ &= \frac{1}{u^{(2)} l^{(1)}} \int_{a_e} (\vec{E}^{(2)} \times \vec{H}^{(1)}) \cdot d\vec{a}_e = \frac{e^{(2)}}{u^{(2)}} = z_{12} \end{aligned} \quad (3.22)$$

the transfer impedances must be equal if the device is electrostatic and the transfer ratios

$$\begin{aligned} h_{21} &= \frac{P^{(1)}}{I^{(1)}} = \frac{1}{u^{(2)} l^{(1)}} \int_{a_a} p^{(1)} \vec{v}^{(2)} \cdot d\vec{a}_a \\ &= \frac{-1}{u^{(2)} l^{(1)}} \int_{a_e} (\vec{E}^{(2)} \times \vec{H}^{(1)}) \cdot d\vec{a}_e = \frac{-e^{(2)}}{u^{(2)}} = -h_{12} \end{aligned} \quad (3.23)$$

will be equal and opposite in sign if the device is electromagnetic (2.62). As indicated in Chapter II, the classical analogy must be used with electrostatic transducers and the mobility analogy with electromagnetic transducers.

### 3.31 Parameters Describing a Reciprocal Transducer

In the following analysis the classical analogy will be used. Strictly speaking, the results should only be applied to electrostatic transducers. The only important difference in the treatment for the mobility analogy is that a negative sign will appear here and there. Therefore, the results for electromagnetic transducers can be



inferred from the following treatment for electrostatic transducers.

The speaker calibration of a transducer is the pressure produced at some point in the far field by a unit current input to the electrical terminals. In terms of the transfer impedance  $z_{21}$  the speaker calibration  $S(r, \theta)$  may be written

$$z_{21}(r, \theta) \xrightarrow{r \rightarrow \infty} S(r, \theta) \quad (3.24)$$

where  $r$  must be large enough so that the measurement is carried out in the far field (symbolically indicated by  $r \rightarrow \infty$ ).

The microphone calibration of a transducer is the open-circuit voltage produced in a free field by a plane wave of unit pressure amplitude incident upon the microphone at an angle  $\theta$ . The plane wave may be generated by a simple source at a very large distance from the transducer. The pressure  $p$  that would be detected by a point pressure detector if it were substituted for the transducer would be

$$p = z_{22} \frac{a}{r} e^{-jkr} u \quad (3.25)$$

where  $z_{22}$  is the driving point impedance of a simple source,  $a$  is the radius of the source,  $r$  is the distance to the

transducer,  $k$  is the wave number, and  $u$  is the volume velocity of the source. Let us define the reciprocity parameter  $J(r)$  as the pressure  $p$  detected by the point pressure detector divided by the volume velocity of the simple source  $u$ .

$$J(r) = \frac{p}{u} = \frac{j\rho c}{2\lambda r} e^{-jkr} \quad (3.26)$$

Here the driving point impedance of the simple source has been evaluated (see Appendix I, Section 9.) and  $\rho$  is the density of air,  $c$  is the velocity of sound, and  $\lambda$  is the wavelength.

For large values of  $r$  the transfer impedance  $z_{12}$  may be written in terms of the microphone calibration  $M(\theta)$  and the reciprocity parameter  $J(r)$

$$z_{12}(r, \theta) \xrightarrow{r \rightarrow \infty} J(r) M(\theta) \quad (3.27)$$

and since the transfer impedances are equal

$$s(r, \theta) = J(r) M(\theta) \quad (3.28)$$

for any reciprocal electrostatic transducer. For reciprocal electromagnetic transducers the speaker calibration will be equal to the negative of the reciprocity parameter times the microphone calibration.

The equations above are applicable in the far field only, but may be generalized by rewriting (3.2) in terms of the reciprocity parameter and the speaker calibration

$$p = S(r_0, \theta) \frac{J(r)}{J(r_0)} \psi(r, \theta) i \quad (3.29)$$

where  $S$  has been evaluated at the reference point where  $p_0$  was measured. This reference point is for convenience on the polar axis and is always in the far field. Now from Fig. 3.2a it is possible to identify the transfer impedances  $z_{21}$  and  $z_{12}$

$$z_{21} = z_{12} = s(r, \theta) \psi(r, \theta) = J(r) M(0) \Psi(r, \theta) \quad (3.30)$$

and this expression is valid at any point in the field outside of a sphere just enclosing the transducer. In the far field  $\psi$  becomes  $\Psi_0$ , the directivity pattern of the microphone. Thus the directivity pattern of a reciprocal transducer is the same whether it acts as a source or a receiver.

In addition the deviation of the speaker response from that of a simple source  $\psi$  is the same as the deviation of the microphone response from that of a point pressure detector. For the microphone this effect may be visualized as a curvature of the wavefronts arriving at the transducer as a result of placing the source in the near field of the microphone. Therefore, the calibration

of a microphone by means of a simple source placed in the near field will differ from the calibration made with the source in the far field. The relationship between these two calibrations may be expressed in terms of the directivity pattern with the aid of the function  $\Psi$ .

The computation of the first few terms of the function  $\Psi$  from the directivity pattern will not only predict the acoustic center and the limit of the far field of a transducer acting as a sound source, but in addition will predict the acoustic center of the transducer acting as a microphone and the point at which the curvature of the wavefronts becomes important. The expressions for  $\epsilon$ , (3.17), (3.18), (3.20), and (3.21) may therefore be interpreted as giving the error incurred by calibrating a microphone with a simple source located at  $r$ .

Thus a reciprocal transducer can be characterized by three parameters: the electrical input impedance, the directivity pattern, and either the speaker or the microphone calibration in the axial direction. All parameters are measured with the transducer immersed in a free field. If the transducer is placed in an enclosure, the change in input impedance can be computed, formally at least, by replacing all reflecting surfaces by sources whose velocity is equal and opposite to that of the incident wave. Integrating the response to a point source of arbitrary location (3.30) over the reflecting surfaces will give an

output voltage that is equal to the current times the change in impedance.

The only other parameter that might be included in a description of the transducer is the scattering pattern. This pattern is proportional to the amplitude of a scattered wave in the far field of the transducer as a result of a plane wave incident at an arbitrary angle. The resulting parameter is a function of both the angle of the incident plane wave and the angle at which the scattered wave is measured. Since the scattered wave is an outgoing solution of the wave equation, the results obtained for the directivity pattern of a source will apply equally well to its scattering pattern.

### 3.32 Reciprocity Calibration

If two transducers, (a) and (b), are placed in a free field, the transfer impedance  $z_{ab}$  between the two electrical ports can be computed

$$z_{ab} = M_a(o) \Psi_a(r, \theta_a) S_b(r, o) \Psi_b(r, \theta_b) \quad (3.31)$$

if one assumes that the pressure at the receiver is not altered appreciably by the wave scattered from the source as a result of the wave scattered from the receiver. This is usually a second order effect at low and moderate frequencies, but at high frequencies multiple reflections

may become quite significant especially if the two transducers have plane, parallel surfaces.

If the results of a comparison calibration between transducers (a) and (b) are included in (3.31) one can write

$$\Psi_a(r, \theta_a) M_a(o) = \left[ \frac{z_{ab}}{J(r)} \frac{M_a(o)}{M_b(o)} \frac{\Psi_a(r, \theta_a)}{\Psi_b(r, \theta_b)} \right]^{\frac{1}{2}} \quad (3.32)$$

where the spacing between transducers for the comparison calibration is large. This expression (3.32) will reduce to the usual reciprocity formula as the spacing is increased and  $\Psi_a$  and  $\Psi_b$  approach the directivity patterns  $\Psi_{a0}$  and  $\Psi_{b0}$ .

An example of the use of (3.32) in the calibration of a special transducer (a simple source on a sphere) is described below. For most practical transducers, however, it is hard to get accurate information about  $\Psi$  by calculation from the geometry of the transducer, by direct measurement, or by computation from the directivity pattern. The directivity gain pattern usually may be measured with little difficulty, but phase information about the pattern is almost always inaccurate. The location of the acoustic center and the limit of the far field can be found for all transducers, and therefore, this information will be of great value in the practical calibration of microphones and sound sources.

### 3.4 The Field of a Spherical Source

In order to gain a better understanding of the acoustic center and the limit of the far field, it is helpful to compute the field of some simple sources. A complete description of the field of a general spherical radiator with axial symmetry can be obtained in terms of the Legendre polynomials  $P_n(\cos \theta)$  and the spherical Hankel functions  $h_n(kr)$ <sup>1</sup>. Two particular cases have been chosen for computation: a point source located on the surface of the sphere on the polar axis, and a spherical piston pulsating in the surface of a sphere. The angle subtended by an arc in the surface of the piston and passing through its center is 120 degrees.

The calculations pertinent to the following discussions will be found in Appendix II.

#### 3.41 Calculation of the Acoustic Center

Fig. 3.3 is a plot of the location of the acoustic center of a point source and a piston source located on the surface of a hard sphere. The horizontal axis of Fig. 3.3 is the wave number  $k$  times the radius of the sphere  $r_1$ . The vertical axis is the location of the acoustic center  $a$  in terms of the radius of the sphere. The distance  $a$  is measured from the origin along the  $\theta = 0$  axis.

<sup>1</sup>See for instance, Morse, P. M., Vibration and Sound, McGraw-Hill, New York, p. 319, 1948.

### Acoustic Center for a Spherical Source

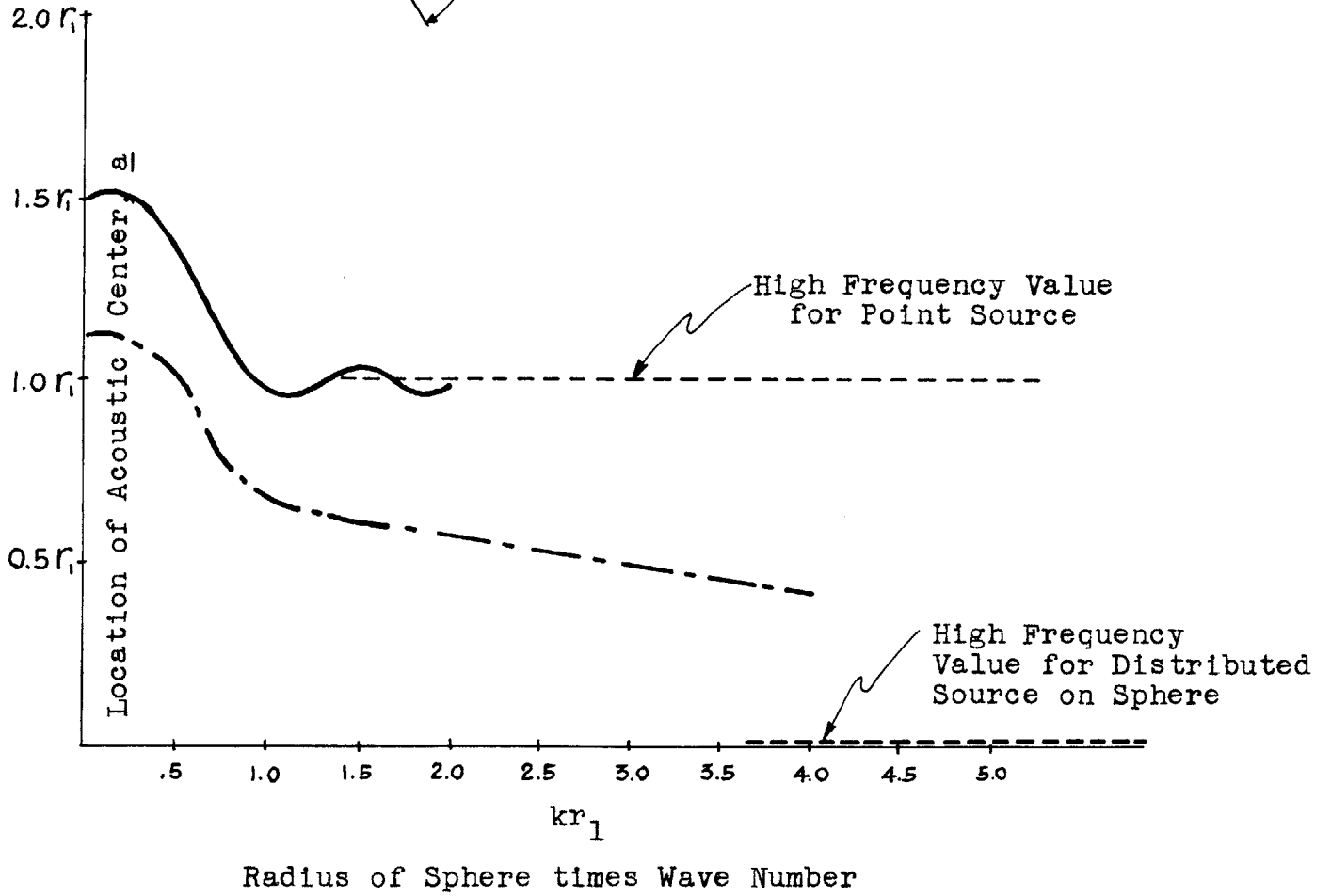
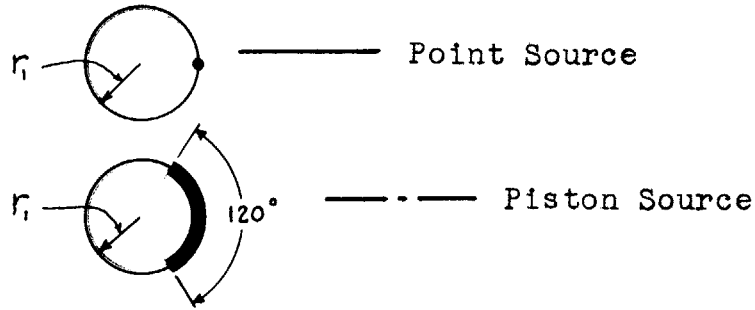


Fig. 3.3 Acoustic Center for Point and Piston Sources on a Sphere (a Measured from Center of Sphere)



At low frequencies the acoustic center for the point source is a half radius in front of the sphere. As the frequency is increased, the center moves toward the surface of the sphere. Above  $kr_1 = 1$  (circumference of the sphere equal to a wavelength) the position of the center oscillates about the surface of the sphere with an ever-decreasing amplitude. At very high frequencies the series expressions involved in the evaluation of the location of the center may be approximated by integrals, and one finds as  $k$  approaches infinity  $a$  approaches unit. This is actually the geometrical optics approximation, since the wavelength will be very small compared to the sphere. The point source appears to be radiating in an infinite baffle and, as a result, acts like a simple source located at  $r = r_1$ .

At very low frequencies the acoustic center for a piston set in a sphere is given by

$$a = \frac{3}{4} r_1 (1 + \cos \theta_0) \quad (3.33)$$

where  $2\theta_0$  is the angle subtended by the piston. When  $\theta_0$  vanishes, this expression should give the acoustic center for a point source on a sphere. Inspection of Fig. 3.3 and (3.33) indicates that this is indeed the case. If the whole sphere is pulsating uniformly ( $\theta_0 = \pi$ ), the right-hand side of (3.33) vanishes. Thus the acoustic center of

a simple source is at its center as one should expect.

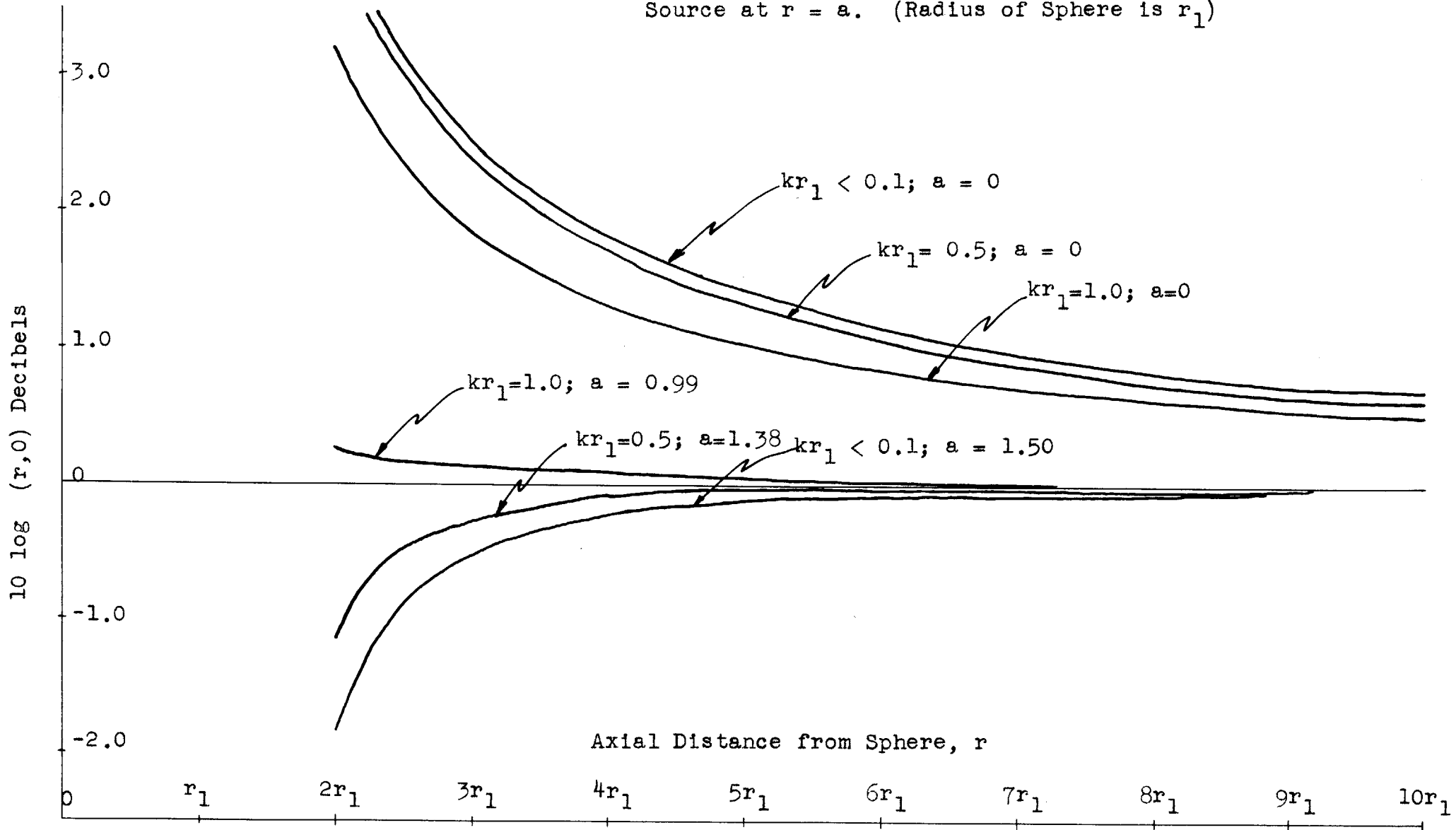
Calculations have been made at higher frequencies for the case  $\theta = \frac{\pi}{3}$ , and the results are plotted in Fig. 3.3. The curve runs parallel to that for a point source up to about  $kr_1 = 1$ , but at higher frequencies gradually drops toward zero. For sources with a well-behaved velocity distribution (no discontinuities in the slope), the directivity pattern is proportional to the velocity distribution. Thus, if all the elements on the surface of the sphere radiate in phase, the directivity pattern will have constant phase. One can conclude that the acoustic center of this sort of source is at the origin at high frequencies.

The piston set in a sphere does not have a well-behaved velocity distribution, but any physical realization of this source will. Therefore, the acoustic center will be at the origin for some high frequency; the sharper the drop in the velocity at the edge of the piston, the higher the frequency.

### 3.42 Calculation of the Field of a Point Source on a Sphere

The pressure on the axis in front of a point source on a sphere has been calculated for three frequencies;  $kr_1 \leq 0.1$ ,  $kr_1 = 0.5$ , and  $kr_1 = 1.0$ . These data are plotted in Fig. 3.4 as deviations from the pressure produced by a point source located at the origin ( $\underline{a} = 0$ ) and then located at

Fig. 3.4 Level of Deviation of Axial Field of a Point Source on a Hard Sphere from that of a Simple Source at  $r = a$ . (Radius of Sphere is  $r_1$ )



the acoustic center as given in Fig. 3.3. This procedure emphasizes the advantage to be gained by choosing the proper acoustic center. Note that the three bottom curves indicate that the difference between the actual pressure and that from an equivalent source is less than 0.5 decibels as close as one diameter away from the surface of the sphere for all three frequencies.

The low frequency curve deviates at larger distances than do the other two. Examination of the series expression for  $\Psi$  at low frequencies (see Appendix II) shows that the  $(1/kr_1)^2$  term has a rather large coefficient that is proportional to  $(kr_1)^2$ . This term could not have been predicted by the construction on the directivity pattern given in Section 3.25. The first term in the complete expression for the error (3.17) is proportional to  $(kr_1)^4$  and the second to  $(kr_1)^2$ . Therefore, at low frequencies the term that was neglected in the graphical construction predominates. This situation indicates that the graphical method may fail at very low frequencies.

At  $kr_1 = 0.5$  the second term of the error (3.17) is still important, but at  $kr_1 = 1.0$  the graphical method predicts the error accurately.<sup>1</sup> This might have been guessed without calculation, since the first term of the error will always predict an increase in  $\Psi$ .

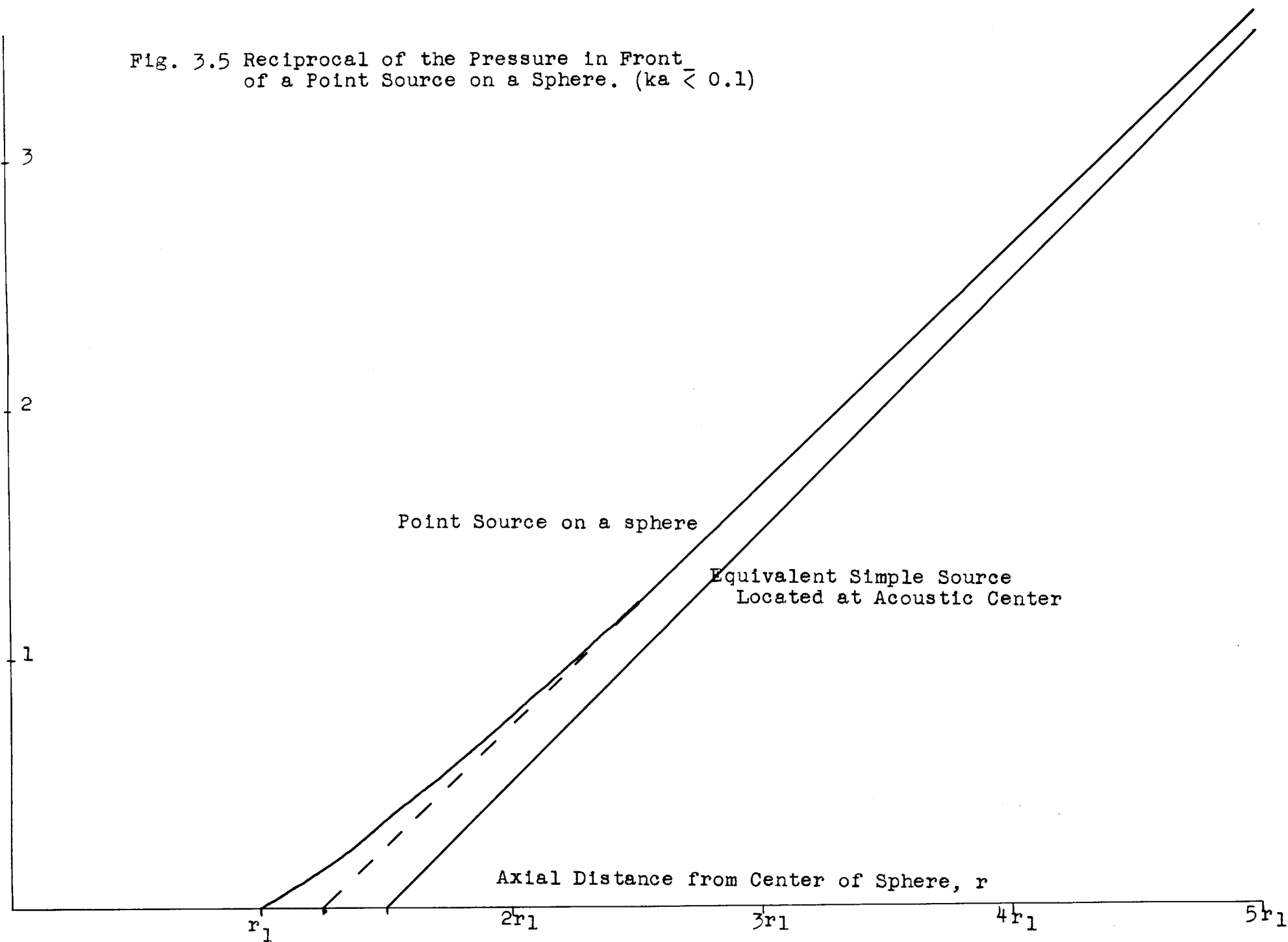
<sup>1</sup>The directivity plots of a point source on a sphere used here are from Morse, P.M., op. cit., p. 322. However, the plots in this reference are not of great enough accuracy to be used in determining the error  $\epsilon$ . For this reason, the original calculations were obtained through the cooperation of the MIT RLE Computing Group.

A series expression for the field of a piston in an infinite baffle for  $\theta = 0$  is given in Appendix II (21). Examination of the error (3.17) for this source shows that the situation is much the same as for the point source on a sphere. The first term of (3.17) is again of the order  $(kr_1)^2$  whereas the second term has both  $(kr_1)^2$  and  $(kr_1)^4$  terms. At low frequencies the second term will predominate and the graphical construction will be invalid. At moderate and high frequencies both terms are about the same size, and the construction will give a good approximation to the error.

The closed form expression for the pressure in front of the sphere at low frequencies given in Appendix II allows one to make an accurate plot of the reciprocal of the pressure without difficulty. Such a plot is shown in Fig. 3.5. It is interesting to note that a limited amount of data taken no farther than  $5r_1$  from the origin would indicate that the acoustic center was located closer to the surface of the sphere than  $\frac{3}{2}r_1$ . Thus, in determining the acoustic center, it is wise to take measurements well beyond the limit of the far field in addition to those taken near the limit.

Fig. 3.5 Reciprocal of the Pressure in Front  
of a Point Source on a Sphere. ( $ka \ll 0.1$ )

Reciprocal of Pressure



### 3.5 Summary

It has been shown that the near field of a sound source is directly related to its directivity pattern. Formulas for the acoustic center and the limit of the far field were developed in terms of this pattern. These formulas help to give the experimenter the answer to one of the most frequent questions in microphone calibration: "How closely can I space source and receiver?"

The calculations for the special sources gave greater meaning to the concepts of acoustic center and the limit of the far field and also pointed out some of the limitations. The real test of the usefulness of these two concepts will come in their application to experimental data.

## CHAPTER IV MEASUREMENTS AND MEASUREMENT TECHNIQUES

### 4.1 Introduction

The material discussed above has been entirely theoretical in nature. The work leading to the discussions in Chapters II and III has helped to produce a more firm and detailed understanding of the phenomenon of reciprocity and the behavior of the field of a transducer. That many of the concepts developed there are useful in practical calibration work will be demonstrated in the present chapter.

Measurements of the directivity patterns and acoustic center have been made for seven different types of commercial transducers:

- 1) Altec-Lansing Model 633-A dynamic microphone
- 2) Shure Rochelle salt Model 9898 crystal microphone
- 3) Western Electric Model 640-AA condenser microphone
- 4) Altec-Lansing Model 21-B condenser microphone
- 5) Altec-Lansing Model 21-C condenser microphone
- 6) Altec-Lansing Model 21-BR condenser microphone
- 7) Altec-Lansing Model L-1 dynamic pressure unit  
mounted in a special spherical housing

In several cases more than one unit of a given type was studied. Throughout the forthcoming discussion reference will be made to these seven types of transducers by their model numbers only.



Following the presentation of the measured data is a section describing experimental techniques of microphone calibration. This discussion includes the method of application of the acoustic center and directivity data to a calibration setup. Also discussed are many of the other limitations and errors that may arise in practice.

#### 4.2 Measurements

All the measurements were carried out in the MIT Acoustics Laboratory anechoic chamber. The free space available was about 14 feet cubed. The chamber actually has a longer dimension, but the full benefit of this additional space could not be realized because of the panel transmission apparatus. The chamber is designed to reflect less than 10 per cent of the incident energy down to about 70 cps. Very few measurements were carried out below 1000 cps, however.

##### 4.21 Experimental Apparatus

Most of the electronic equipment was mounted in a trio of relay racks located just outside the chamber (Fig. 4.1). Included in this equipment are the following items:

- 1) Two-frequency audio oscillator
- 2) Power amplifier
- 3) Pulsed sine wave generator

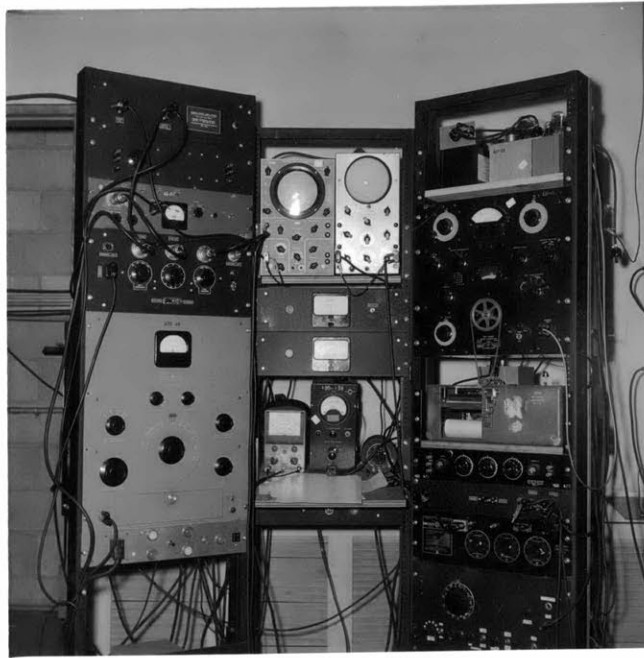


Fig. 4.1 Electronic equipment and control panel.

- 4) Precision attenuators
- 5) Universal microphone preamplifier panel
- 6) Condenser microphone line amplifier
- 7) Amplifier compensated for microphone response to provide uniform output at all audio frequencies.
- 8) Tracking wave analyzer electronically coupled to two-frequency oscillator
- 9) Expanded scale voltmeter for monitoring condenser microphone polarizing voltage
- 10) Expanded scale output meter for making accurate judgments of attenuator settings
- 11) Oscilloscope for monitoring output wave form
- 12) Oscilloscope for determining frequency by Lissajous patterns against frequency standard
- 13) Graphic level recorder mechanically coupled to oscillator

This equipment was found to be quite flexible and was easily adapted to all the experiments conducted. Most of the special equipment was designed and constructed by Mr. B. G. Watters and is described in detail in his thesis.<sup>1</sup> In particular, a special transducer of his design was used extensively (Fig. 4.2). This device is an L-1 pressure unit from a 633-A dynamic microphone enclosed in a spherical housing about two inches in diameter. The acoustic circuit

-----

<sup>1</sup>Watters, B.G., "Sound Sources for Microphone Calibration", MIT Masters Thesis, 1953.

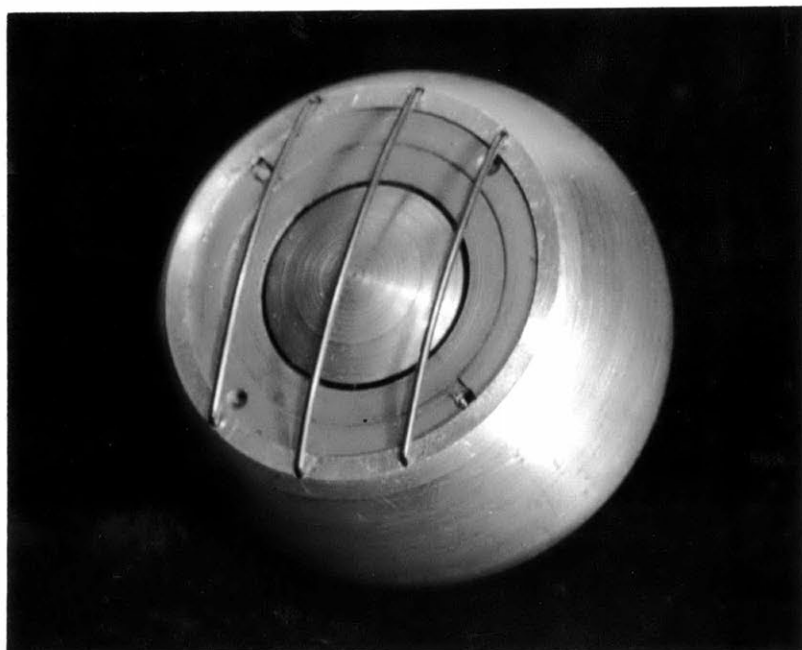


Fig. 4.2 Altec-Lansing L-1 pressure unit mounted  
in a 2-inch sphere.

of the pressure unit has been modified so that the source response of the unit is quite smooth between 1 and 20 kilocycles (kc).

#### 4.22 Scanning Apparatus

An automatic method of scanning the field in front of a sound source was found to be desirable. One of the prime considerations was the accuracy with which the scanning microphone was positioned. For this reason a dismantled lathe bed was used as the basis of the scanner (Fig. 4.3). A small and extremely quiet motor was attached by O-ring belts to the screw. Thus the scanning frame was driven along by means of the lathe carriage.

The information desired from the experiment was the deviation of the sound field from that of a simple source. Therefore, a novel and simple method of recording the position of the microphone was designed. A ten-turn potentiometer was attached to the carriage and geared to a rack fixed on the bed (Fig. 4.4). The audio signal from the oscillator was fed to the potentiometer. The output of the potentiometer was then proportional to the distance travelled by the microphone. This voltage, proportional to distance, was connected to the input of the power amplifier which, in turn, was connected to the sound source. If the scanner starts at the acoustic center of a simple source, the pressure arriving at the microphone

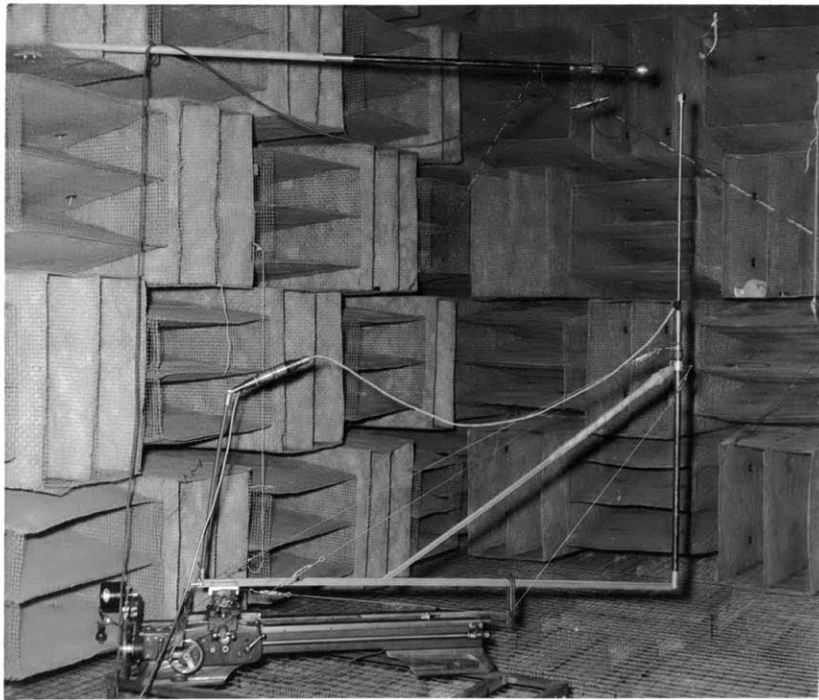


Fig. 4.3 Scanner for plotting field of a sound source.

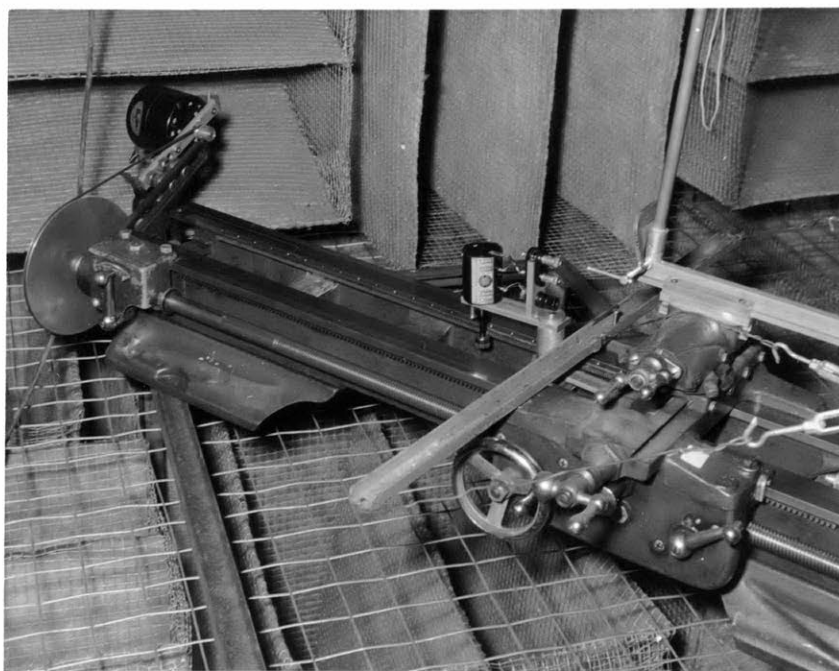


Fig. 4.4 Detail of scanner showing potentiometer.

will be independent of the movement of the scanner.

The scheme described above has several advantages. The voltage output of the microphone will be approximately constant allowing for close examination of any changes. A large dynamic range is not necessary in the measuring equipment. The information about the separation of source and receiver is automatically taken into account, thereby reducing the amount of data necessary. Finally, it is possible to include an adjustable resistor in series with the potentiometer to provide a means for positioning at will the effective acoustic center of the scanner.

#### 4.23 Acoustic Center Measurements

The procedure for making measurements of the acoustic center of a transducer consisted of adjusting the series resistor on successive scans until the curve with the least deviation from a straight line was obtained. The series resistor was calibrated in terms of the number of centimeters between the acoustic center and some arbitrary reference.

Two typical scans are shown in Fig. 4.5. The first was taken at 2 kc and shows clearly the limit of the far field at slightly under 5 cm from the beginning of the scan. At large separations the effects of reflections from the wall of the chamber begin to manifest themselves as standing waves.



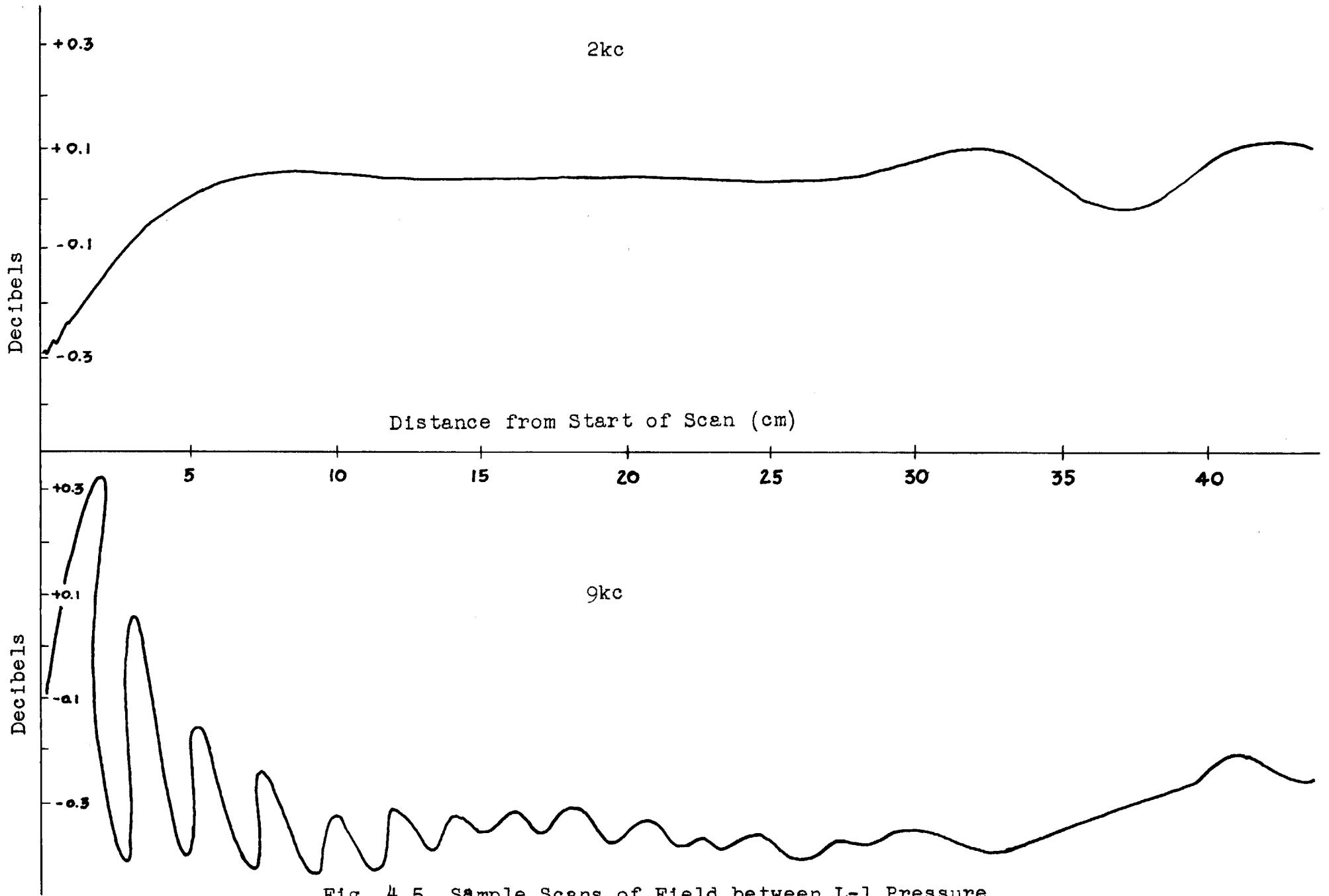


Fig. 4.5 Sample Scans of Field between L-1 Pressure Unit and 640-AA

Note that the vertical scale is quite expanded. The amplitude of the standing waves shown is only about 0.1 db. This large scale was obtained by means of a differencing circuit. The output of the wave analyzer was rectified and compared with a d-c reference voltage. The difference voltage was connected to an Esterline-Angus recording milliammeter and the scans shown in Fig. 4.5 are full size tracings from the original data.

Because of the high sensitivity of the system, great care had to be exercised in order to avoid erroneous readings as a result of amplifier drift. In general, any suspected recording was rerun until several similar plots were obtained. Recordings had to be taken during periods when the line voltage was stable.

The second scan of Fig. 4.5 illustrates the effect of multiple reflections between source and receiver. In this case the L-1 pressure unit and a 640-AA were used. The flat face of the 640-AA evidently served as an ideal reflector at the fairly high frequency of this scan. Other more complicated reflections occur after about 35 cm. These may be caused by the scanning apparatus itself.

In spite of a certain amount of trouble at a few frequencies caused by reflections from the scanner, the scheme was much more satisfactory than others that were tried. Point-by-point measurements were taken with extreme care and perseverance every centimeter for a distance of

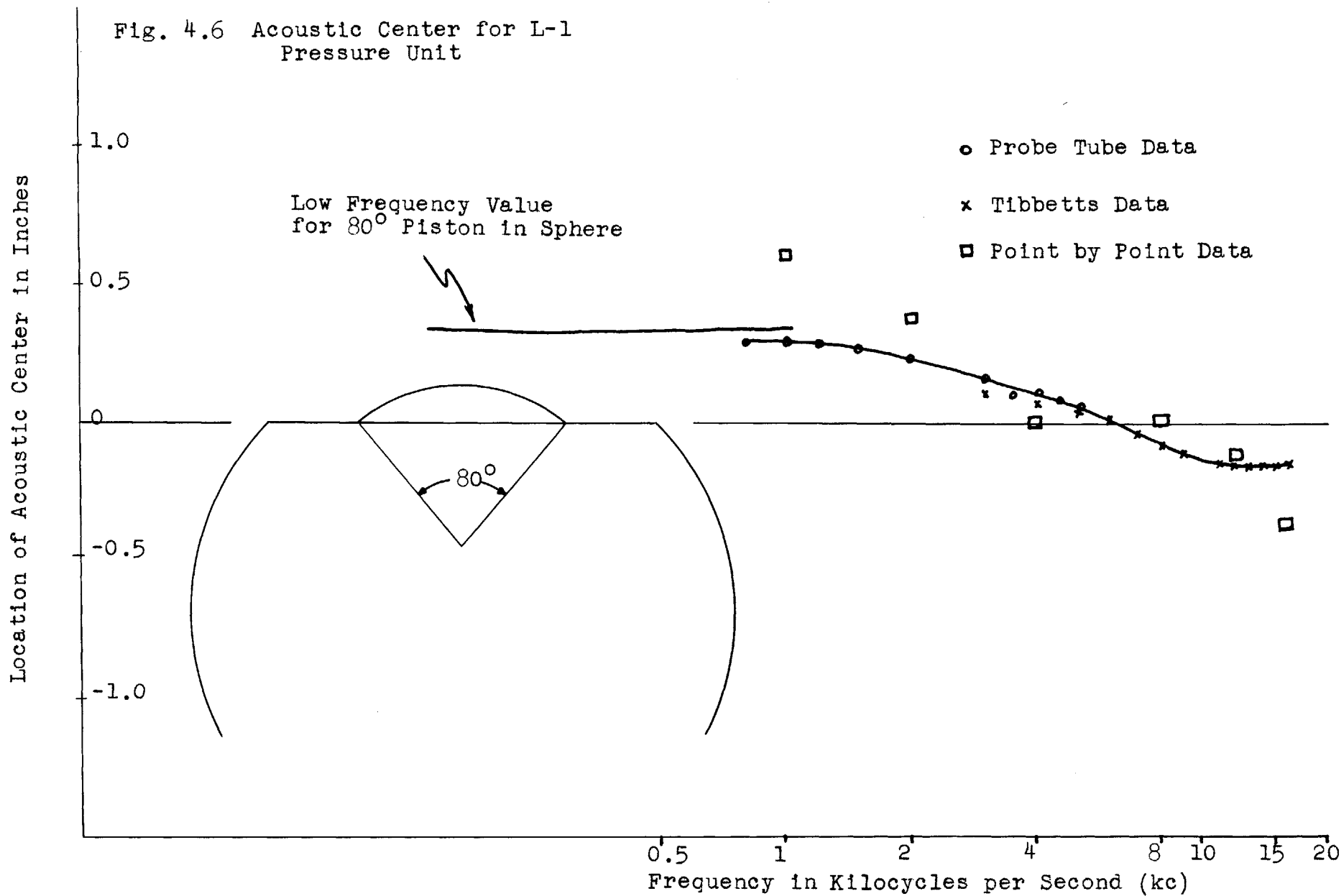
80 centimeters and at five frequencies. From these data it was difficult to guess the acoustic center within a quarter of an inch. The results of these measurements are shown for comparison in Fig. 4.6.

More data were taken on the L-1 unit because it was to serve as the source in the measurement of the centers of the other microphones tested. For the measurements shown in Fig. 4.6 microphones with known acoustic centers were used. At low frequencies a probe tube attached to a 640-AA was employed. However, about about 5 kc the attenuation of the probe became so great that noise and flanking were insurmountable problems.

A Tibbets Rochelle salt Diabow unit was used for measurements from 3 kc up to 16 kc. This unit is about 1/4-inch square and 1/16-inch thick. Its sensitivity when attached to a double-shielded cathode follower input is about -70 db re 1 volt and 1 microbar. Because of the drop in the source sensitivity and the increase in the acoustic background noise, this unit could not be used with accuracy below 3 or 4 kc.

The Diabow unit was mounted on a long tube which acted as the second shield for the shielded wire running up the middle. Shielding problems were critical and trouble was actually experienced as a result of a standing wave between the acoustic and electrostatic field of the transducer.

Fig. 4.6 Acoustic Center for L-1 Pressure Unit



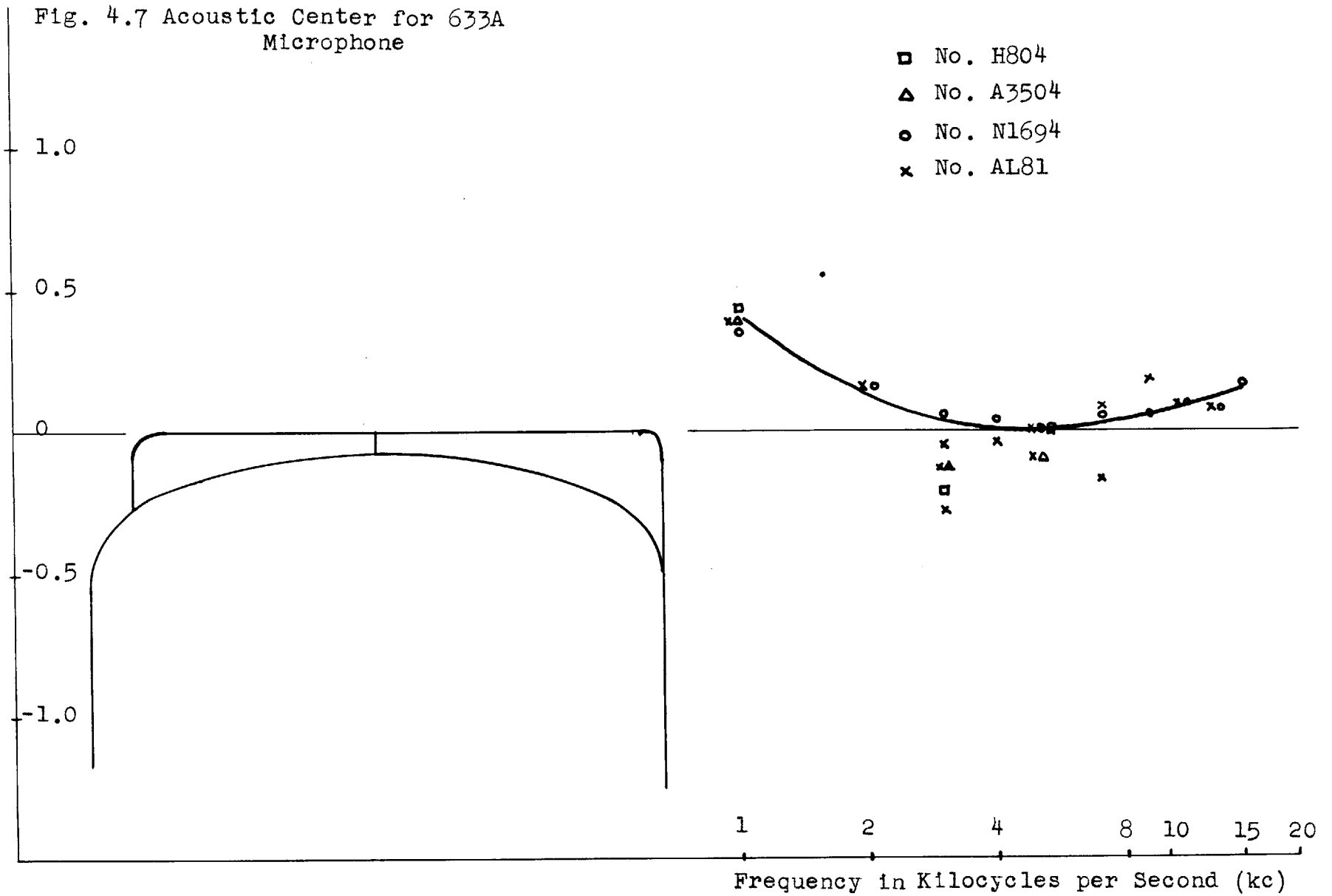
The vertical axis of the data and sketch of the L-1 unit are plotted double size in Fig. 4.6. The reference for the location of the acoustic center is as shown. The data are quite smooth, considering the scale to which they are plotted. In addition, they appear to follow in a general way the predicted curve for a piston in a sphere. The low frequency value is what one would expect for a piston in a sphere subtending an angle of  $80^\circ$  at the origin. The high frequency value is between that for a piston in a sphere and a plane source in an infinite baffle. These data were used as a correction to all the subsequent data taken on acoustic centers.

Figures 4.7 through 4.10 show similar data for the other microphones. The data for the 633-A microphones show an appreciable spread in the region between 3 and 8 kc. This may be explained by the fact that the far field recedes in this frequency range. Perhaps the near field is rather complicated in this range and was included incorrectly in the scans determining the acoustic center.

The 21 series of condenser microphones has the least change in acoustic center as a function of frequency. As one would expect, the addition of the holes moves the acoustic center forward. The accuracy of the data for these three microphones as well as that for the others is dependent on frequency. At high frequencies because of a number of measurement difficulties, the error may be as

Fig. 4.7 Acoustic Center for 633A  
Microphone

Location of Acoustic Center in Inches



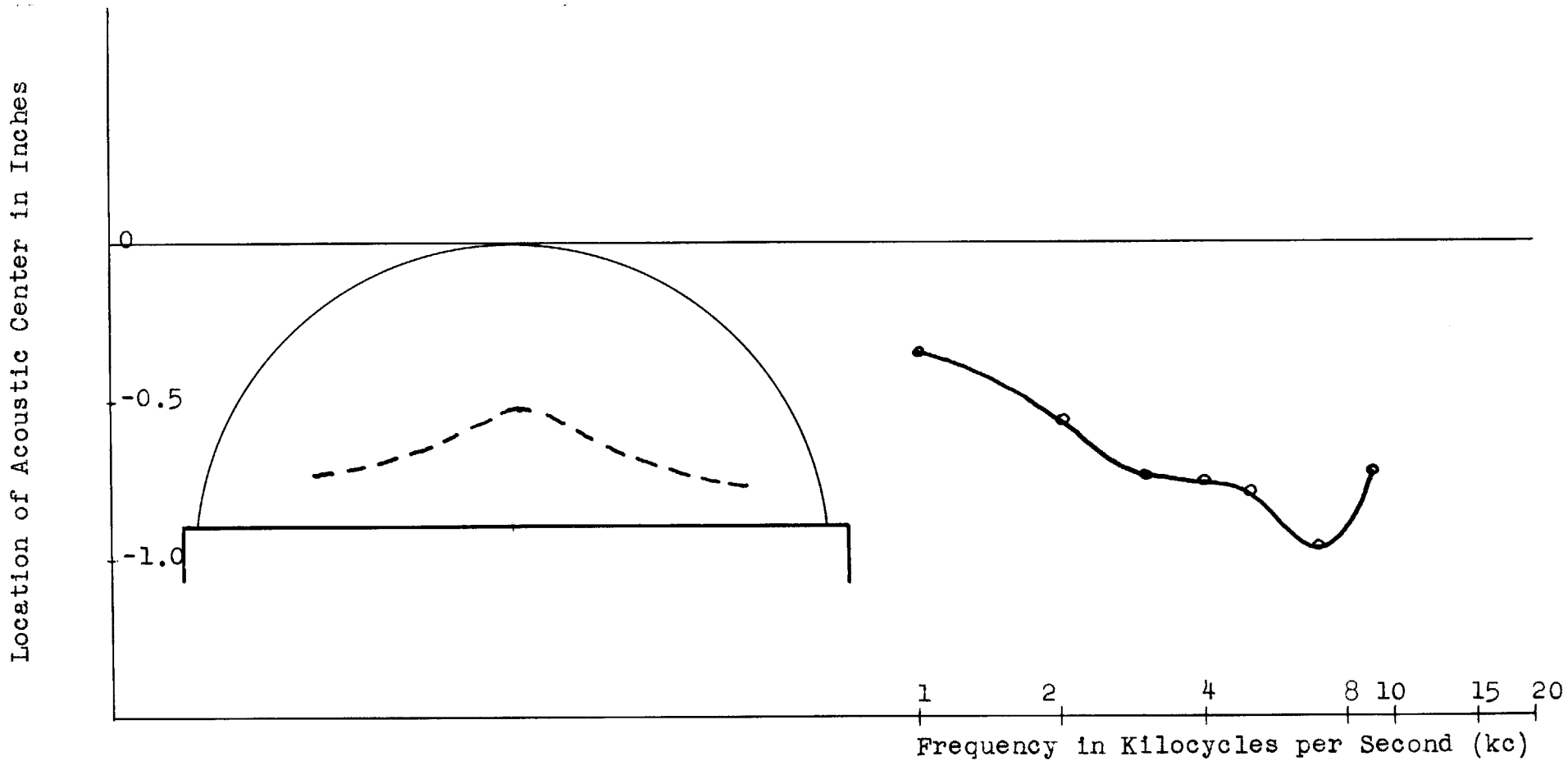


Fig. 4.8 Acoustic Center for 9898 Crystal Microphone

Fig. 4.9 Acoustic Center for 640-AA  
Microphone

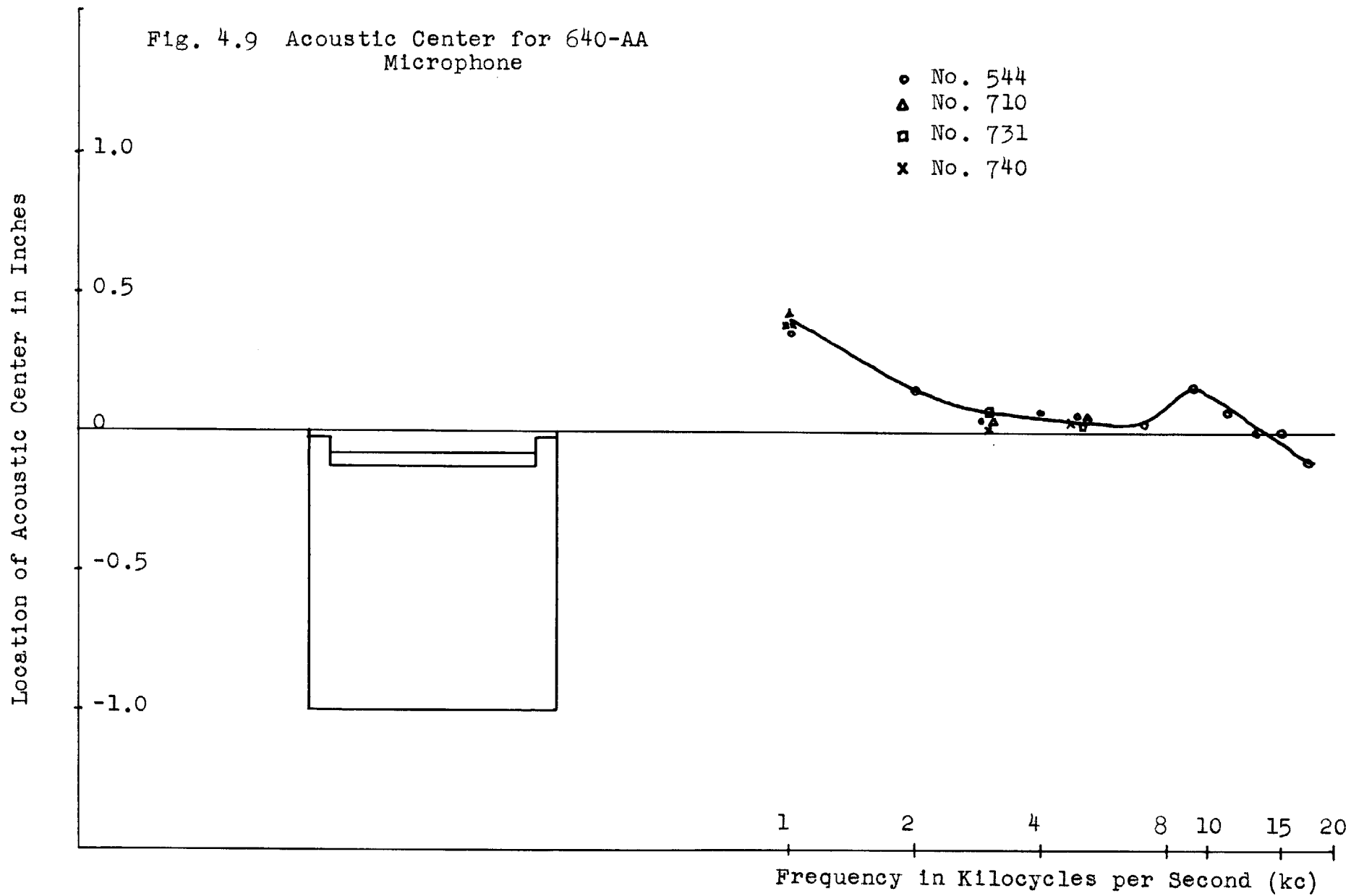
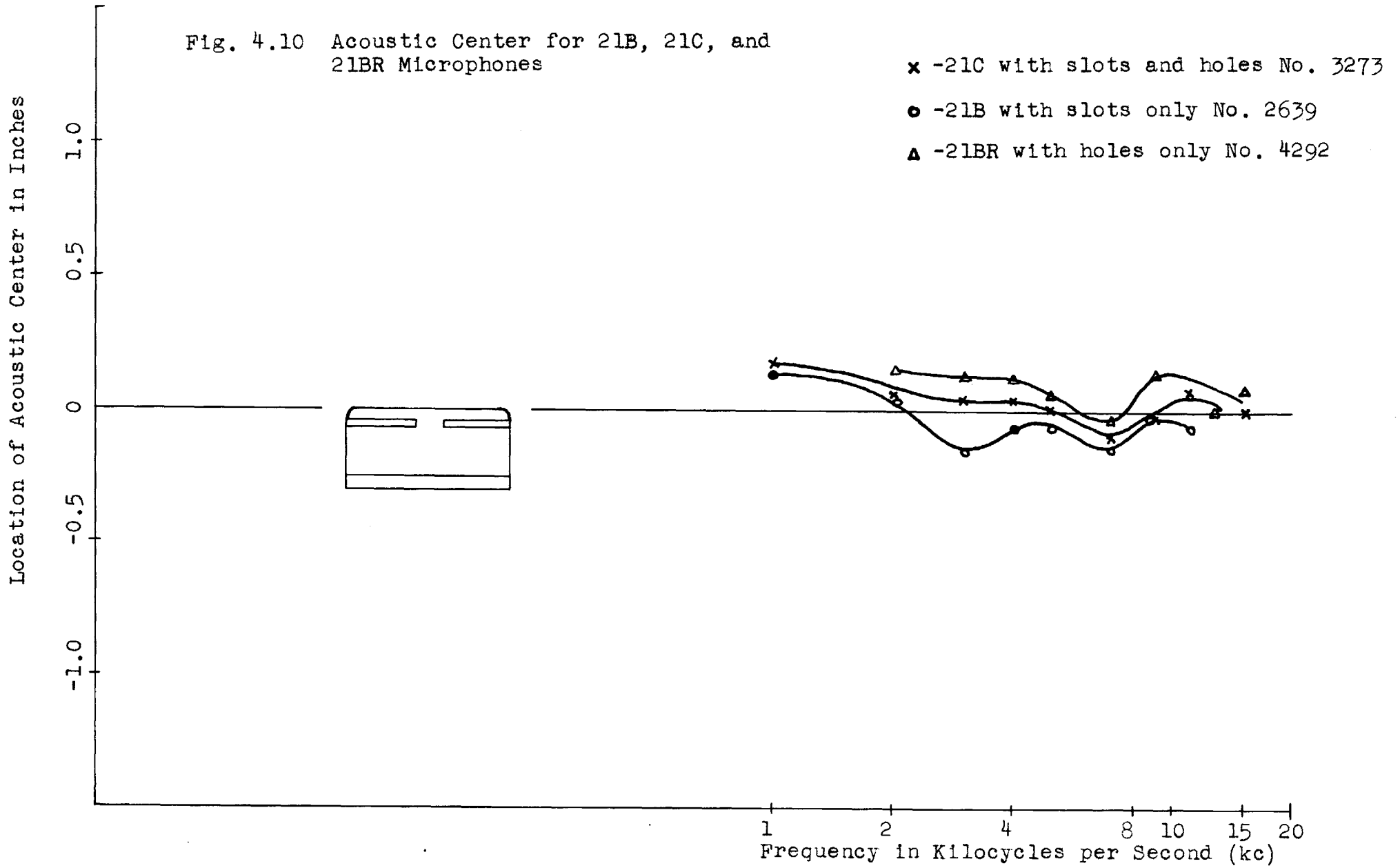




Fig. 4.10 Acoustic Center for 21B, 21C, and 21BR Microphones



large as 0.2 inch. In the remainder of the frequency range except for the 633-A measurements, the error should be less than 0.1 inch.

#### 4.24 Measurements of a Point Source on a Sphere

An experimental verification of the calibration theory set forth in (3.32) was carried out. This equation states that a reciprocity calibration may be carried out in the near field of one or both of the transducers, providing the deviation of the field from that of a simple source is accurately known. In Section 3.42 the near field of a point source on a sphere was calculated. These curves can be utilized in a reciprocity calibration if the second transducer approximates a point receiver and does not cause multiple reflections between the source and the receiver.

An experimental setup that meets these specifications is shown in Fig. 4.11. The sphere is a hollow copper float. The point source on the sphere is approximated by a 633-A microphone mounted flush with the surface of the sphere. The point receiver is a 640-AA microphone with a double-shielded extension cable between it and the preamplifier.

The sphere is 18 cm in diameter and its circumference equals a wavelength ( $kr_1 = 1$ ) at about 600 cps. The sphere is filled with glass wool to prevent resonances caused by sound that leaks into the interior.

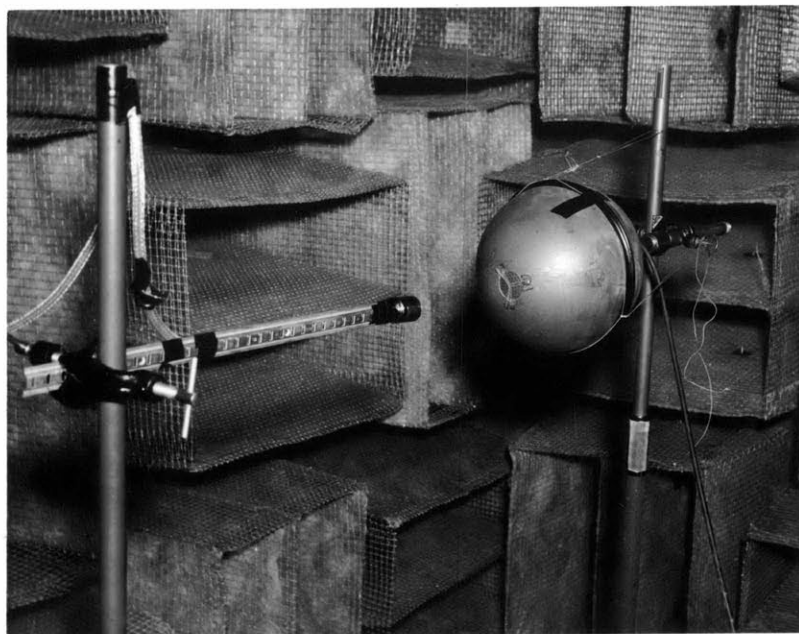


Fig. 4.11 Apparatus for the measurement of the field of a point source on a hard sphere.

Measurements of the field were made in the anechoic chamber from 200 to 1000 cps. A typical plot of these data is shown in Fig. 4.12. The measured points fall on the theoretical curve within 0.1 db from  $2.5r_1$  to  $8r_1$  from the center of the sphere. Therefore, the source proved to be an extremely satisfactory approximation to a point source on a hard sphere. However, at frequencies above 500 cps the first two points begin to depart from the theoretical curve slightly.

Additional measurements were taken with the source and receiver set up in the anechoic chamber control room. These data show that the reflections from the walls of the room begin to be important at greater than  $3r_1$ . Measurements taken closer to the source yielded data that were used in a reciprocity calibration of the 640-AA. The resultant response was within a few tenths of a decibel of the actual calibration.

Of course the reciprocity measurement in the anechoic chamber control room was only part of the complete calibration. It was still necessary to perform a comparison calibration of the 640-AA and the sphere. This was done in the anechoic chamber, but could have been carried out in a moderately dead room for frequencies below 1000 cps. The method for this measurement will be discussed below.

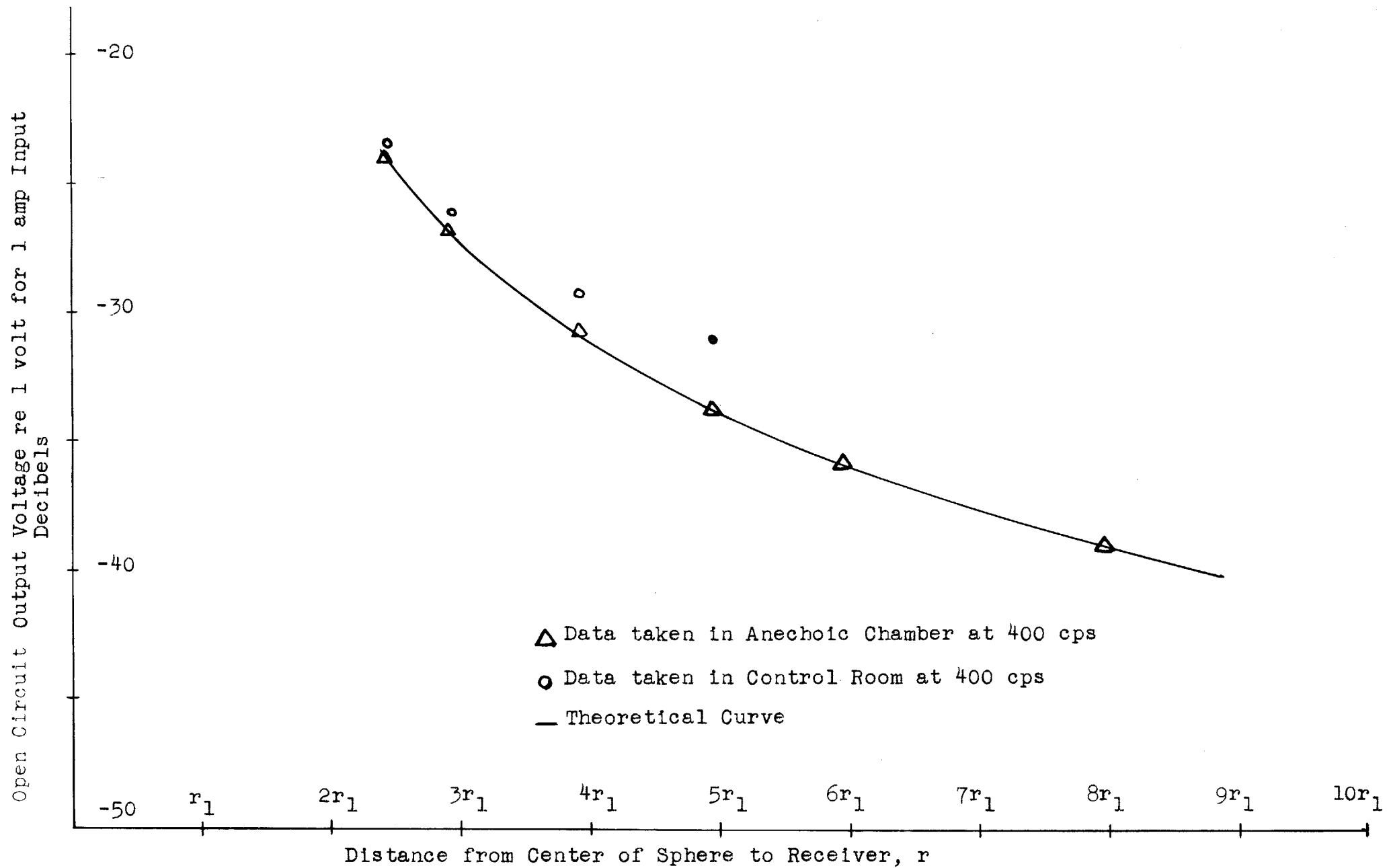


Fig. 4.12 Data on the Field in Front of a Point Source on the Surface of a Hard Sphere

#### 4.25 Directivity Measurements

Directivity gain patterns were automatically recorded at a number of frequencies for all seven types of transducers. The equipment used consists of a rotating boom and a synchronized polar level recorder. The source was placed on the boom and rotated around the microphone at a distance of about 40 cm. This distance was chosen so that reflections from the walls would not be important and yet the spacing would not be so close that the exact position of the center of rotation would be critical.

The data have been traced directly onto Figs. 4.13 through 4.28. To save space only half the plot has been shown in most cases. Fig. 4.17 is an exception which compares the two halves of the directivity gain pattern of a 633-A. At this frequency there is apparently a fairly serious assymetry in this microphone. Other microphones (the 640-AA, for example) do not show any assymetry, thus ruling out the possibility that the difference shown in Fig. 4.17 might be caused by reflections from the walls.

A special plot of the variation in response of the 9898 in the equitorial plane is shown in Fig. 4.20. Since the microphone apparently has axial symmetry, it is rather surprising that variations of the order of 20 db are observed at 8 and 10 kc. These data emphasize the futility of making one calibration at grazing incidence for such

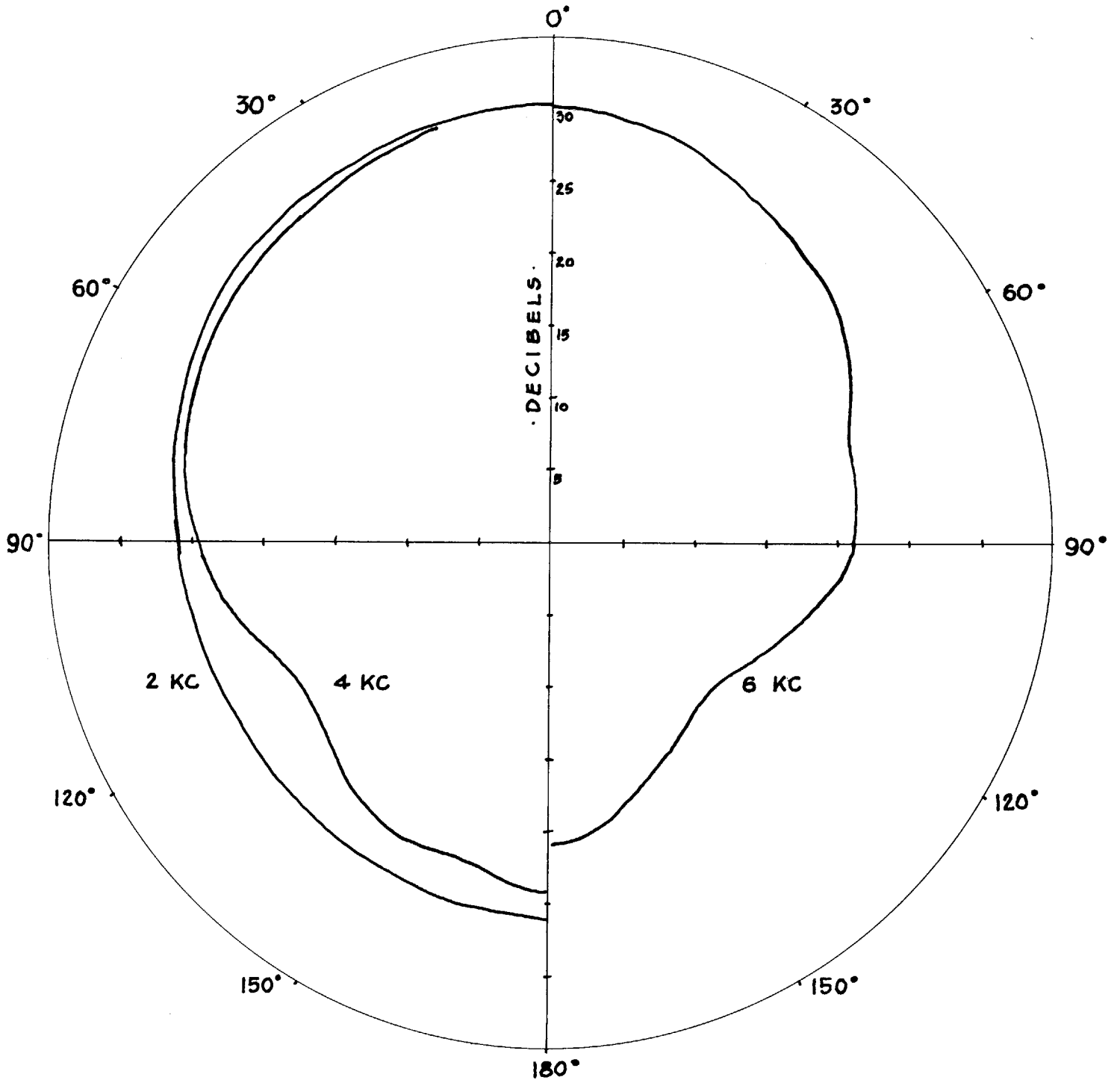


Fig. 4.13 Directivity Gain Patterns of L-1 Pressure Unit

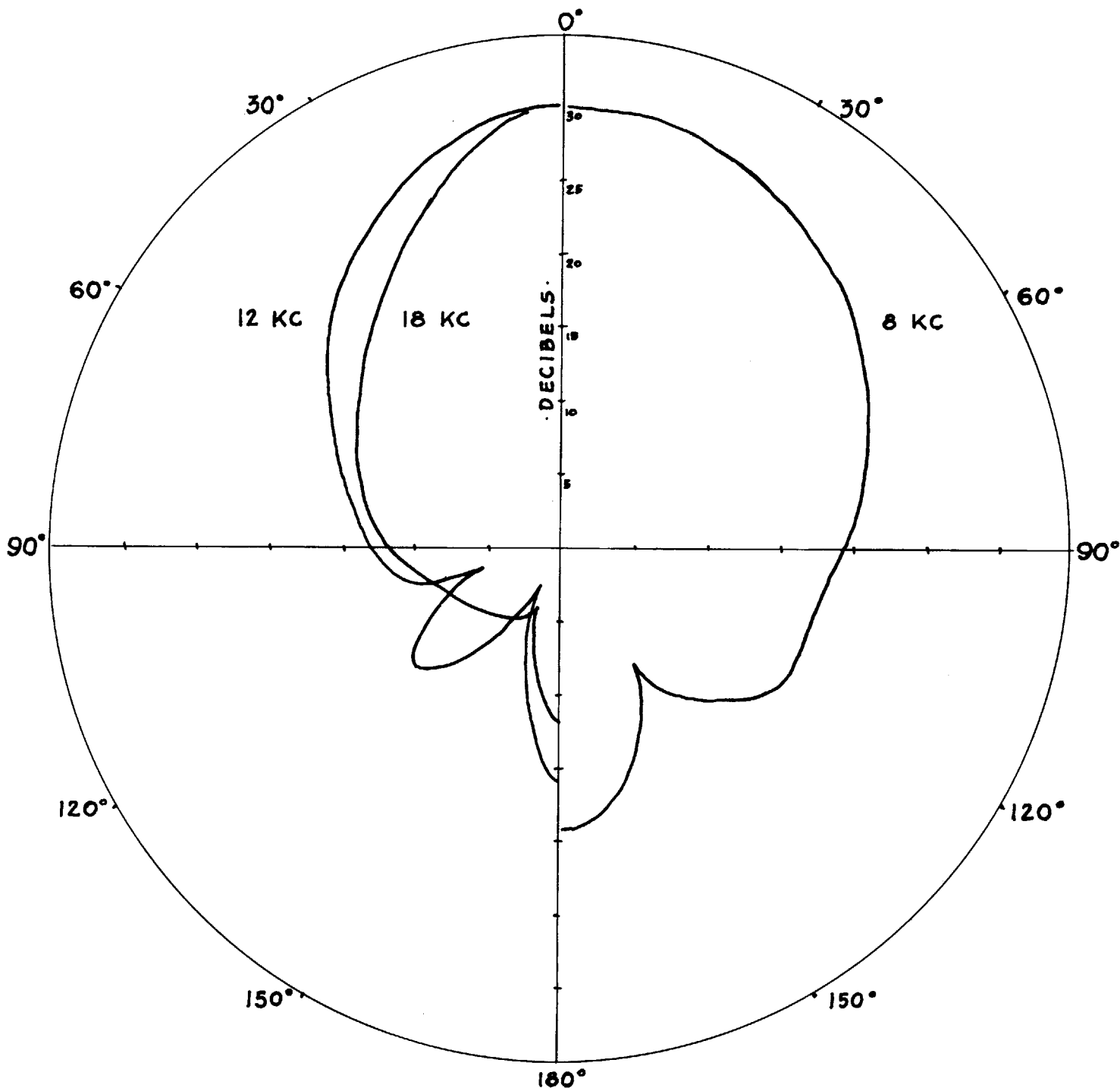


Fig. 4.14 Directivity Gain Patterns of L-1 Pressure Unit



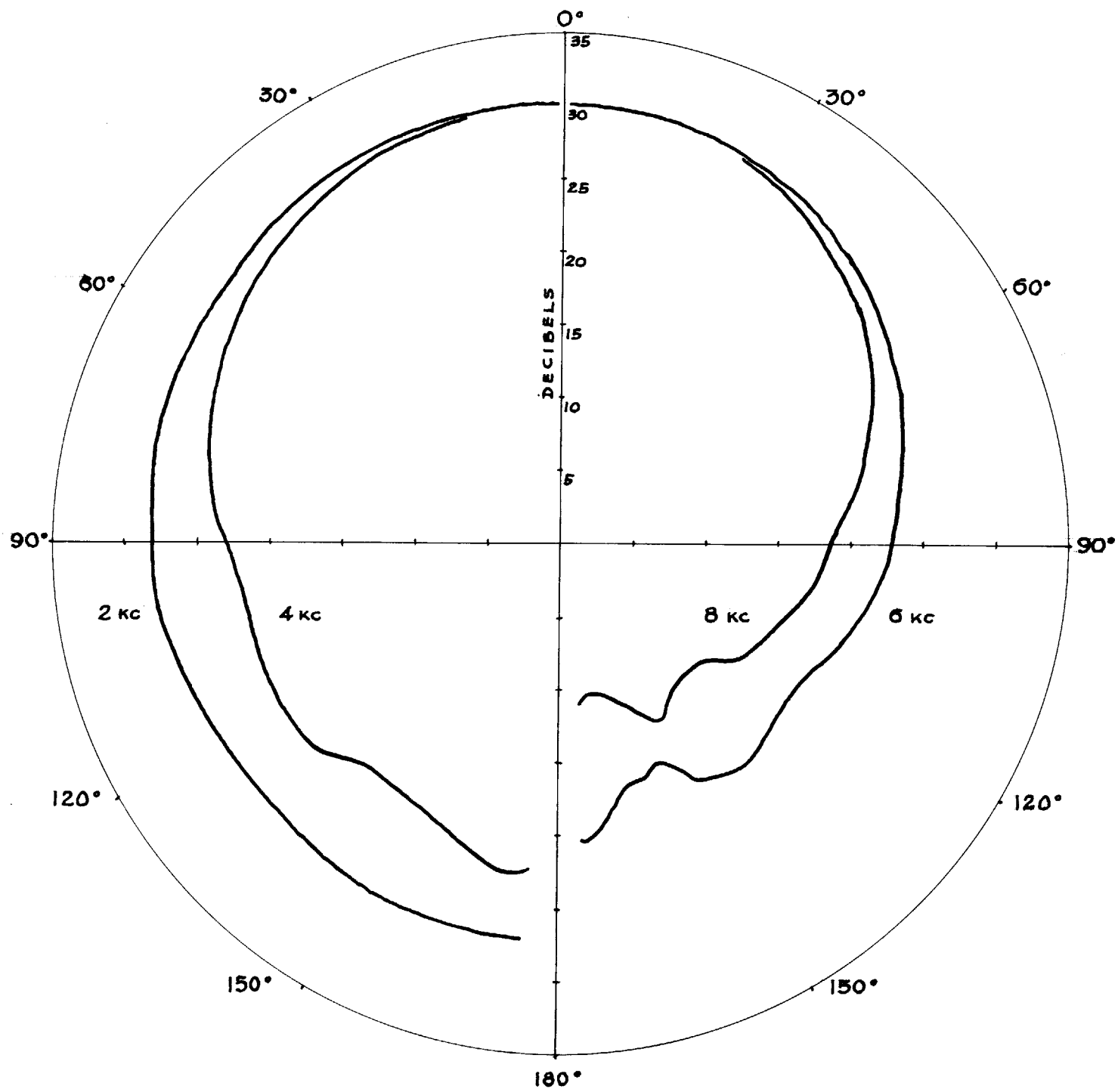


Fig. 4.15 Directivity Gain Patterns of 633-A Microphone

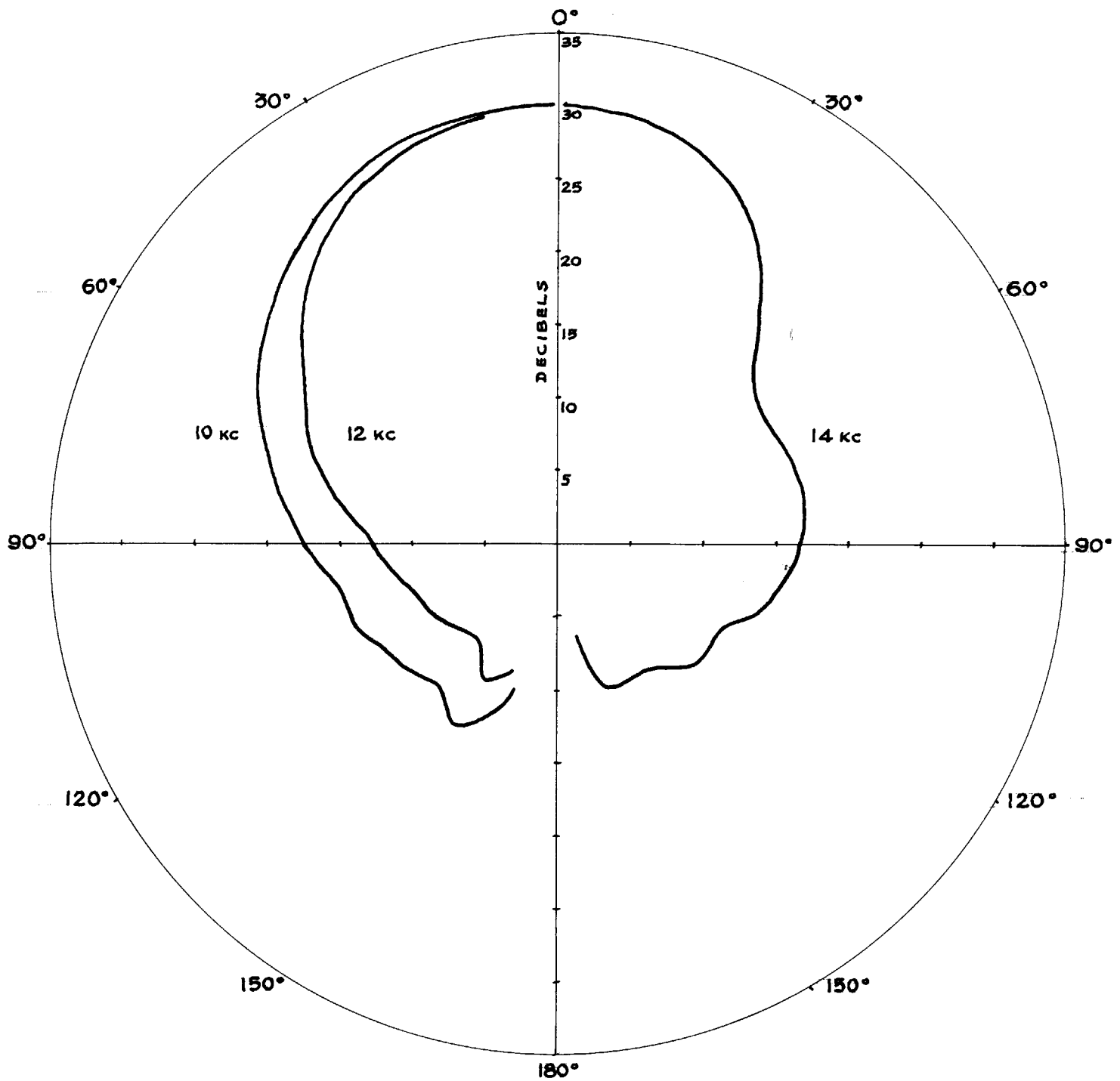


Fig. 4.16 Directivity Gain Patterns of 633-A Microphone

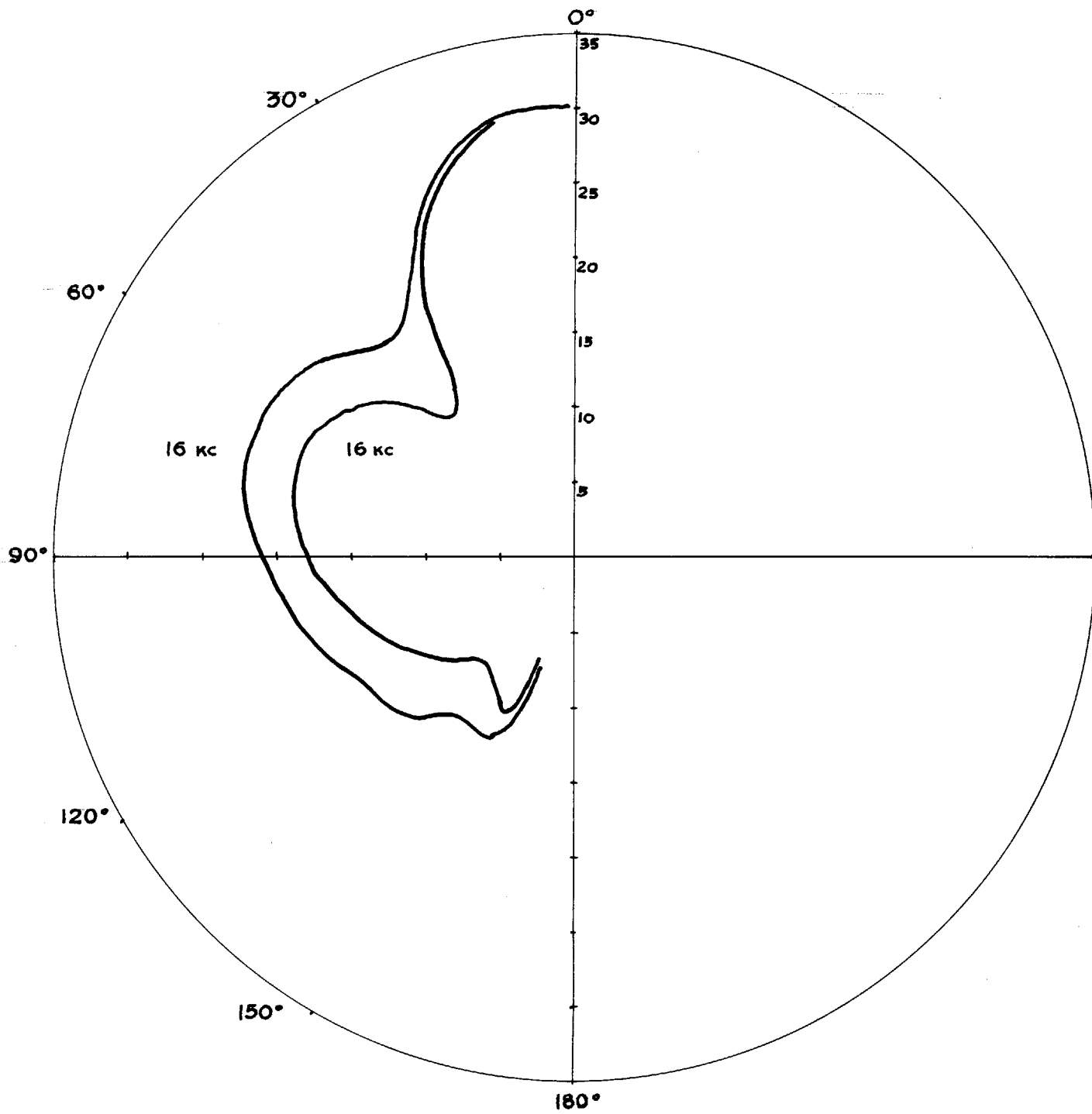


Fig. 4.17 Directivity Gain Patterns of 633-A Microphone

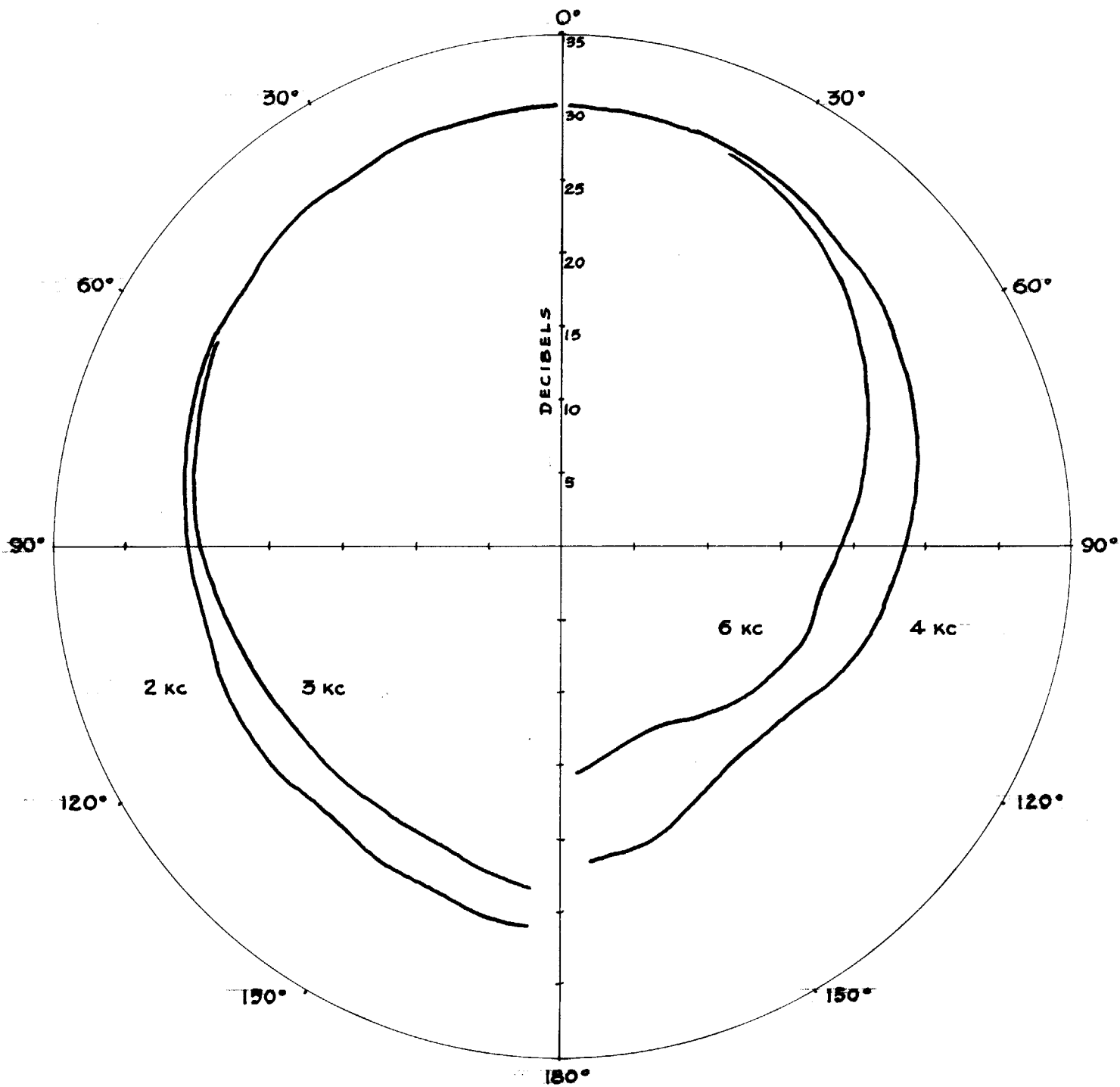


Fig. 4.18 Directivity Gain Patterns of 9898 Microphone

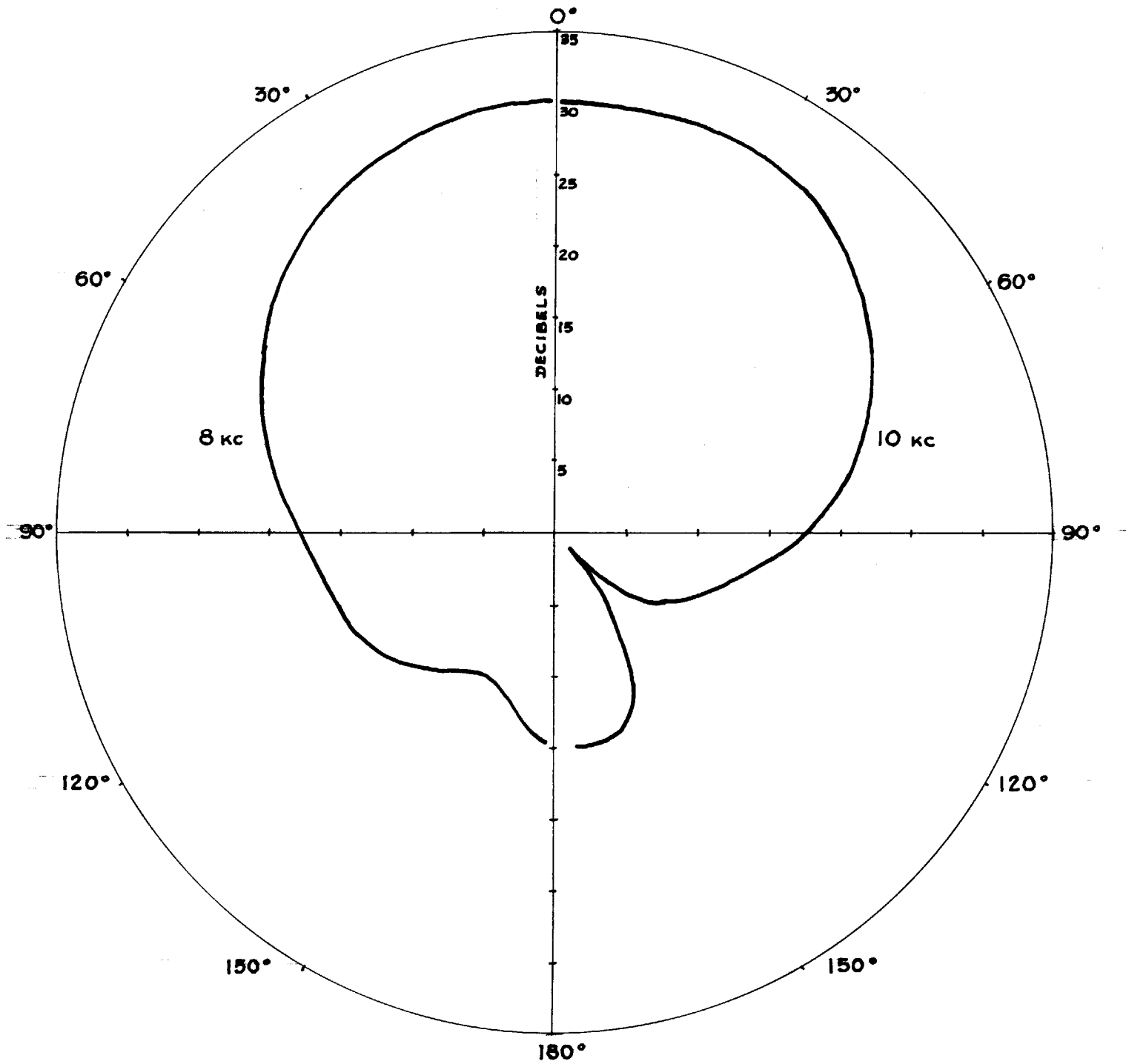


Fig. 4.19 Directivity Gain Patterns of 9898 Microphone

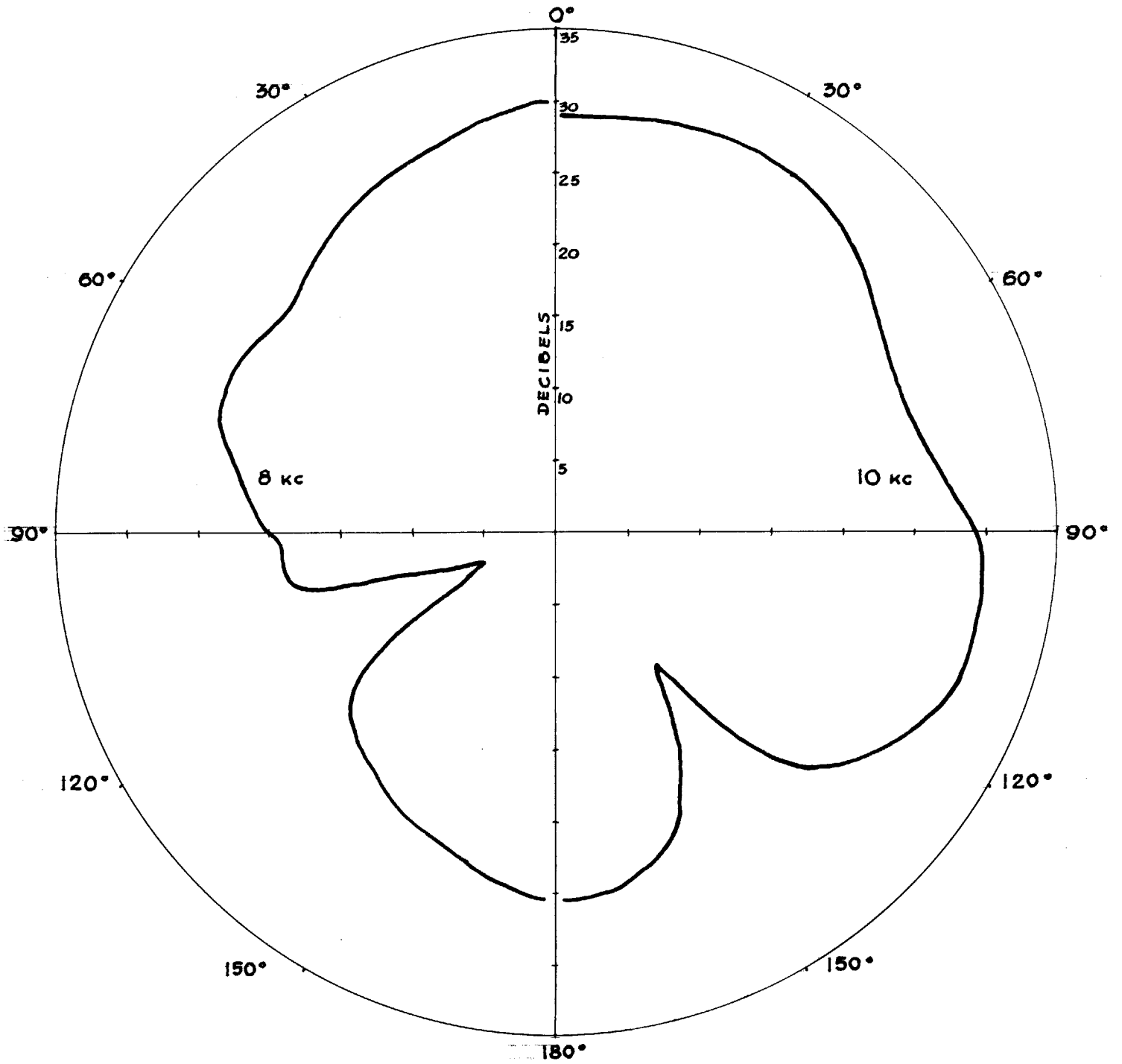


Fig. 4.20 Azimuth Directivity Gain Patterns of 9898 Microphone

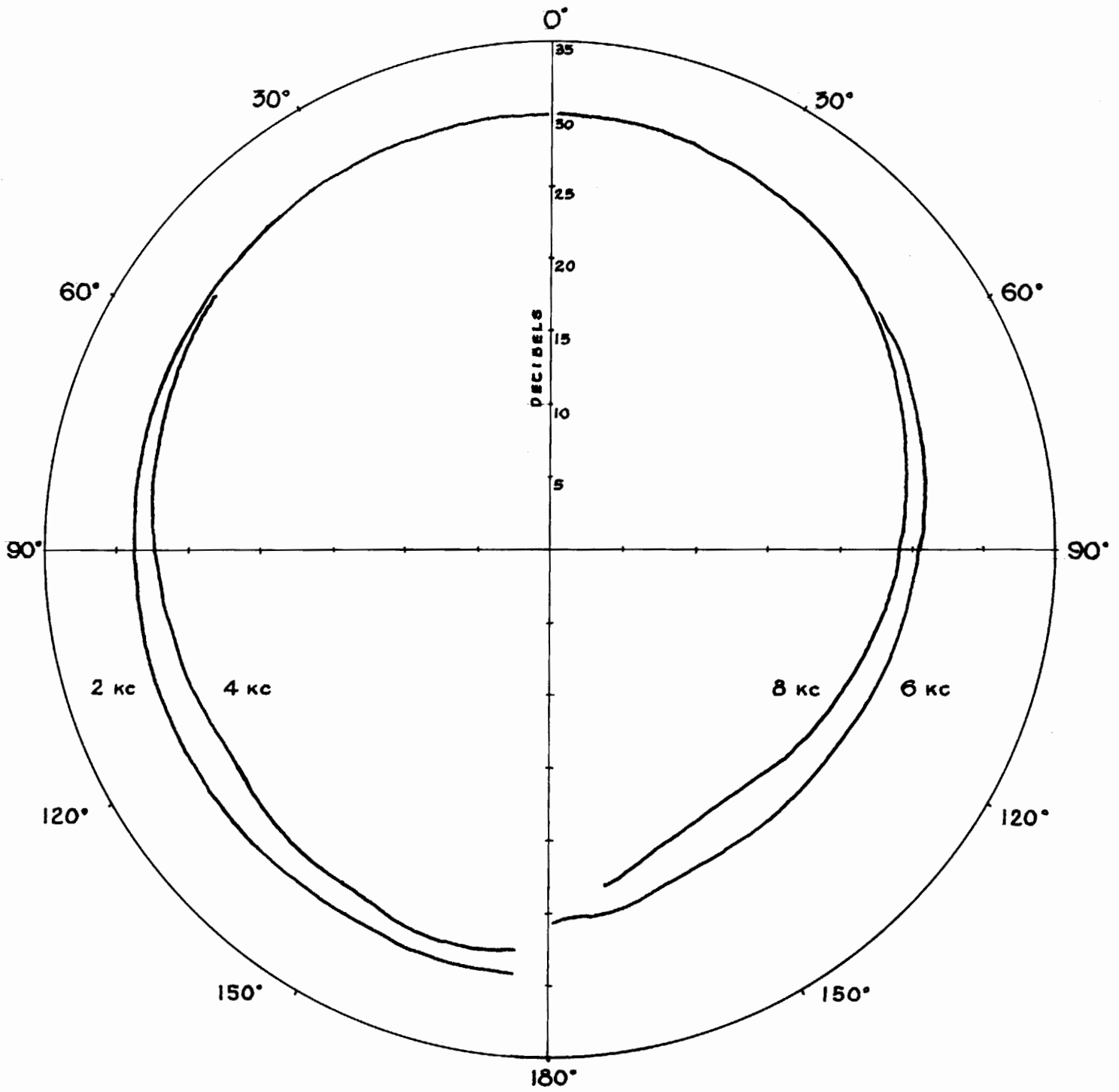


Fig. 4.21 Directivity Gain Patterns of 640-AA Microphone

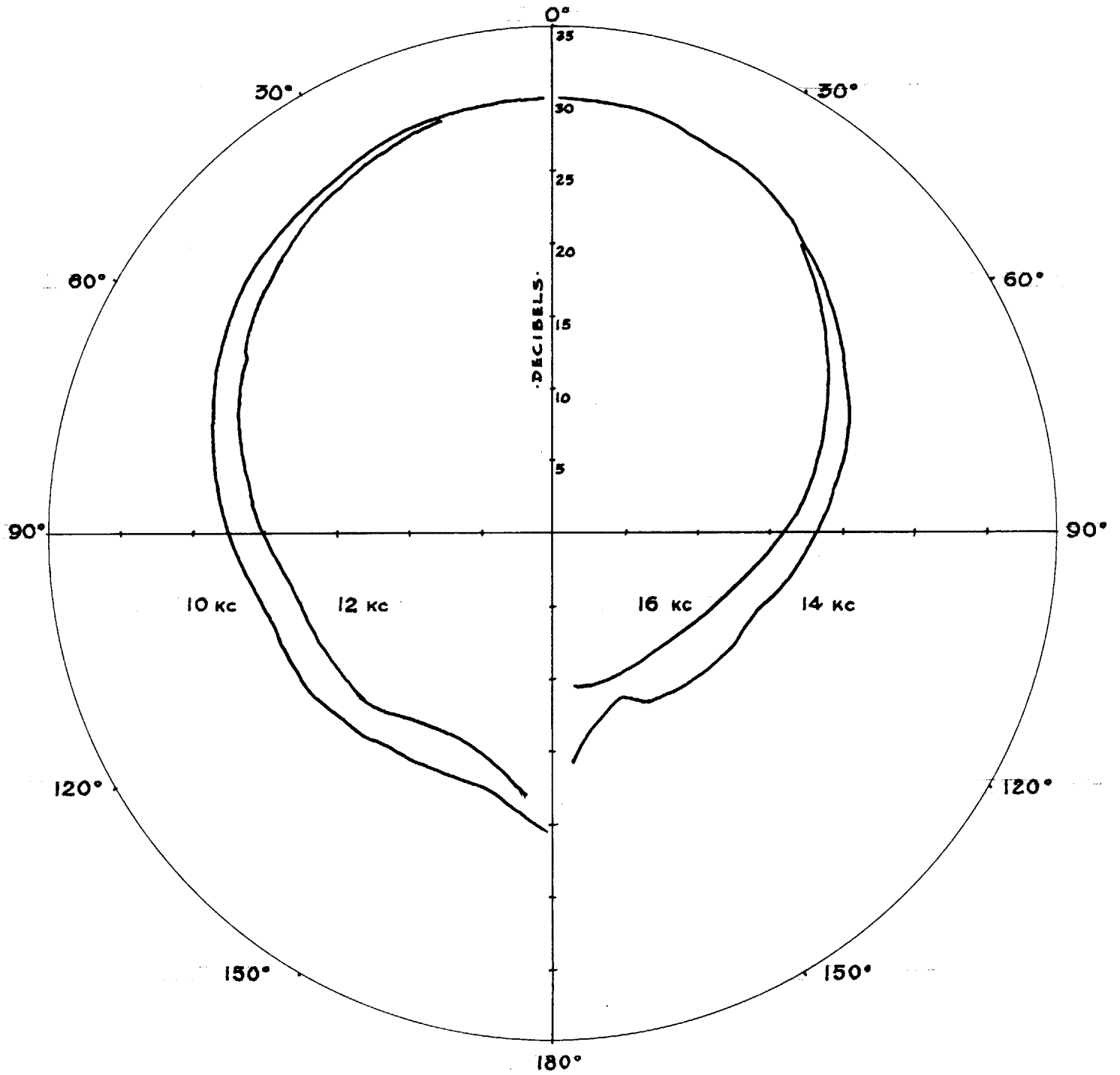


Fig. 4.22 Directivity Gain Patterns of 640-AA Microphone



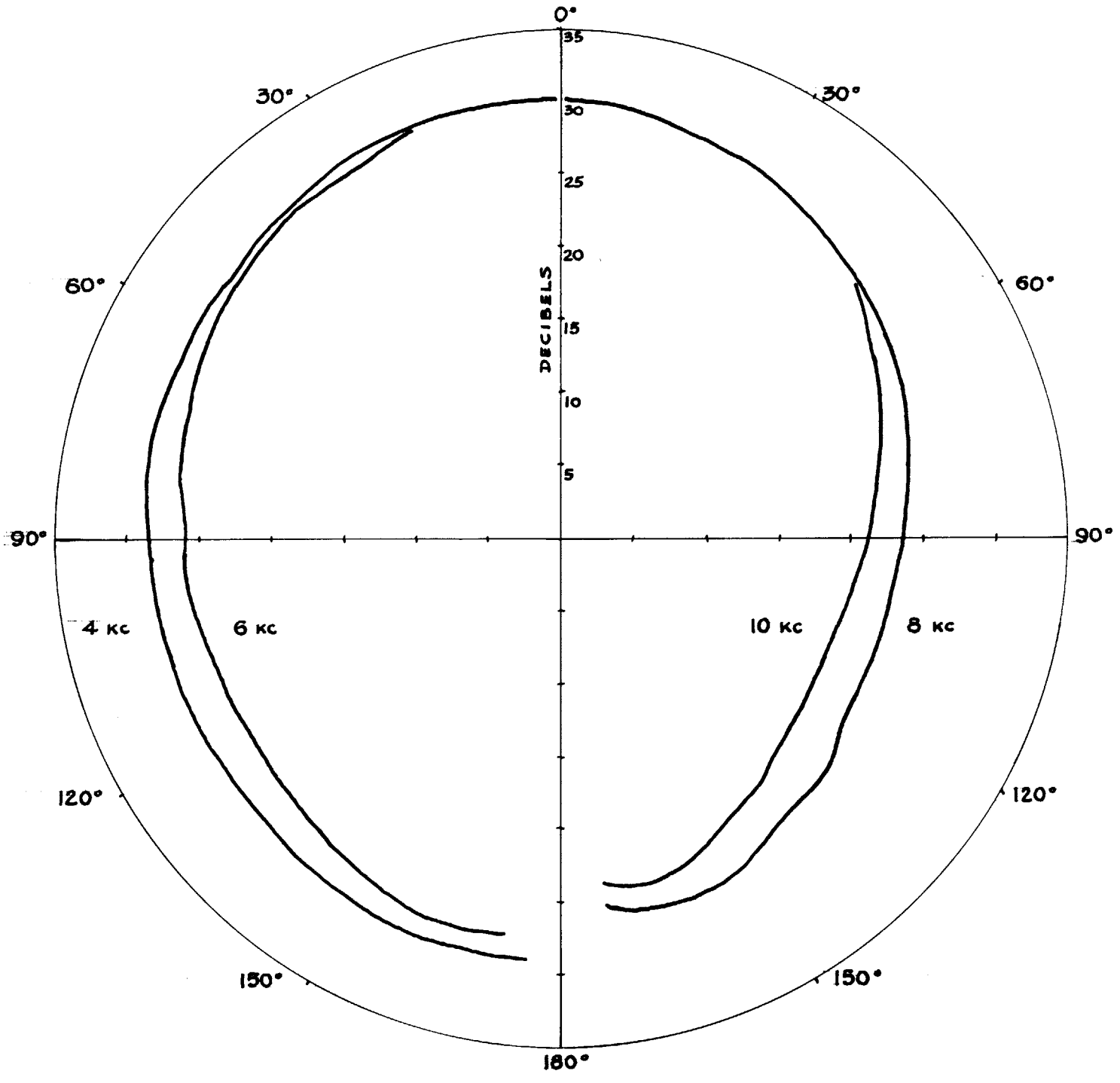


Fig. 4.23 Directivity Gain Patterns of 21-B Microphone

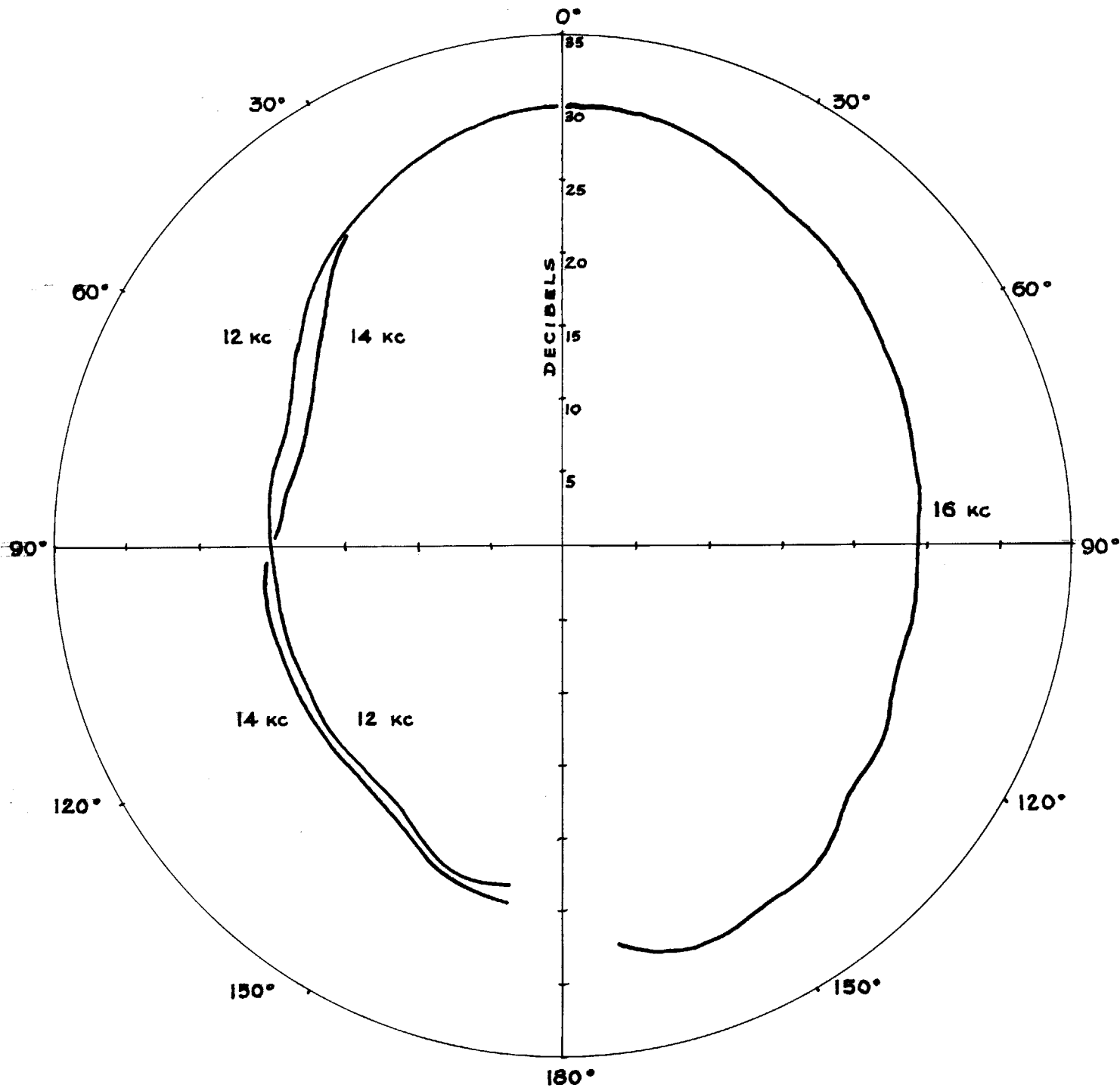


Fig. 4.24 Directivity Gain Patterns of 21-B Microphone

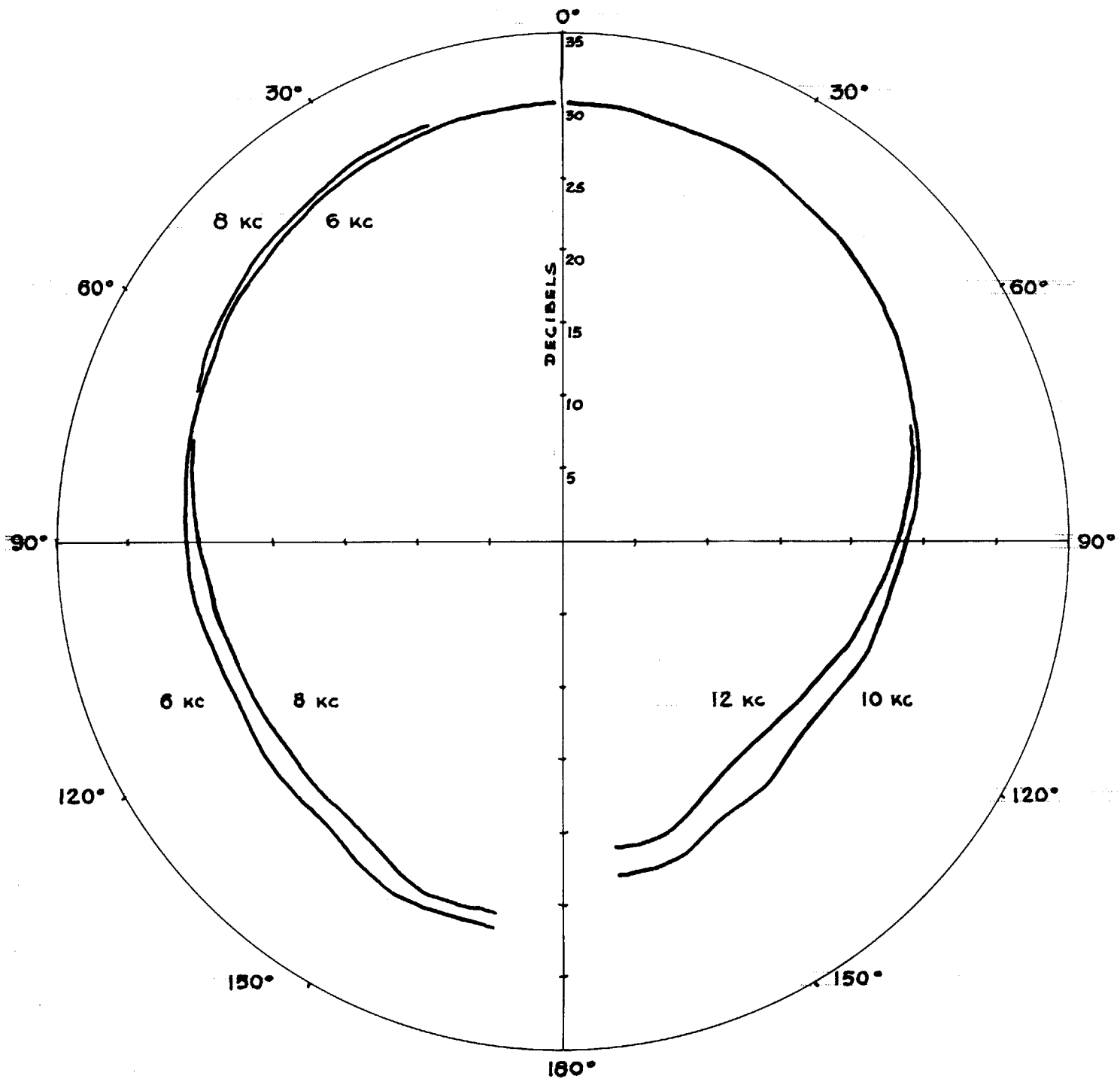


Fig. 4.25 Directivity Gain Patterns of 21-C Microphone

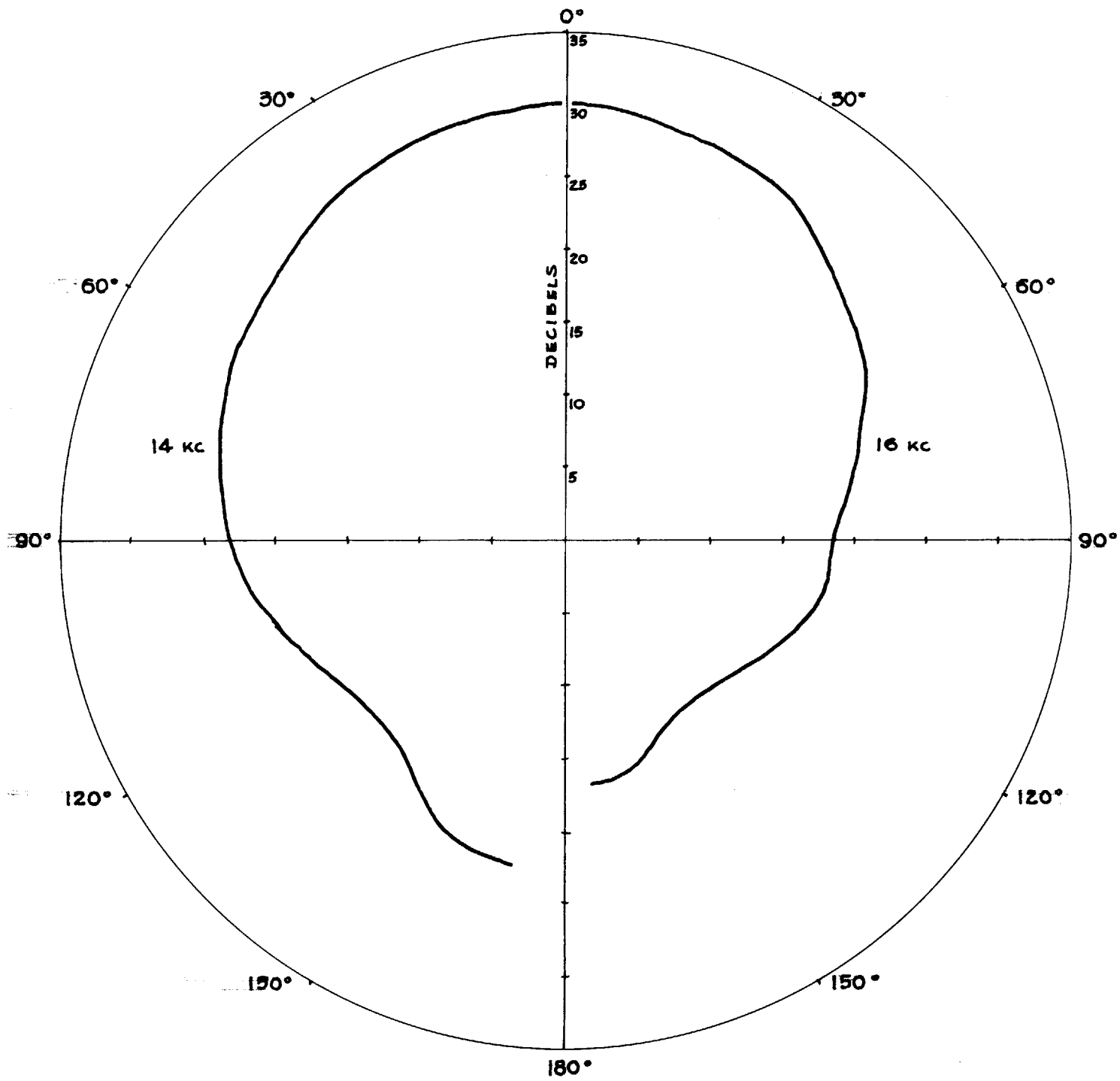


Fig. 4.26 Directivity Gain Patterns of 21-C Microphone

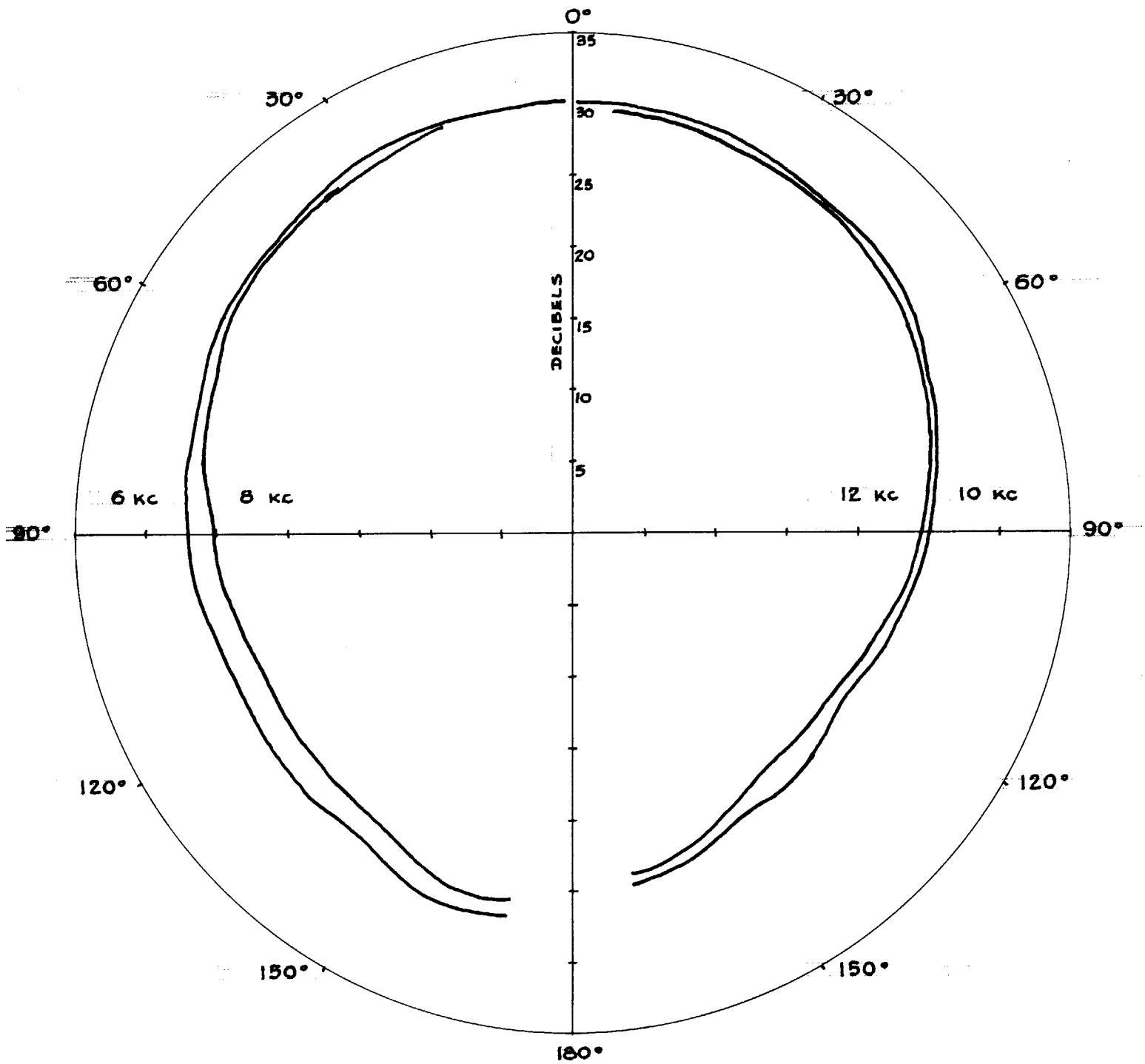


Fig. 4.27 Directivity Gain Patterns of 21-BR Microphone

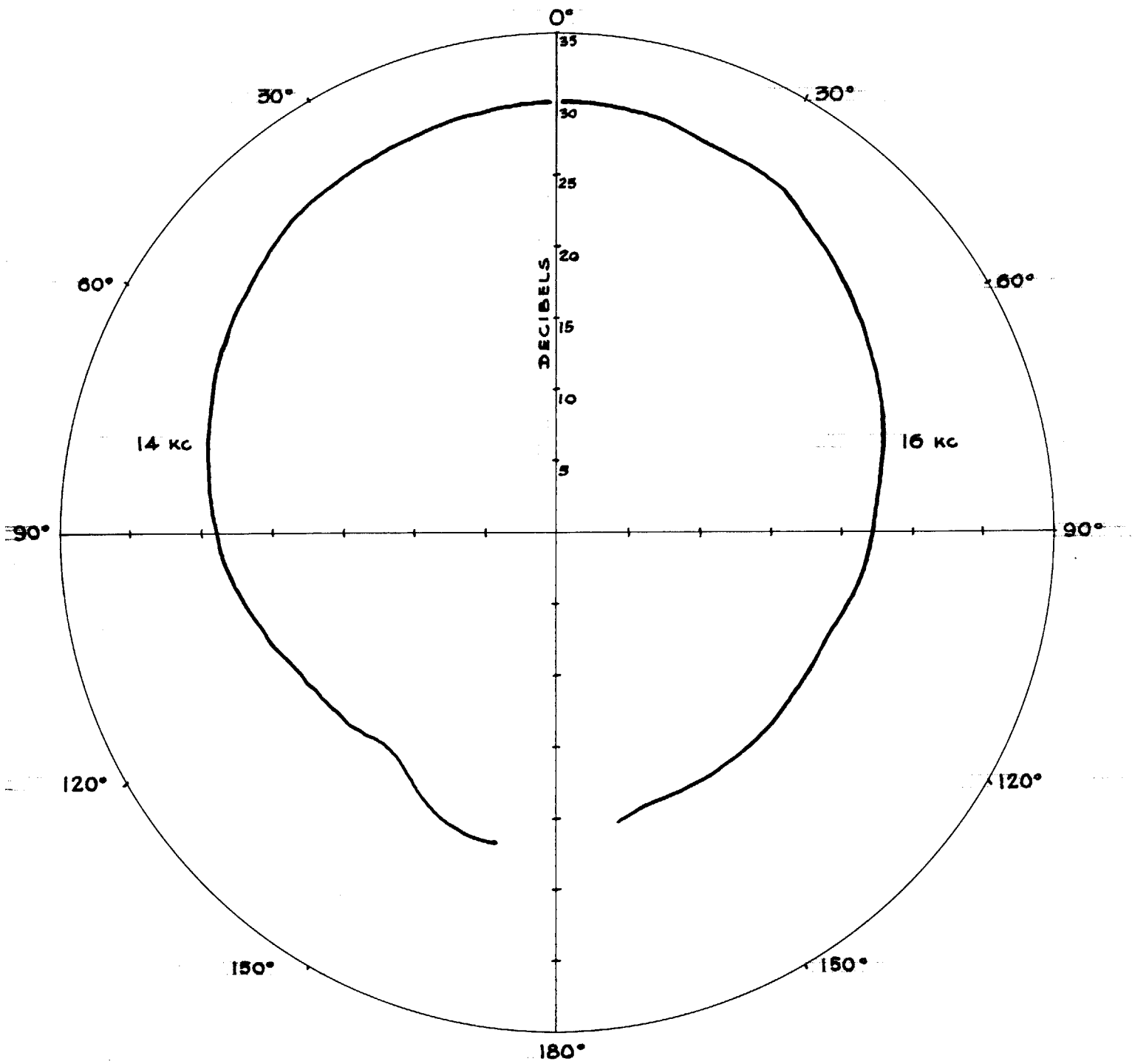


Fig. 4.28 Directivity Gain Patterns of 21-BR Microphone

a microphone. If one expects to find an average grazing response, azimuth directivity gain plots such as those in Fig. 4.20 must be run at all the higher frequencies.

The accuracy of these directivity gain patterns will be greatest for situations where the sensitivity is highest. When the source is positioned at angles of  $90^\circ$  and greater with respect to the axis of the microphone, sound energy reflected from the wall of the chamber may arrive at the microphone in the normal direction. The output voltage caused by the reflected wave may be comparable to that caused by the direct wave, and hence the rear two quadrants of the pattern may be in error by several decibels at high frequencies. The portions of the patterns that are on the major lobe should be accurate to about one decibel, the practical limit of the recorder.

#### 4.26 Calculation of the Limit of the Far Field

The graphical construction described in Section 3.25 was applied to the directivity gain patterns (Figs. 4.13-4.28). The results are plotted to show the minimum distance to which a point receiver may be brought without observing more than a 3 per cent deviation from the pressure radiated by a simple source. This minimum distance for the L-1 unit is shown in Fig. 4.29a. Also shown in this figure are the equivalent distances taken directly from the scanner data. The prediction by means of the

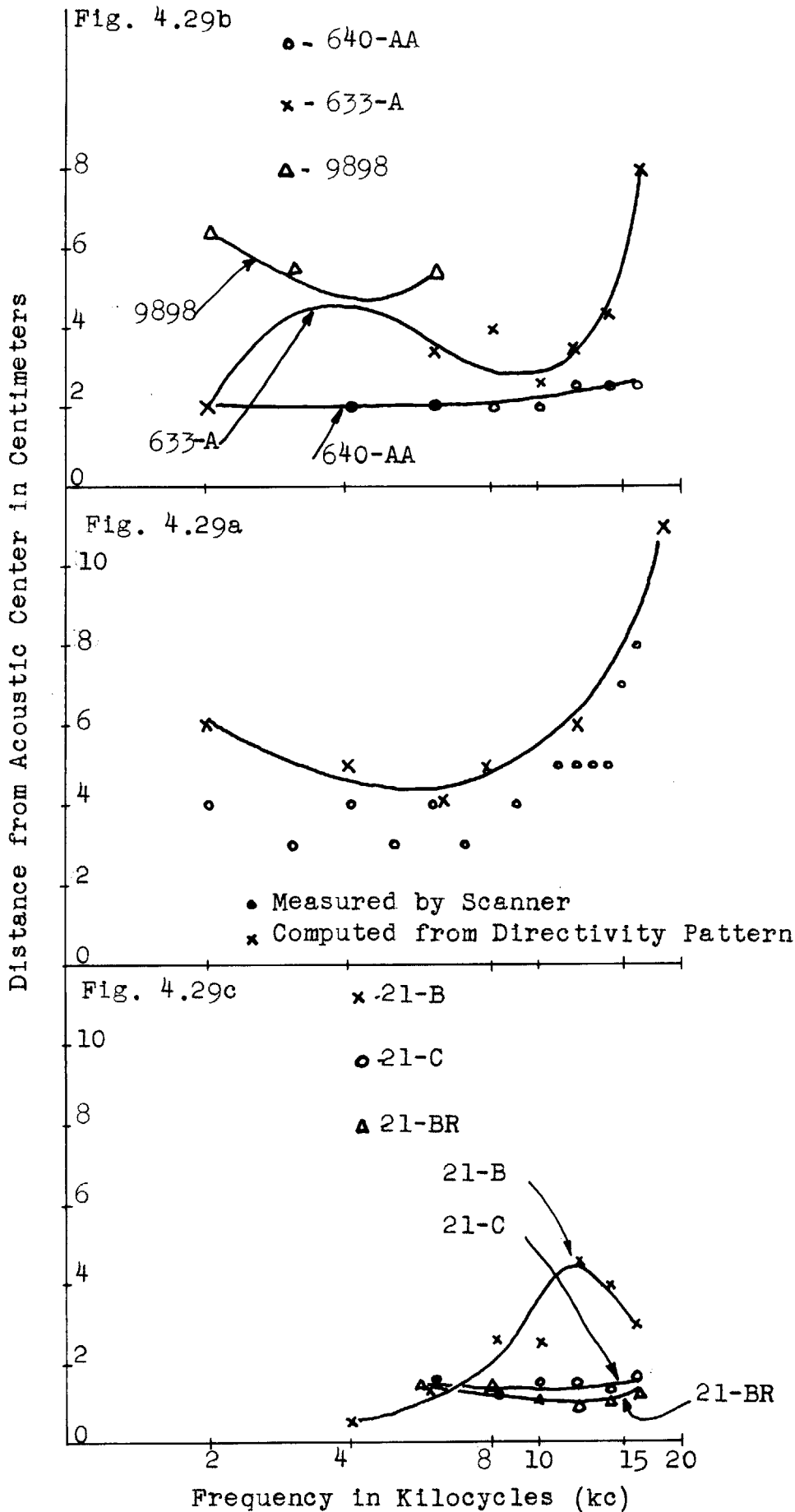


Fig. 4.29 Distance at which the Field of Several Microphones Departs by 3% from the Field of a Simple Source



graphical construction seems to give a good indication of the actual field, and, if anything, the estimate is a little conservative. The scanner data are rather scattered because the point at which the pressure deviates by 3 per cent apparently depends on higher order terms which are neglected in the graphical construction. The scanner plots rarely made a smooth turn away from the horizontal line.

The data for the other microphones (Figs. 4.29b and c) indicate that the condenser microphones have the smallest near fields. The far field of the 21-B recedes around 12 kc as a result of the dipole action of the slots. This phenomenon is almost completely absent from the 21-C even though the slots have not been eliminated. Apparently the holes tend to shunt the volume velocity from the slots.

#### 4.3 Measurement Techniques

The data of the previous sections and the theory of Chapters II and III, together with additional information gained through experience enable us to delineate the physical limitations on the free-field calibration of microphones. Let us assume that a reciprocity calibration of a certain transducer is to be carried out over a specified frequency range and with a specified accuracy. The experimenter may ask:

- 1) Is the transducer to be calibrated reciprocal?
- 2) How closely can source and receiver be spaced?
- 3) What will be the error caused by reflections?
- 4) May pulse techniques be used to advantage?
- 5) Should the data be recorded point by point or automatically?
- 6) What errors may occur in the measurement of electrical quantities?
- 7) What factors should be considered in the selection of a sound source?

With the aid of the material in the foregoing plus a certain amount of practical experience, it is possible to give engineering answers to these questions.

#### 4.31 Linearity and Reciprocity

As shown in Chapter II, the transducers used in a reciprocity calibration will in general be reciprocal for incremental signals. In any case one can prove that they are reciprocal by making measurements of the electrical transfer impedance of a pair of transducers. Equality of these two transfer impedances for an arbitrary second transducer will be sufficient grounds for concluding that the first is reciprocal. It is wise to make the measurement with two completely different types of transducers

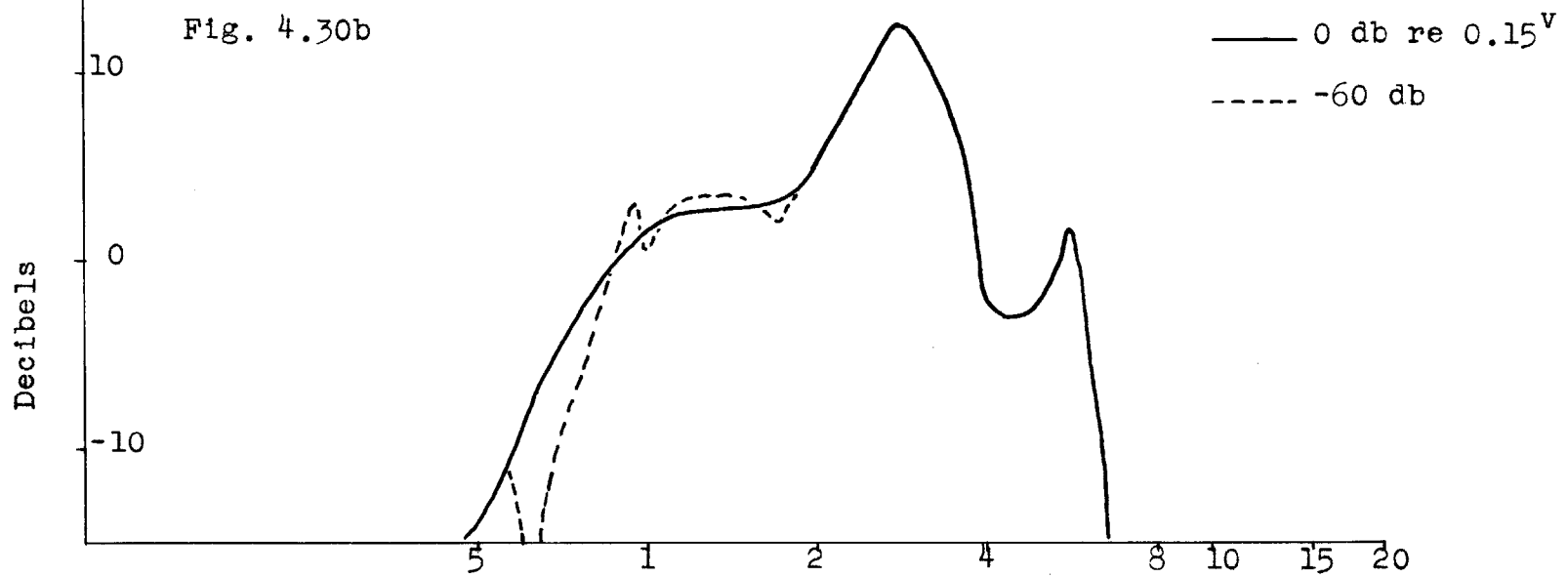
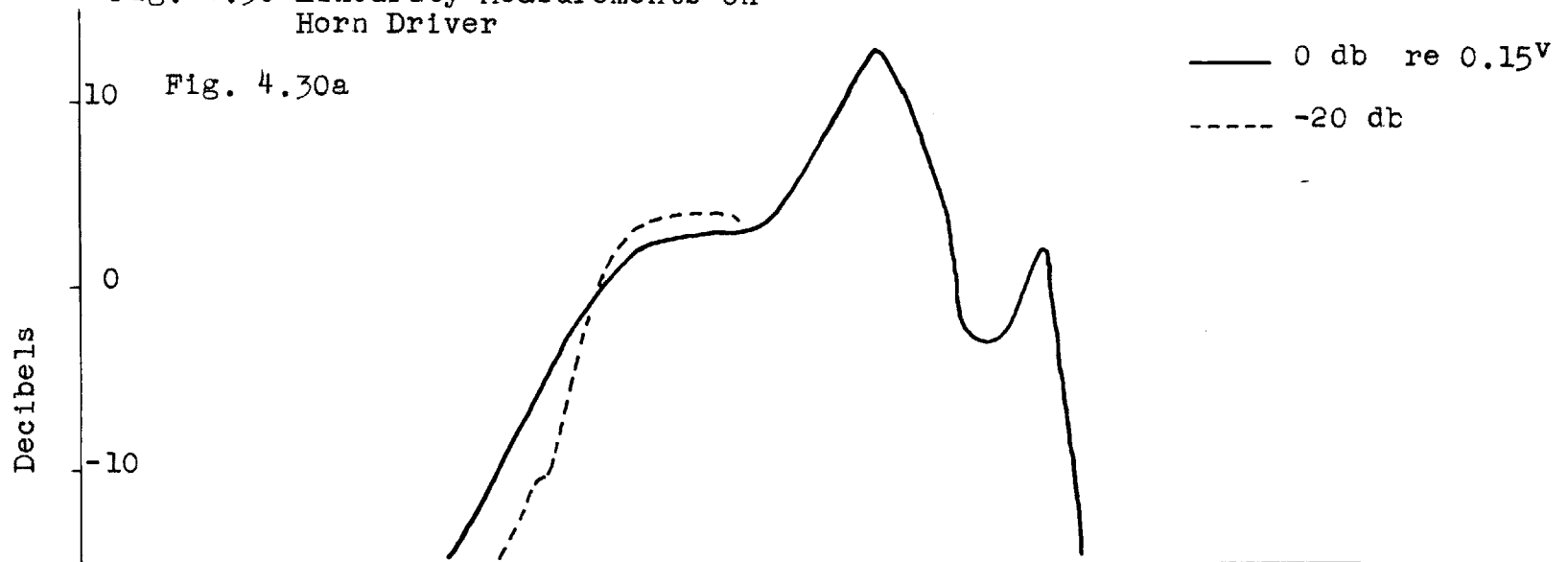
because it is possible that an identical nonreciprocal mechanism may exist in two transducers of the same type.

Let us assume that the transducers under consideration exhibit reciprocity for incremental signals. The question that the experimenter must still answer is, "At what level will nonlinearities become important?"

A small, low-noise microphone should be placed as close as possible to the transducer whose linearity is to be studied. The frequency response is recorded for several different input levels. Any changes in the shape of the response indicate errors that will occur in a reciprocity calibration.

Every effort should be made to make measurements at input levels that correspond to the output levels obtained when the transducer operates as a microphone. An illustration of this point is shown in Fig. 4.30a and b. The response of an Altec-Lansing bull-horn driver was measured at close range with a 640-AA microphone. The heavy curve in both Fig. 4.30a and b was measured with a fairly small voltage (about 40db below rated voltage) applied to the driver. However, reductions in the applied voltage of 20db (Fig. 4.30a) and 60db (Fig. 4.30b) show important changes in the frequency response of the source. A limited number of measurements over a range of about 10 db might not show significant nonlinearities. It can be concluded

Fig. 4.30 Linearity Measurements on  
Horn Driver



that the horn driver will be a satisfactory reciprocal transducer above 2 kc, but not below.

In general it is not safe to assume that a transducer is linear until measurements of the sort described above have been conducted. Horn drivers will, in general, exhibit nonlinearities like those shown in Fig. 4.30. Cone loudspeakers show even more erratic behavior. At frequencies near the rim resonance the exact form of the cone break-up will be strongly influenced by the level of the input voltage. In some cases the cone may not break up in exactly the same way even when the same voltage is applied a second time. Dynamic microphones like the 633-A show nonlinearities at low frequencies for extremely small inputs. Most high quality transducers are linear and reciprocal throughout some usable portion of the frequency range, and it is always possible to use a number of sources of different types in order to cover the entire audio range.

The data shown in Fig. 4.30 were recorded through a narrow band wave analyzer, thus eliminating the contribution to the response of the higher harmonics. Often a harmonic can be detected with greater ease than a corresponding change in the fundamental. Unfortunately there is no general relationship between the levels of the harmonics and the change in the fundamental. It is interesting to note, however, that even harmonics alone can never cause changes in the fundamental. This is a result of the

fact that a nonlinear element that is an even function of some generalized coordinate can never produce a contribution to the fundamental or any odd harmonics.

A pertinent example of this kind of nonlinearity is that introduced by the square term of a condenser microphone.<sup>1</sup> No matter how great the second harmonic distortion may be, this transducer will exhibit no changes in the fundamental. Of course, changes in the fundamental may occur for other reasons. A nonlinear compliance will usually cause changes in the fundamental and the resultant failure of the device to obey reciprocity.

Hysteresis mechanisms are basically nonlinear and may therefore introduce violations of reciprocity. For incremental variations in the coordinates, the area enclosed by the hysteresis loop may be approximated by an ellipse. This does not represent a nonlinearity but merely the presence of a small linear dissipative element. As the area enclosed by the loop increases, the direction of the major axis or the ratio of the major to minor axis may begin to change. It is at this point that the device becomes nonreciprocal. In any case a test of linearity by a method similar to that employed above will indicate the maximum level at which the device may be operated linearly.

---

<sup>1</sup>Cox, J.R., "Nonlinear Analysis of the Condenser Microphone," Quarterly Progress Report of the MIT Acous. Lab., p. 4, Oct.-Dec., 1951.

#### 4.32 Spacing of Source and Receiver

The limit of the far field can be predicted with satisfactory accuracy from the directivity pattern (Section 4.26). However, spacings as close as those indicated in Fig. 4.29 are probably not useful. The location of the acoustic center varies slightly for different microphones of the same type. Therefore, it will be necessary to space the transducers far enough apart to reduce these individual variations to negligible proportions or, alternatively, to find the position of the center of each transducer.

If a calibration is to be conducted for which the desired accuracy is of the order of 0.5 db, it is suggested that the average values of the acoustic center be used. In the worst case (that of the 633-A) this accuracy could be maintained for a spacing of 5 inches, providing that multiple reflections are unimportant. This will, in general, be true at this spacing at low and moderate frequencies. At high frequencies it may be necessary to use other techniques.

If a greater accuracy is desired and space is limited, it may be wise to find the exact location of the acoustic center. Point by point measurements of the field at several different spacings will serve to define the acoustic center accurately if measurements close to but not in the near field are made. Knowledge of the limit of the far field is necessary

in order to eliminate errors like that illustrated for the point source on a sphere (Fig. 3.5).

#### 4.33 Reflections

The wave impedance of a spherical wave is

$$\frac{p}{v} = \rho^c \frac{1}{1 + \frac{1}{jkr}} \quad (4.1)$$

At low frequencies the reciprocal of  $jkr$  predominates even at large distances from the source. Thus, if the wall of an anechoic space is the order of a wavelength from the source, the wave impedance will not be matched by the wall impedance even if the wall is perfectly absorbing. Therefore, the reactive term of (4.1) causes a reflection at the wall. This problem has been treated in detail by Ingard<sup>1</sup> and the simplified result

$$\frac{Q_i}{Q_s} = \frac{1}{2kr} + R_o \quad (4.2)$$

may be obtained from his work if one assumes that the wall has an impedance that is close to the characteristic impedance of air and that the angle of incidence is normal. Here the original source strength is  $Q_s$ , the image source strength is  $Q_i$ , the reflection coefficient of the wall is  $R_o$ , the

---

<sup>1</sup>Ingard, U., "On the Reflection of a Spherical Sound Wave from an Infinite Plane," Jour. Acous. Soc. Am., v. 23, p. 329, 1951.



distance from the image of the source to the receiver is  $r$ . If the reflection coefficient is  $R_0 = 0.1$ , the two terms of (4.2) will be about equal in magnitude when the source is located a half wavelength from the wall. A source placed closer to the wall will tend to nullify the effect of the absorbing material. If the wall has greater absorption, the source should be spaced even farther away in order that the first term in 4.2 does not predominate.

Thus the low frequency limit of an anechoic enclosure is determined by its size and the absorption of the walls. Calibrations in the 100 cps to 1000 cps range may be carried out with less expense in a large but only moderately absorptive room. At higher frequencies it is profitable to make the enclosure smaller and increase the absorption of the walls.

Above 1 kc or 2 kc the first term of (4.2) may be neglected by comparison with the reflection coefficient. The directivity patterns of both source and receiver must now be considered, however. The wall may be replaced by an image source with a strength of  $R_0$  times the strength of the original source. The directivity pattern of the image source will naturally be the image of the original pattern. The worst reflections will usually be from the wall opposite the major lobe of the source. It will be assumed then that this is the wall under consideration. Obviously the least error resulting from the image source

will be incurred when the major lobe of the directivity pattern of the receiver faces the source. Other orientations such as that required for a grazing incidence calibration will result in a greater error.

It is suggested, therefore, that all reciprocity calibrations be carried out with both transducers at normal incidence. If calibrations at other angles are required, they may be obtained from the directivity pattern and the normal incidence calibration. Lacking a directivity pattern for the transducer, a comparison calibration at the required angle may be carried out for several different orientations in the anechoic space so that errors caused by reflections will be smoothed. The recording of the directivity pattern is naturally subject to the same errors, but a large amount of data will have been recorded, and the effect of reflections may be smoothed somewhat by eye.

Let us consider two transducers facing each other. The spacing between them has already been determined by considerations similar to those discussed in Section 4.32. The error caused by reflections may be approximated by replacing the six walls of the enclosure by the images of the source. The strength of these images will be equal to the original source strength times (4.2). On the average the reflected intensity for a cubicle enclosure will be

six times the intensity reflected from one wall, since the contributions of the image sources can be expected to add incoherently.

Again taking the example of  $R_0 = 0.1$ , the above considerations lead to a ratio of path lengths for the direct to the reflected sound of 1:5 for an error of 0.5 db and about 1:25 for an error of 0.1 db. At low frequencies the reactive part of the impedance of a spherical wave will cause additional reflections.

#### 4.34 Pulse Techniques

For frequencies greater than about 5 kc a train of sine waves a few cycles long can often be used to advantage. An oscillographic display of the microphone response to such a pulsed sine wave will yield considerable information about the magnitude of reflections and the total path length involved. One may ignore the direct pulse and expand the scale of the display so that the reflections are examined in detail. It is then possible to track down the offending reflecting surface with great rapidity, whereas plots of the field yield little information other than the fact that reflections are present.

The space length of the pulse should be 6 to 12 inches so that distances of this order of magnitude can be resolved on the oscilloscope screen. This corresponds to a minimum

pulse length of 2.5 cycles at 5 kc or 8 cycles at 16 kc. Thus at low frequencies the bandwidth of the pulse will be quite wide, and it is often necessary to accept a longer pulse length unless the responses of the transducers are smooth. A short pulse passed through a transducer that has an irregular response (such as the 9898) will produce a ringing in the transducer that may be mistaken for reflections. This ringing phenomena may be detected by bringing the receiver into the near field of the source so that the effect of reflections may be neglected.

In addition to use in studying reflections pulse techniques may be employed directly in calibration work. More emphasis is placed on the requirement that the frequency response of the transducer be smooth, however, For instance, if a portion of the response of a microphone can be approximated by a simple resonant circuit with a certain Q, the output of the microphone when exposed to a pulse of sound will approach some steady-state value. When the output is a fraction of a decibel (db) from the final value, one may make the approximation

$$db = 8.6 e^{-\left(\frac{fd}{3Q}\right)} \quad (4.3)$$

where d is the space length of the pulse in feet received before the time of observation and f is the frequency in

kc. For instance, if  $Q = 5$  and  $f = 5$  kc, almost 20 feet of the pulse must be received before the output of the microphone is within 0.1 db of the steady-state value. Thus unless the space is large or the microphone response smoother than above, pulse techniques will be of little value in eliminating reflections from the walls.

In some cases multiple reflections between source and receiver will cause errors. The beginning of this kind of difficulty is shown in the lower scan of Fig. 4.5. At higher frequencies sizeable variations in the field will be found at much larger spacings. For both the L-1 pressure unit and the 640-AA the frequency response is quite smooth, and it was found that by pulsing the source it was possible to eliminate these multiple reflections at frequencies above 10 kc. When this technique is used, great care must be exercised to be sure that the signal is of sufficient duration to approximate steady-state conditions.

#### 4.35 Methods of Data Taking

There are two basic methods of recording the data: discrete measurements at a number of frequencies and continuously recording the output as a function of frequency. The point-by-point method can yield results with accuracies in the vicinity of 0.1 db, but it is extremely laborious

and time consuming. It is necessary to obtain a Lissajous pattern at each frequency and to obtain a balance between the acoustic signal and that introduced by means of the insert resistor. If the calibration is irregular, many points will have to be taken within a small frequency range.

On the other hand, if automatic recording techniques are employed, the irregularity of the response is of no consequence. However, the accuracy of the data obtained will be considerably less than 0.1 db. The recorder that was used in this work had 0.25 db steps but was often in error by 0.5 db. In the continuous recording technique it is not possible to record frequency accurately. Small inaccuracies in positioning the paper or slippage in the drive can cause sizeable errors.

A combination of the two techniques can often be used profitably. The frequencies at which point-by-point measurements should be taken in order to obtain the response curve with the minimum amount of data can be chosen with the aid of an automatic recording. If accuracy of the order of 0.5 db is required, it is often possible to take only a few discrete points. The remainder of the curve may be interpolated from the data recorded automatically. If the frequency scale is in error, the discrete data will disclose this. In some cases the frequency scale may be

translated, and it will be possible to shift the automatic recording so that it will fit the discrete data.

#### 4.36 Electrical Measurements

The electrical measurements of magnitude of the transfer impedance  $z_{ab}$  can be accomplished by comparison with a calibrated attenuator. If the current into the source is adjusted so that it is the same as that into the attenuator, and if the attenuator is adjusted so that the voltage introduced by the insert resistor is the same as that produced by the microphone, the transfer impedance will be directly related to the attenuator setting. An accurately calibrated attenuator can yield data with an error of less than 0.1 db.

The insert resistor must always be in series with the equivalent voltage generator of the microphone. If the impedance of the microphone is low, there is no problem. If the impedance is high, for instance, a condenser microphone, it is necessary to take special precautions to be sure that no shunting capacitance appears between the microphone and the insert resistor. Watters<sup>1</sup> has shown that the insert resistor may be located at the line amplifier if the circuitry is arranged so that this capacitance is negligible.

---

<sup>1</sup>Watters, B.G., ibid.

In the calibration of condenser microphones the polarizing voltage must be accurately measured. Since the microphone must face a high impedance, it is not practical to measure this voltage directly. Usually a cathode follower preamplifier is employed in such a way that the voltage across the cathode resistor supplies the microphone bias. The cathode voltage is then closely related to the bias voltage. However, if any current flows between grid and cathode, the polarizing voltage may deviate appreciably from the cathode voltage.

Figure 4.31 shows the variations in the sensitivity of a 640-AA microphone as a function of the voltage across the cathode resistor of the preamplifier. The straight line shows the variation in sensitivity to be expected if the polarizing voltage were known accurately.

The data of Fig. 4.31 were taken with the microphone mounted first on a Cruft and then on an Altec-Lansing preamplifier. The Cruft preamplifier had a 10-megohm resistor connected between grid and cathode. The Altec-Lansing preamplifier was measured as built with the grid open. A 2-megohm resistor was then inserted between grid and cathode.

The open-grid condition increases the uncertainty of the measurement of the polarizing voltage. Grid current plus very small currents flowing through the extremely high leakage resistance of the tube evidently cause these



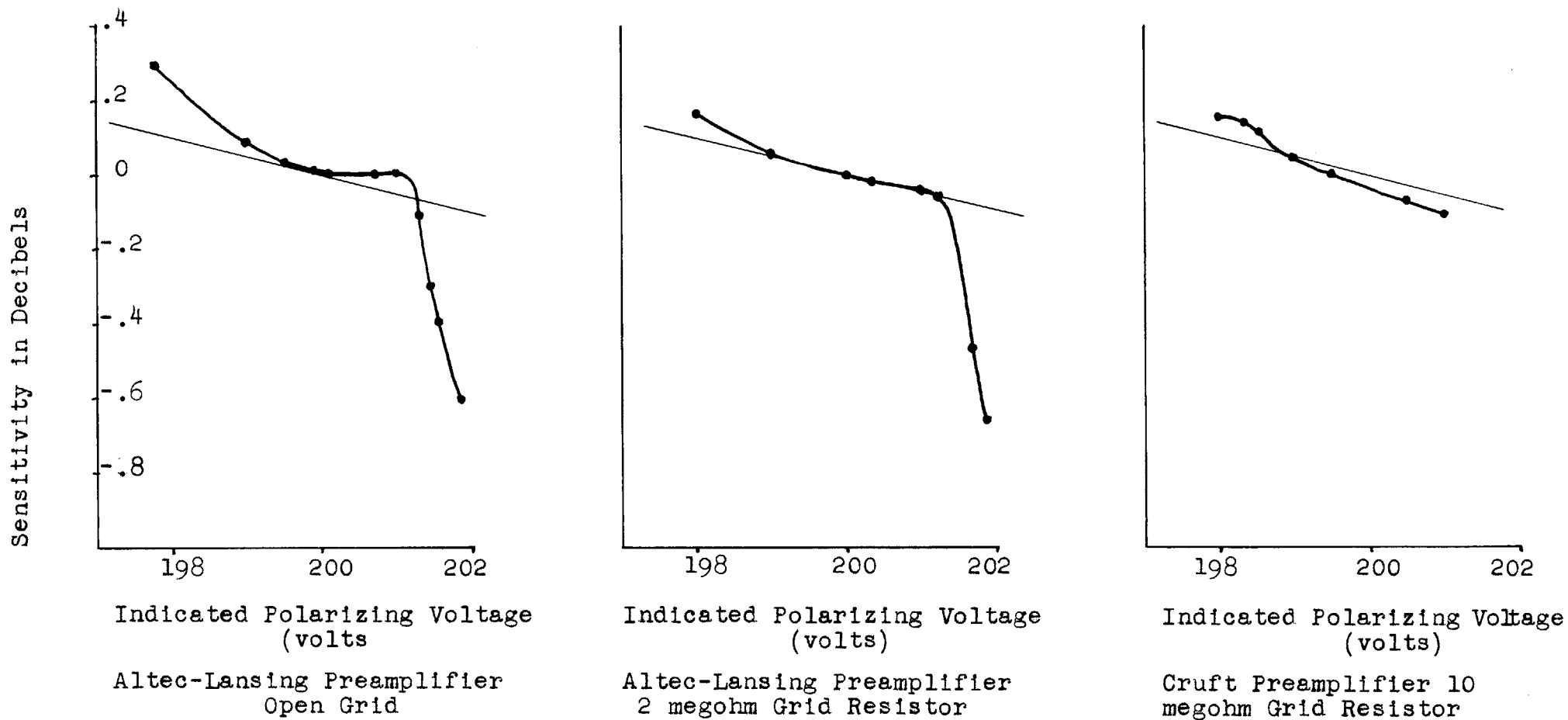


Fig. 4.31 Variations in Sensitivity of 640-AA with Indicated Polarizing Voltage

variations. The 2-megohm grid resistor reduces the variation of the grid bias markedly, but at a slight sacrifice in the signal to noise level and in the low frequency sensitivity. Usually these sacrifices can be tolerated in microphone calibration work.

#### 4.37 Selection of a Sound Source

The selection of a sound source is an important step in the instrumentation for reciprocity calibration. There are a number of desirable characteristics that one should bear in mind. The frequency response should be smooth, the front of the source should be free from flat surfaces, the near field should be small, the acoustic center should change smoothly with frequency, and the response should be practically independent of time and minor variations in temperature and pressure.

It is important to have a source with a smooth frequency response for two reasons. First, small changes in frequency should not cause large changes in the electrical output. Such a situation makes the source impractical for use with automatic recording equipment and inconvenient for use when point-by-point data is taken. Second, a smooth frequency response is desirable for pulse measurements.

The front of the source should not be flat so that multiple reflections between source and receiver are minimized. A spherical shape will diffuse the wave reflected

from the microphone most effectively. The L-1 pressure unit has a dome-shaped diaphragm mounted in a spherical housing (Fig. 4.2 - note that the diaphragm is removed in this photograph), and even though the L-1 unit is larger, this configuration was found to be more satisfactory than that of the 640-AA (Fig. 4.9).

A smooth directivity pattern will usually insure that a sound source has a small near field. This will be a great advantage in conducting calibrations in a small enclosure as discussed in Section 4.32. However, a smooth directivity pattern does not always insure that it is possible to make calibrations at close spacing. As in the case of the 640-AA, a flat face may cause multiple reflections.

An acoustic center that does not change irregularly as a function of frequency is desirable for use in calibrations at close spacing. Erratic behavior of the acoustic center, like erratic behavior of the response, will cause large changes in electrical output for small changes in frequency. Such behavior will make the accurate measurement of the acoustic center more difficult, since scans of the field at a large number of frequencies will be necessary.

Finally, the stability of the source under normal variations of pressure and temperature should be observed. The 640-AA microphones are by far the most stable of those

studied. The 21 series of condenser microphones prove to be slightly less stable in general. A few of the 21 series microphones exhibit quite large instabilities, but this is probably a production difficulty that will be eliminated in the future. The 633-A microphones have excellent short-term stability, but their sensitivity may change by several tenths of a decibel over a period of days or weeks. In practice it was found that the L-1 pressure unit (used in 633-A microphones) need to be calibrated against the 640-AA only at the beginning and end of a group of calibration runs. At the end of the runs, from 2 to 4 hours, later the sensitivity was found to be unchanged. The stability of the crystal microphones is poor because both the coupling constant and the electrical capacitance depend on temperature. The 9898 microphone is better than most crystal microphones in this respect, but not as stable as the other microphones studied.

#### 4.4 Summary

The measurements and techniques discussed in this chapter should be of assistance in the instrumentation for the free-field calibration of microphones. Given microphones of the type studied here and given the desired accuracy, one should be able to determine the optimum spacing of source and receiver. If one knows the reflection coefficient of the acoustic material to be used on

the walls of the enclosure, it is possible to compute the minimum dimensions that will be consistent with the given error.

In addition a number of other pertinent topics have been discussed including reciprocity linearity, pulse techniques, data taking, electrical measurements, and selection of a sound source. It is hoped that this information will lead to microphone calibrations of increased accuracy.

## APPENDIX I

### 1. Energy Functions and Reciprocity for Sinusoidal Signals

Section 2.27 contained a proof stating that a reciprocal system must have a kinetic energy that is a function of the velocities only and a potential energy that is a function of the displacements only. The dissipation function was shown to be a function of the velocities only. Each one of these functions was a quadratic form with no explicit dependence on time.

Under the above conditions and with sinusoidal signals the kinetic energy  $\mathcal{T}$  is

$$\mathcal{T} = \frac{1}{8} (I e^{j\omega t} + I^* e^{-j\omega t}) L (I e^{j\omega t} + I^* e^{-j\omega t}) \quad (1)$$

where  $L$  is the square matrix

$$L = \left[ \frac{\partial^2 \mathcal{T}}{\partial \dot{q} \partial \dot{q}} \right] \quad (2)$$

The kinetic energy given in (1) can be separated into two parts, an average part  $\mathcal{T}_{av}$  that is independent of time,

$$\mathcal{T}_{av} = \frac{1}{4} I L I^* \quad (3)$$

and a double frequency part  $\mathcal{T}_{df}$

$$\mathcal{T}_{df} = \frac{1}{4} I L I \quad (4)$$

so that

$$\mathcal{T} = \mathcal{R}_e \{ \mathcal{T}_{av} + \mathcal{T}_{df} e^{2j\omega t} \} \quad (5)$$

The potential energy  $\mathcal{V}$  can be separated in the same fashion. An  $\omega^2$  factor will appear because it is necessary to express the charges in terms of the currents.

$$\mathcal{V}_{av} = \frac{1}{4\omega^2} \mathbf{I} \mathbf{S} \mathbf{I}^* \quad (6)$$

$$\mathcal{V}_{df} = -\frac{1}{4\omega^2} \mathbf{I} \mathbf{S} \mathbf{I} \quad (7)$$

where the square matrix  $\mathbf{S}$  is

$$\mathbf{S} = \left[ \frac{\partial^2 \mathcal{V}}{\partial \mathbf{q} \partial \mathbf{q}} \right] \quad (8)$$

Likewise the two parts of the dissipation function  $\mathcal{F}$  are

$$\mathcal{F}_{av} = \frac{1}{4} \mathbf{I} \mathbf{R} \mathbf{I}^* \quad (9)$$

$$\mathcal{F}_{df} = \frac{1}{4} \mathbf{I} \mathbf{R} \mathbf{I} \quad (10)$$

where the square matrix  $\mathbf{R}$  is

$$\mathbf{R} = \left[ \frac{\partial^2 \mathcal{F}}{\partial \dot{\mathbf{q}} \partial \dot{\mathbf{q}}} \right] \quad (11)$$

Utilizing the matrices L, S, and R, the Lagrange equations may be written in a more compact fashion,

$$L\ddot{q}] + S\dot{q}] = e] = e_s] - R\dot{q}] \quad (12)$$

Sinusoidal behavior of the system will be described by

$$j\omega LI + RI + \frac{SI}{j\omega} = E_s = ZI \quad (13)$$

the familiar electrical network equations. Following the analysis of Bode<sup>1</sup>, it is possible to evaluate the driving point impedances and admittances in terms of the energy functions. The complex power absorbed by the network is

$$I^*E_s = I^*RI + j\omega \left( I^*LI - \frac{I^*SI}{\omega^2} \right) \quad (14)$$

which in terms of the average energy functions is

$$I^*E_s = 4\mathcal{P}_{av} + 4j\omega\mathcal{L}_{av} \quad (15)$$

where the average Lagrangian  $\mathcal{L}_{av}$  is

$$\mathcal{L}_{av} = \mathcal{T}_{av} - \mathcal{V}_{av} \quad (16)$$

---

<sup>1</sup> Bode, H. W., Network Analysis and Feedback Amplifier Design, D. Van Nostrand Co., New York, p. 128, 1945.



The complex power into the network may be expressed in terms of the admittance matrix

$$I E_s^* = (I^* E_s)^* = E_s Y E_s^* \quad (17)$$

The  $n^{\text{th}}$  driving point admittance may be evaluated by setting all the driving forces or voltages except  $E_{sn}$  equal to zero,

$$Y_{nn} = \frac{E_{sn} Y_n E_{sn}^*}{|E_{sn}|^2} = 4 \frac{\mathcal{Y}_{av}^{(n)} - j\omega \mathcal{L}_{av}^{(n)}}{|E_{sn}|^2} \quad (18)$$

where the superscript (n) indicates that the energy and dissipation functions have been evaluated with only  $E_{sn}$  non-zero.

To illustrate the dual representation of the system, consider the alternate definition of the energy and dissipation functions

$$\mathcal{T}_d = \frac{1}{2} \dot{\lambda} C \lambda \quad (19)$$

$$\mathcal{V}_d = \frac{1}{2} \lambda \Gamma \lambda \quad (20)$$

$$\mathcal{W}_d = \frac{1}{2} \dot{\lambda} G \lambda \quad (21)$$

The notation here is electrical. The results can be applied equally well to a mechanical system, however, with  $\lambda$  standing for the momenta instead of the fluxes. The dual

of (13) is

$$j\omega CE + GE + \frac{\Gamma E}{j\omega} = I_s = YE \quad (22)$$

where  $I_s$  is a matrix containing the driving currents or velocities. The  $n^{\text{th}}$  driving point impedance is

$$Z_{nn} = 4 \frac{\mathcal{V}_{dav}^{(n)} - j\omega \mathcal{X}_{dav}^{(n)}}{|I_{sn}|^2} \quad (23)$$

where notation similar to that in (18) has been employed.

The proof of the reciprocity of systems described by (13) or (22) is extremely simple. It is only necessary to remember that  $L$ ,  $\Gamma$ ,  $R$ ,  $G$ ,  $S$ , and  $C$  are symmetrical matrices, since they were all derived from quadratic forms. By inspection of (13) and (22), one sees that  $Z$  and  $Y$  are also symmetrical. A more formal proof utilizes the two experiments (1) and (2).

$$I^{(1)} E_s^{(2)} = I^{(1)} R I^{(2)} + j\omega \left( I^{(1)} L I^{(2)} - \frac{I^{(1)} S I^{(2)}}{\omega^2} \right) \quad (24)$$

and clearly

$$I^{(1)} E_s^{(2)} - I^{(2)} E_s^{(1)} = 0 \quad (25)$$

the condition for reciprocity.

Evaluation of one of the transfer admittances in terms of the energy and dissipation functions is somewhat more difficult than that carried through above for the driving point admittances and apparently has not been reported before. In experiment (m) all the source voltages except  $E_{sm}$  vanish. In experiment (n) all except  $E_{sn}$  vanish.

$$I^{(m)} E_s^{(n)} = E_{sm} Y_{mn} E_{sn} = I^{(m)} R I^{(m)} + j\omega \left( I^{(m)} L I^{(n)} - \frac{I^{(m)} S I^{(n)}}{\omega^2} \right) \quad (26)$$

Utilizing the notation

$$\tilde{\sigma}_{df}^{(m \pm n)} = \frac{1}{4} (I^{(m)} \pm I^{(n)}) L (I^{(m)} \pm I^{(n)}) = \tilde{\sigma}_{df}^{(m)} \pm \frac{1}{2} I^{(m)} L I^{(n)} + \tilde{\sigma}_{df}^{(n)} \quad (27)$$

the expression for the transfer admittance  $Y_{mn}$  becomes

$$Y_{mn} = \frac{1}{E_{sm} E_{sn}} \left( \sigma_{df}^{(m+n)} - \sigma_{df}^{(m-n)} + j\omega \left\{ \tilde{\sigma}_{df}^{(m+n)} - \tilde{\sigma}_{df}^{(m-n)} + \mathcal{V}_{df}^{(m+n)} - \mathcal{V}_{df}^{(m-n)} \right\} \right) \quad (28)$$

Interchanging m and n will not alter the result as long as the energy and dissipation functions are quadratic forms.

## 2. Lagrange Equations for a Distributed System

Assuming that the necessary conditions for reciprocity in a lumped system will also have to hold in a distributed system, makes it possible to simplify the analysis greatly. Therefore, let us assume that the system has a kinetic energy density  $\underline{T}$  that can be written in the form

$$\underline{T} = \frac{1}{2} \dot{q} \underline{L} \dot{q} \quad (29)$$

where the elements of the symmetrical matrix  $L$  are independent of time. This is exactly the same as the kinetic energy of a lumped system.

The potential energy density  $\underline{V}$  will, however, be considerably more complicated. In general it will depend on the coordinates themselves and their derivatives with respect to each of the space coordinates.

$$\underline{V} = \frac{1}{2} \left[ q \begin{array}{c} \frac{\partial q}{\partial x_1} \\ \frac{\partial q}{\partial x_2} \\ \frac{\partial q}{\partial x_3} \end{array} \right] \left[ \begin{array}{cccc|c} V_{00} & V_{01} & V_{02} & V_{03} & q \\ \hline V_{10} & V_{11} & V_{12} & V_{13} & \frac{\partial q}{\partial x_1} \\ V_{20} & V_{21} & V_{22} & V_{23} & \frac{\partial q}{\partial x_2} \\ V_{30} & V_{31} & V_{32} & V_{33} & \frac{\partial q}{\partial x_3} \end{array} \right] \quad (30)$$

This description of the potential energy is overly clumsy and the following symbolic notation will be useful:

$$\left[ \begin{array}{c} q \\ \frac{\partial q}{\partial x_1} \\ \frac{\partial q}{\partial x_2} \\ \frac{\partial q}{\partial x_3} \end{array} \right] = \left[ \begin{array}{c} q \\ \nabla q \end{array} \right] \quad (31)$$

It should be remembered that each element of the matrices shown in (30) and (31) is itself a matrix. Each one of the submatrices associated with the coordinates in (30), for instance have as many elements as there are generalized coordinates.

Utilizing (31) the potential energy may be written

$$\underline{\mathcal{V}} = \frac{1}{2} \underline{q} : \underline{\nabla} q \cdot \begin{bmatrix} V_{00} & \underline{\vec{V}}_x \\ \underline{\vec{V}}_x & \underline{\vec{V}} \end{bmatrix} \cdot \begin{bmatrix} q \\ \underline{\nabla} q \end{bmatrix} \quad (32)$$

where the square matrix of (30) has been partitioned as indicated by the dotted lines and

$$\underline{\vec{V}}_x = [V_{01} \ V_{02} \ V_{03}] = \begin{bmatrix} V_{10} \\ V_{20} \\ V_{30} \end{bmatrix}_t \quad (33)$$

$$\underline{\vec{V}} = \begin{bmatrix} V_{11} & V_{12} & V_{13} \\ V_{21} & V_{22} & V_{23} \\ V_{31} & V_{32} & V_{33} \end{bmatrix} \quad (34)$$

Note that elements of the submatrix  $\underline{\vec{V}}$  may be grouped together to form a dyadic. Such dyadics have nine elements and operate on the vector  $\underline{\nabla} q$  to produce a new vector. Similarly elements in the submatrix  $\underline{\vec{V}}_x$  may be grouped together to form a vector. Each vector will, of course, have three elements and will operate on  $\underline{\nabla} q$  to produce a scalar

or on  $q$  to produce a vector.

The equations of motion derived from the kinetic and potential energies given in (29 and (32) will, in general, have terms involving the coordinates themselves. These terms will be in addition to the usual terms involving the first spatial derivatives and the second spatial and time derivatives. This circumstance will, in general, make it impossible to set up a dual representation of the system. As will be seen below, one cannot find a satisfactory set of new coordinates that makes it possible to express the potential energy in terms of the time derivatives of these coordinates.

Although distributed systems whose potential energies contain the coordinates themselves in addition to their spatial derivatives can be shown to display reciprocity, they will not be included in the following general discussion. With this simplification the Lagrangian density  $\underline{\mathcal{L}}$  becomes

$$\underline{\mathcal{L}} = \underline{\mathcal{T}} - \underline{\mathcal{V}} = \underline{\dot{q}} [\underline{\mathcal{T}} \dot{q}] - \underline{\nabla} q \cdot \underline{\vec{V}} \cdot \underline{\nabla} q \quad (35)$$

which yields the Lagrange equations

$$\underline{\mathcal{T}} \ddot{q}] - \underline{\nabla} \cdot \underline{\vec{V}} \cdot \underline{\nabla} q] = -f] \quad (36)$$

where  $f$  is the generalized force density vector opposing at any point forces not included in the Lagrangian density; i.e., viscous forces. The power density removed from the

conservative part of the system as a result of these forces is

$$\begin{aligned} \underline{\dot{q}} f] &= \underline{\dot{q}} \vec{\nabla} \cdot \vec{V} \cdot \vec{\nabla} q] - \underline{\dot{q}} T \ddot{q}] & (37) \\ &= \vec{\nabla} \cdot (\underline{\dot{q}} \vec{V} \cdot \vec{\nabla} q]) - \underline{\vec{\nabla} \dot{q}} \cdot \vec{V} \cdot \vec{\nabla} q] - \underline{\dot{q}} T \ddot{q}] \end{aligned}$$

but this can be rewritten in terms of the time derivative of the energy density  $\mathcal{H}$

$$\underline{\dot{q}} f] = \vec{\nabla} \cdot (\underline{\dot{q}} \vec{V} \cdot \vec{\nabla} q]) - \frac{\partial \hat{T}}{\partial t} - \frac{\partial \mathcal{H}}{\partial t} = -\vec{\nabla} \cdot \vec{\mathcal{I}} - \frac{\partial \mathcal{H}}{\partial t} \quad (38)$$

where  $\vec{\mathcal{I}}$  stands for the negative of vector within the parentheses. Clearly the power absorbed by the dissipative mechanisms within a volume plus the total power flow out of the volume plus the rate of increase of the stored energy within the volume must vanish. Thus  $\vec{\mathcal{I}}$  is identified with the outward intensity vector (Poynting vector) when (38) is integrated over a volume

$$\int \underline{\dot{q}} f] dv + \int \vec{\mathcal{I}} \cdot d\vec{a} + \frac{\partial}{\partial t} \int \mathcal{H} dv = 0 \quad (39)$$

### 3. Dual Representation of the System

In most physical problems the intensity vector  $\vec{I}$  can be written in a symmetrical fashion in terms of components that have the dimensions of a generalized velocity and components that have the dimensions of a generalized stress. The above observation can be stated in a general way by defining the dual set of coordinates  $\lambda$

$$\vec{M} \dot{\lambda}] = \vec{V} \cdot \vec{\nabla} q] \quad (40)$$

where  $\vec{M}$  is a dimensionless matrix whose elements are vectors independent of space and time. The purpose of  $\vec{M}$  is to combine the new coordinates in a manner analogous to the combining of element voltages to get node voltages in a lumped system<sup>1</sup>. Like the lumped system case the matrix M need not be square. This is a result of the fact that the number of node equations necessary to describe a system need not be the same as the number of loop equations.

In terms of the new coordinates the intensity vector becomes

$$\vec{I} = -\dot{q} \vec{M} \dot{\lambda}] \quad (41)$$

-----  
<sup>1</sup>In a lumped electrical system one may write the node voltages in terms of the capacitance and inductance voltages with the aid of a similar M matrix where the q's are the charges associated with the loop currents  $\dot{q}$ . Substitution of these expressions into the homogeneous Lagrange equations for the loop charges q will show that the node fluxes  $\lambda$  also satisfy the Lagrange equations.



an expression that is symmetrical in appearance. In this case  $\lambda$  will have the dimensions of a generalized momentum per unit area.

One should not expect to be able to find the dual of a system which involves the arbitrary forces described by the matrix  $f]$ , since these forces may have no dual presentation. Therefore, consider only the homogeneous Lagrange equations

$$T\ddot{q}] - \vec{\nabla} \cdot \vec{V} \cdot \vec{\nabla} q] = 0 \quad (42)$$

If the new coordinates defined by (40) are substituted into (42), one finds that

$$\vec{\nabla} \cdot \vec{M} \lambda] = \vec{M} \cdot \vec{\nabla} \lambda] = T\ddot{q}] \quad (43)$$

since  $\vec{M}$  is independent of space.

Thus, in terms of the dual coordinates the kinetic energy density is

$$\underline{T} = \frac{1}{2} \underline{\vec{\nabla} \lambda} \cdot (\vec{M})_t T^{-1} \vec{M} \cdot \vec{\nabla} \lambda] \quad (44)$$

and the potential energy density is

$$\underline{\mathcal{V}} = \frac{1}{2} \dot{\lambda} \underline{(\vec{M})}_t \cdot \vec{V} \cdot \vec{M} \dot{\lambda}] \quad (45)$$

where the inverse of the matrices  $T$  and  $\vec{V}$  are obtained in the usual fashion. Since each element of  $\vec{V}$  is a dyadic, it

may be more straightforward to take the inverse of the expanded form (34) and then recombine elements to form the dyadics.

Utilizing the dual matrices

$$T_d = \vec{M}_t \cdot \vec{V}^{-1} \cdot \vec{M} \quad (46)$$

$$\vec{V}_d = \vec{M}_t T^{-1} \vec{M} \quad (47)$$

it is possible to define a dual Lagrangian density  $\underline{\mathcal{L}}_d$

$$\underline{\mathcal{L}}_d = \frac{1}{2} \underline{\dot{\lambda}} T_d \underline{\dot{\lambda}} - \frac{1}{2} \underline{\vec{\nabla}} \lambda \vec{V}_d \underline{\vec{\nabla}} \lambda = - \underline{\mathcal{L}} \quad (48)$$

which is identical in form to the original. The actual magnitudes of the two are, however, opposite in sign. Both expressions for the Lagrangian density will obey Hamilton's principle and both  $q$  and  $\lambda$  will satisfy a set of Lagrange equations.

#### 4. Reciprocity for Distributed Systems

Let us perform two separate experiments, (1) and (2), on a system described by the Lagrange equations (36). If the system undergoes sinusoidal motion, these equations for

the (1) experiment will be

$$j\omega T J^{(1)} - \frac{1}{j\omega} \vec{\nabla} \cdot \vec{V} \cdot \vec{\nabla} J^{(1)} = -F^{(1)} \quad (49)$$

where the J matrix gives the complex amplitude of the  $\dot{q}$ 's; i.e.,

$$\dot{q}] = \text{Re} \{ J e^{j\omega t} \} \quad (50)$$

and the F matrix is defined in terms of the f's in a similar fashion. By analogy with the treatment of lumped systems, (49) is multiplied by  $J^{(2)}$

$$j\omega J^{(2)} T J^{(1)} - \frac{1}{j\omega} J^{(2)} \vec{\nabla} \cdot \vec{V} \cdot \vec{\nabla} J^{(1)} = -J^{(2)} F^{(1)} \quad (51)$$

The second term of this expression may be expanded to get

$$j\omega J^{(2)} T J^{(1)} + \frac{1}{j\omega} \vec{\nabla} J^{(2)} \cdot \vec{V} \cdot \vec{\nabla} J^{(1)} - \frac{1}{j\omega} \vec{\nabla} \cdot (J^{(2)} \vec{V} \cdot \vec{\nabla} J^{(1)}) = -J^{(2)} F^{(1)} \quad (52)$$

An expression identical to this (52) except with the superscripts interchanged can be obtained by starting with the Lagrange equations for the (2) experiment. The volume integral of the difference of these two expressions is

$$\frac{1}{j\omega} \int d\vec{a} \cdot (J^{(2)} \vec{V} \cdot \vec{\nabla} J^{(1)} - J^{(1)} \vec{V} \cdot \vec{\nabla} J^{(2)}) = - \int (J^{(2)} F^{(1)} - J^{(1)} F^{(2)}) d\tau \quad (53)$$

The vanishing of the righthand side of this equation is the reciprocity condition for distributed systems. The similarity between this expression and the equivalent for lumped systems can be seen if one substitutes  $S$ , the matrix that is the dual of the  $J$

$$j\omega \vec{M}S = \vec{V} \cdot \vec{\nabla} J \quad (54)$$

into the lefthand side of (53) to get the reciprocity condition

$$\int d\vec{a} \cdot (J^{(1)} \vec{M}S^{(1)} - J^{(2)} \vec{M}S^{(2)}) = 0 \quad (55)$$

In the lumped constant case a summation over all the ports of the system was implied. For distributed systems this summation becomes an integral over the surface of the system. If no arbitrary forces are present within the system, the  $F$  matrix will vanish and the system will satisfy the reciprocity condition (55).

##### 5. Dissipation in Distributed Systems

If the forces  $F$  do work on dissipative mechanisms of the viscous type, it is possible to demonstrate that the entire system will still display reciprocity. The form of these forces must be similar to the general description of the conservative forces. This statement results from a consideration of the matrix product,  $JF$ . In order that the righthand side of (53) vanish,  $JF$  must lead to a quadratic

form in the generalized velocities and the spatial derivatives of the generalized velocities. The most general form for  $JF$  is, therefore, a quadratic form similar to (30) for the potential energy except that  $q$  would be replaced by  $\dot{q}$  plus a divergence term that will vanish when integrated over the volume of the system.

With these considerations in mind, the general form for the viscous forces is

$$F = \vec{\nabla} \cdot \hat{R} \cdot \vec{\nabla} J + R_{oo} J \quad (56)$$

where the  $\hat{R}$  and  $R_{oo}$  matrices must be symmetrical. The righthand member of (53) becomes

$$-\int (J^{(1)} F^{(1)} - J^{(2)} F^{(2)}) dv = + \int d\vec{a} \cdot (J^{(2)} \hat{R} \cdot \vec{\nabla} J^{(1)} - J^{(1)} \hat{R} \cdot \vec{\nabla} J^{(2)}) \quad (57)$$

which will vanish if there is either no dissipation or no power flow at the boundary surface. The dual matrix  $S$  may be defined differently so that these viscous terms are included in the lefthand side of (53). This corresponds to the rearrangement in the node voltages that might take place when resistances are added to an otherwise lossless network.

A simpler method of handling viscous forces would have been to transfer them from the righthand side of the Lagrange equations (49) and include them in the conservative forces. This method is not quite as straightforward as that used above because it hides the mechanics of the proof. It does have the virtue of a simplified notation.

In summary, systems whose behavior is described by the differential equations

$$j\omega T J - \frac{1}{j\omega} \vec{\nabla} \cdot \vec{V} \cdot \vec{\nabla} J = 0 \quad (58)$$

where  $T$  and  $\vec{V}$  may be complex, will be reciprocal and therefore satisfy (55).

### 6. Relationship to Green's Function

Suppose that power is fed into the system by means of simple point sources. On the boundary surface of the system, the intensity vector is zero, and therefore, the integral (55) will vanish except for the small spherical surfaces surrounding the point sources. Assume that in the (1) experiment the  $k^{\text{th}}$  coordinate has an impulse at the point  $\vec{r}^{(1)}$

$$J_k^{(1)} \Big|_{\vec{r} \sim \vec{r}^{(1)}} \cong |\vec{r} - \vec{r}^{(1)}|^{-1} \quad (59)$$

and in the (2) experiment the  $l^{\text{th}}$  coordinate has an impulse at the point  $\vec{r}^{(2)}$

$$J_l^{(2)} \Big|_{\vec{r} \sim \vec{r}^{(2)}} \cong |\vec{r} - \vec{r}^{(2)}|^{-1} \quad (60)$$

If these functions are substituted into the reciprocity condition, only the coefficients of  $\nabla J_k^{(1)}$  and  $\nabla J_l^{(2)}$  will remain

$$J_i^{(1)}(\vec{r}^{(2)}) \int d\vec{a} \cdot \vec{V}_{ik}(\vec{r}^{(2)}) \cdot \vec{n} = J_j^{(2)}(\vec{r}^{(1)}) \int d\vec{a} \cdot \vec{V}_{jl}(\vec{r}^{(1)}) \cdot \vec{n} \quad (61)$$

where  $\vec{n}$  is a unit vector normal to the surface of integration and summation over the repeated indices is implied. The integral averages the diagonal components of the dyadics  $\vec{V}_{j\ell}$  and may be eliminated with the aid of the Spur of the dyadics. The Spur is written  $|V_{j\ell}|$  and is equal to the sum of the diagonal elements of  $\vec{V}_{j\ell}$ .

$$J_i^{(1)}(\vec{r}^{(2)})|V_{ik}(\vec{r}^{(2)})| = J_j^{(2)}(\vec{r}^{(1)})|V_{j\ell}(\vec{r}^{(1)})| \quad (62)$$

If the matrix  $\vec{V}$  has only diagonal elements (remember that each element of the matrix is a dyadic which is not necessarily diagonal or symmetric), the summation may be eliminated, yielding a more familiar form for the reciprocity of the Green's function. That is, an impulse of magnitude  $|V_{jj}(\vec{r}^{(1)})|$  located at  $\vec{r}^{(2)}$  will produce a response at  $\vec{r}^{(1)}$  that is equal to that produced at  $\vec{r}^{(2)}$  by an impulse of magnitude  $|V_{ii}(\vec{r}^{(2)})|$  located at  $\vec{r}^{(1)}$ . A similar but more complicated relationship could be developed for a dipole source instead of a point source. For an electromagnetic field the Spur of  $\vec{V}_{j\ell}$  will be zero, and therefore, it becomes necessary to use the dipole source.

## 7. Generalized Impedance

A generalized impedance for a distributed system should bear a close relationship to the impedance of a lumped system.

A convenient bridge between the two kinds of systems are the Lagrangians. In Section 1. of this Appendix, it was shown that a driving point impedance may be written in terms of the average Lagrangian  $\mathcal{L}_{av}$ . For a distributed system, it is possible to proceed in an analogous fashion by evaluating the volume integral of the average Lagrangian density

$$4j\omega\mathcal{L}_{av} = \int j\omega(J^*TJ - \frac{1}{\omega^2}\vec{\nabla}J^*\cdot\vec{\nabla}J)dv = \int \frac{d\vec{a}\cdot(J^*\vec{\nabla}\cdot\vec{\nabla}J)}{j\omega} \quad (63)$$

where the system under consideration is conservative, and therefore,  $T$  and  $\vec{\nabla}$  are real. If an impedance matrix can be defined, one would expect that a matrix product of the form  $I^*ZI$  would be equal to the surface integral on the right.

So that the situation may be visualized more easily, let us assume that the surface integral is zero over all the boundary surface of the system except over an area  $A$ . There will be a set of solutions, or eigenfunctions, to the differential equations describing the system that will be zero at the boundary except over  $A$ . These eigenfunctions will be denoted by  $A_{\ell}^{(k)}(x_1, x_2, x_3)$ , the  $k^{\text{th}}$  solution for the  $\ell^{\text{th}}$  coordinate. If these eigenfunctions form a complete set at the surface  $A$ , a linear combination of them can always be found that will be equal to each of the elements of the matrix  $J$ . Therefore, it is possible to write the matrix equation



$$J = A^{(k)} I^{(k)} \quad (64)$$

where  $A^{(k)}$  is a diagonal matrix whose elements are  $k^{\text{th}}$  solutions for each of the coordinates. The constants  $I_{\rho}^{(k)}$  are independent of the spatial coordinates and form the column or row matrix  $I^{(k)}$ . Summation over the repeated superscripts is implied.

The definition of a generalized impedance matrix becomes clear when the set of solutions (64) is substituted into (63)

$$4 j \omega \mathcal{L}_{av} = I^{(k)*} \left( \int \frac{\vec{\nabla} A^{(k)} \cdot \vec{\nabla} A^{(j)*}}{j \omega} \cdot d\vec{a} \right) I^{(j)} \quad (65)$$

making it possible to identify the impedance matrix coupling the  $j^{\text{th}}$  and  $k^{\text{th}}$  modes of the system

$$Z^{(kj)} = \frac{1}{j \omega} \int \vec{\nabla} A^{(k)} \cdot \vec{\nabla} A^{(j)*} \cdot d\vec{a} \quad (66)$$

From experience with lumped systems, one would expect that the product at the right of (65) should equal complex power. Comparison of this expression with (38) where the time dependent intensity vector  $\vec{\mathcal{I}}$  is defined, allows us to define a complex intensity vector  $\vec{\mathcal{I}}_{av}$ .

$$4 j \omega \mathcal{L}_{av} = - \int \vec{\mathcal{I}}_{av} \cdot d\vec{a} = I^{(k)*} Z^{(kj)} I^{(j)} \quad (67)$$

and as expected the integral of the complex intensity over the area  $A$  flowing out of the system gives the negative of the total complex power flowing into the system.

If on the surface  $A$  the matrix  $J$  is chosen so that all its elements except  $J_n$  are zero, one gets the set of driving point impedances

$$4j\omega \mathcal{L}_{av}^{(n)} = I_n^{(k)*} Z_{nn}^{(kj)} I_n^{(j)} \quad (68)$$

and if the distribution of  $J_n$  on  $A$  is such that only the  $k^{\text{th}}$  mode is excited, the impedance  $Z_{nn}^{(kk)}$  may be written in terms of the average Lagrangian density for these conditions

$$Z_{nn}^{(kk)} = \frac{4j\omega \mathcal{L}_{av}^{(n)(k)}}{|I_n^{(k)}|^2} \quad (69)$$

Another simplification of the general result occurs when  $J$  is constrained to be independent of the coordinates over the area  $A$ . The matrix  $A^{(k)}$  is diagonal and therefore possesses a simple inverse. If a unit matrix composed of  $A^{(k)}$  and its inverse is substituted into (65), the result may be written

$$4j\omega \mathcal{L}_{av} = J^* \left[ (A^{(k)})^{-1} \int \frac{\vec{\nabla} A^{(k)} \cdot \vec{V} \cdot d\vec{a}}{j\omega} \right] J \quad (70)$$

and a different set of impedances defined

$$Z = (A^{(k)})^{-1} \frac{1}{j\omega} \int \vec{\nabla} A^{(k)} \cdot \vec{\nabla} \cdot d\vec{a} \quad (71)$$

In this case the mode impedances no longer play a part because  $J$  has been constrained to behave in a certain way and the impedance is associated with the total reaction on the area  $a$ . It is possible to go one step further. The matrix  $J$  could have been made up of prescribed functions over  $a$ . The amplitude of  $J$  could then be taken from under the integral as in (71). The impedance would then be modified to contain the normalized prescribed function both inside and outside of the integral sign.

#### 8. Some Distributed Systems that Obey Reciprocity

Up to this point the discussion has been in extremely general terms. In this section, however, certain physical systems will be examined to see if they satisfy the conditions necessary for reciprocity.

One of the simpler distributed systems is the fluid. It may be described in terms of the three coordinates of a packet of fluid,  $\delta_1$ ,  $\delta_2$  and  $\delta_3$  plus the time derivatives of these coordinates. A  $\vec{\delta}$  vector may be formed from the  $\delta$  matrix with the aid of a unit vector matrix  $\vec{a}$  so that

$$\vec{\delta} = \begin{bmatrix} \delta_1 \\ \delta_2 \\ \delta_3 \end{bmatrix} = \begin{bmatrix} \vec{a} & \delta \end{bmatrix} \quad (72)$$

A change in the volume of the fluid  $\Delta v$  is

$$\Delta v = v_0 \vec{\nabla} \cdot \vec{\delta} = v_0 \vec{\nabla} \cdot \underline{\hat{a}} \delta] = v_0 \underline{\hat{a}} \cdot \vec{\nabla} \delta] = v_0 \underline{\nabla} \delta] \quad (73)$$

if only linear terms are included and rectangular coordinates are used. The  $\underline{\nabla}$  matrix is a column matrix formed from the three scalar elements of the del operator. The zero subscripts indicate rest conditions. The potential energy density  $\underline{v}$  is equal to the work done per unit volume during a compression or expansion of the fluid

$$\underline{v} = - \frac{p \Delta v}{v_0} = -p \vec{\nabla} \cdot \vec{\delta} \quad (74)$$

and if the total pressure  $p$  is dependent on the change in volume only, it is possible to write

$$\underline{v} = -p_0 \vec{\nabla} \cdot \vec{\delta} - v_0 \left. \frac{\partial p}{\partial v} \right|_{v_0} (\vec{\nabla} \cdot \vec{\delta})^2 \quad (75)$$

where terms higher than quadratic have been discarded. The matrix  $\underline{\hat{V}}$

$$\underline{\hat{V}} = \underline{\hat{a}} ] \left( -v_0 \left. \frac{\partial p}{\partial v} \right|_{v_0} \right) \underline{\hat{a}} \quad (76)$$

can be identified and substituted into the expression for the potential energy density

$$\underline{v} = -p_0 \underline{\hat{a}} \cdot \vec{\nabla} \delta] + \vec{\nabla} \delta \cdot \underline{\hat{V}} \cdot \vec{\nabla} \delta] \quad (77)$$

which except for the linear term is the form assumed in the general discussion. If (77) is substituted into the general Lagrange equations, this linear term of  $\underline{V}$  will yield the gradient of  $p_0$ . Therefore, unless  $p_0$  is constant, the Lagrange equations become non-linear and non-reciprocal. If  $p_0$  is constant, however, no trouble is experienced. Note that for constant  $p_0$  this extra term will drop out in the total potential energy, since  $\nabla \cdot \vec{\delta}$  may be integrated directly and will vanish at the boundary surface if none of the fluid is allowed to cross.

The kinetic energy density for the fluid is, of course

$$\underline{T} = \frac{1}{2} \rho \vec{\delta} \cdot \vec{\delta} = \frac{1}{2} \underline{\dot{\delta}} \underline{T} \underline{\dot{\delta}} \quad (78)$$

where  $\rho$  is the density of the fluid. If  $\rho$  is not a function of the displacement of the packet  $\vec{\delta}$ , the matrix  $T$

$$T = \begin{bmatrix} \rho & 0 & 0 \\ 0 & \rho & 0 \\ 0 & 0 & \rho \end{bmatrix} \quad (79)$$

will be in the proper form for reciprocity.

Therefore, the limitations on a fluid or acoustic system in order that it obey reciprocity are simply those of linearity. Variations in the ambient pressure  $p_0$  as a result of winds or vortex motion may cause reciprocity to fail.

The kinetic energy density of an elastic medium is the same as that for a fluid (78), but the potential energy density is

$$\underline{V} = \frac{1}{8} (\nabla \delta] + \nabla] \delta) \cdot [\vec{C}] \cdot (\nabla S] + \nabla] \delta) = \vec{G} \cdot [\vec{C}] \cdot \vec{G} \quad (80)$$

where  $[\vec{C}]$  is a matrix containing the 81 Hooke's law constants for an anisotropic elastic medium. Actually, since  $[\vec{C}]$  and the strain matrix  $\vec{G}$  are symmetric, there are only 21 independent components of  $[\vec{C}]$ .

The matrix  $\vec{V}$  is

$$\vec{V} = \vec{N}_t \cdot [\vec{C}] \cdot \vec{N} \quad (81)$$

where the dyadic matrix  $\vec{N}$  is

$$\vec{N} = \frac{1}{2} \begin{bmatrix} 2 \vec{a}_1 \vec{a}_1 + \vec{a}_2 \vec{a}_2 + \vec{a}_3 \vec{a}_3 & \vec{a}_1 \vec{a}_2 & \vec{a}_1 \vec{a}_3 \\ \vec{a}_2 \vec{a}_1 & \vec{a}_1 \vec{a}_1 + 2 \vec{a}_2 \vec{a}_2 + \vec{a}_3 \vec{a}_3 & \vec{a}_2 \vec{a}_3 \\ \vec{a}_3 \vec{a}_1 & \vec{a}_3 \vec{a}_2 & \vec{a}_1 \vec{a}_1 + \vec{a}_2 \vec{a}_2 + 2 \vec{a}_3 \vec{a}_3 \end{bmatrix} \quad (82)$$

It should not be surprising that an equation as complicated as (80) can be written in terms of the dyadic matrix  $\vec{V}$ , since this represents the most general quadratic form containing all the spatial derivatives of all the coordinates. Both  $\underline{T}$  and  $\underline{V}$  have been written in the standard form, and it can

therefore be concluded that the linear model of a anisotropic, heterogeneous, elastic medium is reciprocal.

It is not clear whether electrostatic or electromagnetic energy should be associated with kinetic or potential energy. However, the energy density must be

$$\underline{H} = \frac{1}{2} E [\epsilon] E + \frac{1}{2} H [\mu] H \quad (83)$$

where the matrix E contains the elements of electric field strength,  $[\epsilon]$  is the dielectric matrix, H is the magnetic field strength, and  $[\mu]$  is the permeability matrix. Suppose that the generalized coordinates are chosen so that

$$\underline{\vec{a}} \dot{\lambda} = \underline{\vec{a}_1 \vec{a}_2 \vec{a}_3} \begin{bmatrix} \dot{\lambda}_1 \\ \dot{\lambda}_2 \\ \dot{\lambda}_3 \end{bmatrix} = \vec{E} = \underline{\vec{a}} E \quad (84)$$

Utilizing one of Maxwell's equations

$$\underline{\vec{a}} \cdot \vec{\nabla} \times \vec{E} = -[\mu] \dot{H} = +\vec{\nabla} \cdot (\underline{\vec{a}} \times \underline{\vec{a}})_t E \quad (85)$$

it is possible to write the magnetic field strength in terms of the coordinates

$$H = -[\mu]^{-1} \vec{\nabla} \cdot [\vec{x}] \lambda = -[\mu]^{-1} [\vec{x}] \cdot \vec{\nabla} \lambda \quad (86)$$

where the vector matrix

$$[\vec{x}] = \begin{bmatrix} 0 & -a_3 & a_2 \\ a_3 & 0 & -a_1 \\ -a_2 & a_1 & 0 \end{bmatrix} = (\vec{a}) \times \underline{a}_t \quad (87)$$

has been substituted for the cross product terms. The energy in terms of these coordinates is

$$\underline{H} = \frac{1}{2} \dot{\lambda} [\epsilon] \dot{\lambda} + \frac{1}{2} \underline{\nabla} \lambda \cdot [\vec{x}]_t [\mu]^{-1} [\vec{x}] \cdot \underline{\nabla} \lambda \quad (88)$$

Identifying  $\hat{V}$  and  $\tau$  with

$$\hat{V} = [\vec{x}]_t [\mu]^{-1} [\vec{x}] \quad (89)$$

$$\tau = [\epsilon] \quad (90)$$

makes it clear that a anisotropic, heterogeneous, electromagnetic medium will satisfy reciprocity if it is linear.

The dual variables  $\dot{q}] = H$  give for the intensity vector

$$\vec{d} = -\dot{q} \underline{M} \dot{\lambda} = -\dot{q} [\vec{x}] \dot{\lambda} = \dot{\lambda} [\vec{x}] \dot{q} = \vec{E} \times \vec{H} \quad (91)$$

and the energy density

$$\underline{H} = \frac{1}{2} \dot{q} [\mu] \dot{q} + \frac{1}{2} \underline{\nabla} q \cdot [\vec{x}]_t [\epsilon]^{-1} [\vec{x}] \underline{\nabla} q \quad (92)$$

as one should expect. The dual matrices  $T_d$  and  $\hat{V}_d$  are therefore



$$\tau_d = [\mu] \quad (93)$$

$$V_d = [\vec{X}]_t [\epsilon]^{-1} [\vec{X}] \quad (94)$$

The  $\widehat{R}$  matrix describing the losses due to expansive friction  $\gamma$  in a fluid may be obtained easily by analogy to the  $\widehat{V}$  matrix for a fluid. The losses resulting from the shearing of the fluid  $\eta$  may be included by analogy to the  $\widehat{V}$  matrix for an elastic medium. Thus,

$$\widehat{R} = \gamma \vec{\alpha} ] \underline{\vec{\alpha}} - \eta \vec{N}_t \cdot \vec{N} \quad (95)$$

which is symmetrical, since  $\gamma$  and  $\eta$  are scalars denoting the second and first viscosity coefficients. Therefore, the addition of viscous forces to fluid medium does not destroy reciprocity. Although the reciprocity of the lossless systems considered above is well known, the author believes that viscous forces have never before been considered explicitly.

For resistive losses in a conductive medium, the current density vector is analogous to the dissipative force density. In this case the  $R_{oo}$  matrix is simply

$$R_{oo} = [\sigma] \quad (95)$$

where  $[\sigma]$  is the conductivity matrix which must be symmetric for reciprocity. In the dual representation the dissipative force density is

$$f] = \nabla \cdot [\hat{x}] [\epsilon]^{-1} [\sigma] E \quad (96)$$

If  $[\epsilon]^{-1}[\sigma]$  does not vary markedly with space, it is possible to write for the dual matrix  $R_{oo d}$

$$R_{oo d} = [\epsilon]^{-1} [\sigma] [\mu] \quad (97)$$

which in general will not be symmetrical.

The material of this section up to this point has shown that electromagnetic, fluid, and elastic systems are reciprocal. It has really been an exercise in fitting some well-known equations into the formalism that was used in the general proof of reciprocity. There is no doubt that the straightforward method of proving reciprocity for these systems taken one at a time would have been simpler. When all three types of systems are combined, however, the simplification and insight provided by the general method becomes apparent.

As the first example of a mixed system, let us examine a general mechanical system that is undergoing steady rotation motion. The kinetic energy density becomes

$$\underline{T} = \frac{\rho}{2} \left( \vec{r} \cdot \vec{r} + \{ (\vec{r}_0 + \vec{r}) \times (\vec{\omega}_0 + \vec{\omega}) \}^2 \right) \quad (98)$$

where  $\vec{r}_0$  is the radius vector from the center of rotation,  $\vec{r}$  is the incremental radial displacement vector of a packet of material originally located at  $\vec{r}_0$ ,  $\vec{\omega}_0$  is the steady angular rotation vector and  $\vec{\omega}$  is the incremental angular rotation vector. The quadratic terms of the kinetic energy density are given by

$$\underline{T} = \frac{\rho}{2} \left( \vec{r} \cdot \vec{r} + 4(\vec{r} \times \vec{\omega}_0) \cdot (\vec{r}_0 \times \vec{\omega}) + (\vec{r}_0 \times \vec{\omega})^2 + (\vec{r} \times \vec{\omega}_0)^2 \right) + \underline{T}' \quad (99)$$

where  $\underline{T}'$  contains the remaining terms. The presence of the cross term between the radial displacement and the angular velocity indicates that the system will not obey reciprocity.

The potential energy of the system will be unchanged whether expressed in a stationary or a rotating coordinate system. This follows from the fact that the stress dyadic depends on differences in displacement rather than on the displacements themselves.

Let us investigate the possibility of using a dual coordinate system for the rotational coordinates. By analogy to the lumped system discussed in Section 2.27, substitute the angular momentum density into (99). The last three terms of (99) will then be included in an apparent potential energy of the system if the angular momentum density is assumed to

be a generalized coordinate. Unfortunately the potential energy itself will now have cross terms between the radial displacement and the time derivatives of the angular momentum density.

In general it is not possible, therefore, to make such a rotating system reciprocal. For the special case of an incompressible medium, the potential energy is of no consequence. It is possible, then, to make the change to the dual coordinates to obtain reciprocity.

Since (99) is actually the Lagrangian of a system with no potential energy, one wonders why it cannot be substituted directly into the Lagrange equations. As shown in Section 2.27, the quadratic expression will yield the correct equations of motion, but the computation of the energy from these equations will not contain the cross term between radial displacement and angular velocity. This is another indication of the fact that the energy of a linear but non-reciprocal system is not uniquely related to the Lagrangian.

Turning to a general electroacoustic system, the total energy density will be made up of the mechanical kinetic energy density  $\underline{T}_m$

$$\underline{T}_m = \frac{1}{2} \underline{\dot{s}} \cdot \underline{\dot{s}} \quad (100)$$

the mechanical potential energy density  $\underline{V}_m$

$$\underline{V}_m = \frac{1}{2} \vec{G} \cdot \vec{S} \quad (101)$$

and the electromagnetic energy density  $\underline{\mathcal{H}}_e$

$$\underline{\mathcal{H}}_e = \frac{1}{2} \mathbf{E} \mathbf{D} + \frac{1}{2} \mathbf{H} \mathbf{B} \quad (102)$$

where  $\dot{\mathbf{s}}]$ ,  $\vec{\mathbf{S}}$ ,  $\vec{\mathbf{G}}$ ,  $\mathbf{E}$ ,  $\mathbf{D}$ ,  $\mathbf{H}$ , and  $\mathbf{B}$  are matrices containing the components of velocity, stress, strain, electric field intensity, electric displacement, magnetic field strength, and magnetic induction.

Piezoelectric and magnetostrictive coupling effects are taken into account by the constitutive relations

$$\mathbf{D} = [\epsilon] \mathbf{E} + [\vec{\alpha}] \cdot \vec{\mathbf{G}} \quad (103)$$

$$\mathbf{B} = [\mu] \mathbf{H} + [\vec{\beta}] \cdot \vec{\mathbf{G}} \quad (104)$$

$$\vec{\mathbf{S}} = [\vec{\mathbf{C}}] \cdot \vec{\mathbf{G}} - [\vec{\alpha}]_t \mathbf{E} - [\vec{\beta}]_t \mathbf{H} \quad (105)$$

where  $\epsilon$ ,  $\mu$ ,  $\mathbf{C}$ ,  $\alpha$  and  $\beta$  are the dielectric, permeability, Hooke's law, piezoelectric coupling and magnetostrictive coupling matrices. The total energy of the electromechanical system may be computed by adding the components (100) through (102). The variables  $\mathbf{D}$ ,  $\mathbf{B}$ , and  $\vec{\mathbf{S}}$  may be eliminated with the aid of the relations (103) through (105).

$$\underline{\mathcal{H}} = \frac{1}{2} \underline{\dot{\mathbf{s}}} \rho \dot{\mathbf{s}}] + \frac{1}{2} \vec{\mathbf{G}} \cdot [\vec{\mathbf{C}}] \cdot \vec{\mathbf{G}} + \frac{1}{2} \mathbf{E} [\epsilon] \mathbf{E} + \frac{1}{2} \mathbf{H} [\mu] \mathbf{H} \quad (106)$$

The coupling terms apparently drop out of the expression. However, both sets of electromagnetic coordinates  $q$  and  $\lambda$  must be used to express the energy in this form. In order to eliminate one or the other of these variables it is necessary to use one of Maxwell's relations

$$-\vec{\nabla} \cdot [\vec{x}] E = \dot{B} + \vec{\nabla} \cdot [\vec{x}] \vec{a} \cdot (\underline{B}_0 [\vec{x}] \dot{\delta}) \quad (107)$$

$$\vec{\nabla} \cdot [\vec{x}] H = \dot{D} + \rho_e \dot{\delta} \quad (108)$$

where the effects of the moving medium have been included and all non-linear terms excluded. It has been assumed that a strong steady magnetic induction with components  $B_0$  may be present. Similarly, a large steady charge  $\rho_e$  may also be present. Since losses cannot be included in the formulation of the equations of motion by Hamilton's principle except by inclusion as external forces, it must be assumed that these dissipative mechanisms are temporarily outside of the system. Therefore, all conductors have infinite conductivity and all dielectrics have zero conductivity.

Expressing the two Maxwell's relations given above in terms of the coordinates  $q$  and  $\lambda$ , it is possible to write

$$-\vec{\nabla} \cdot [\vec{x}] \lambda = B + \vec{\nabla} \cdot [\vec{\beta}_m] \delta = [\mu] H + [\vec{\beta}] \cdot \vec{G} + \vec{\nabla} \cdot [\vec{\beta}_m] \delta \quad (109)$$

$$\vec{\nabla} \cdot [\vec{x}]_q = D + \rho_e \delta = [\epsilon] E + [\vec{\alpha}] \cdot \vec{G} + \rho_e \delta \quad (110)$$

where the abbreviation

$$[\vec{\beta}_m] = [\vec{x}] \vec{\alpha} \cdot \underline{B}_e [\vec{x}] \quad (111)$$

has been used. If using (109),  $H$  is eliminated from the expression for the total energy, the result may be expressed in terms of the  $\delta$ ,  $\dot{\delta}$ ,  $\vec{\nabla}\delta$ ,  $\vec{\nabla}\lambda$ , and  $\dot{\lambda}$ . The coupling described by  $[\vec{\alpha}]$  and  $\rho_e$  will not appear in the energy, and therefore, the equations of motion derived from this expression by means of Hamilton's principle will not show any evidence of electrostatic coupling. This is the kind of situation that arose in the derivation of the equations of motion for a rotating system.

The electrostatic coupling will be included in the total energy if  $E$  is eliminated with the aid of (111). In this case, however, the magnetic coupling described by the matrices  $[\vec{\beta}]$  and  $[\vec{\beta}_m]$  will disappear. One must conclude that both electrostatic and magnetic coupling cannot be present simultaneously if reciprocity is to apply. Furthermore, a linear system with both kinds of coupling cannot be described by a Lagrangian, since the linear Lagrange equations are always reciprocal.

Utilizing the coordinates  $\lambda$  and allowing no electrostatic coupling, the application of Hamilton's principle will give the equations of motion

$$\begin{aligned} e\ddot{\delta}] - \vec{\nabla} \cdot (\vec{N}_t \cdot [\vec{c}] \cdot \vec{G} - \vec{N}_t \cdot [\vec{h}]_t H + [\vec{h}_m]_t H) \\ = -\vec{\nabla} \cdot (\gamma \vec{a}] \underline{\vec{a}} - \eta \vec{N}_t \cdot \vec{N}) \cdot \vec{\nabla} \delta \end{aligned} \quad (112)$$

$$[\epsilon] \ddot{\lambda}] - \vec{\nabla} \cdot [\vec{x}] [\mu]^{-1} (\vec{\nabla} \cdot [\vec{x}] \lambda] + [\vec{h}] \cdot \vec{G} + \vec{\nabla} \cdot [\vec{h}_m] \delta]) = -[\sigma] \dot{\lambda}] \quad (113)$$

If electromagnetic but no electrostatic coupling is present, the  $q$  coordinates must be used and the equations of motion are

$$\begin{aligned} e\ddot{\delta}] - \vec{\nabla} \cdot (\vec{N}_t \cdot [\vec{c}] \cdot \vec{G} - \vec{N}_t \cdot [\vec{a}] E) - \rho_e E \\ = -\vec{\nabla} \cdot (\gamma \vec{a}] \underline{\vec{a}} - \eta \vec{N}_t \cdot \vec{N}) \cdot \dot{\delta}] \end{aligned} \quad (114)$$

$$\begin{aligned} [\mu] \ddot{q}] - \vec{\nabla} \cdot [\vec{x}] [\epsilon]^{-1} (\vec{\nabla} \cdot [\vec{x}] q] - [\vec{a}] \cdot \vec{G} - \rho_e \delta]) \\ = -[\epsilon]^{-1} [\sigma] [\mu] \dot{q}] \end{aligned} \quad (115)$$

These two sets of equations describe reciprocal systems of great generality. The first pair describe coupling resulting from piezoelectric effects and the presence of a steady charge. The second pair describe coupling resulting from magnetostrictive effects and the presence of a steady field. Both sets include losses resulting from expansive friction, shearing



viscosity and electrical conductive losses. If the equations are written in terms of the complex magnitudes of the variables, it is possible to include many other kinds of loss by assuming that the parameters on the lefthand side of these equations may be complex.

#### 9. Some Examples of the Impedance of a Distributed System

The driving point impedance at a point source is particularly simple to evaluate. The radius of the sphere is chosen small enough so that it can oscillate in only one mode\* i.e., constant amplitude over the surface. The A matrix (64) giving the dependence on the space coordinates of the generalized velocities, degenerates to the single element

$$A_{kk} = \frac{a}{r} \quad (116)$$

where  $r$  is the radial coordinate and  $a$  the radius of the sphere. The point source driving point impedance of the  $k^{\text{th}}$  coordinate becomes

$$Z_{kk} = + \frac{|V_{kk}|}{j\omega} 4\pi a \quad (117)$$

where  $|V_{kk}|$  is the contracted form of the dyadic.

Let us evaluate this result for a pressure point source in acoustic medium. Defining the dual matrix  $M$  in terms of the incremental pressure  $p$

$$\vec{Q} = -\underline{\dot{S}} \vec{M} p = \underline{\dot{S}} \vec{a}] p = \dot{\delta} p \quad (118)$$

makes it possible to write for the dual matrix  $\vec{V}_d$

$$\vec{V}_d = \vec{M}_t T^{-1} \vec{M} = \frac{[\vec{a}, \vec{a}]}{p} \quad (119)$$

thus the driving point impedance of an acoustic point source is

$$Z = \frac{u^o}{p^o} = \frac{4\pi a}{j\omega p} \quad (120)$$

where  $u^o$  is the complex volume velocity and  $p^o$  the complex pressure.

The definitions of the two principle kinds of impedance for acoustic systems may be written in terms of the complex intensity vector  $\vec{Q}_{av}$  when either one or the other of the dual pair of coordinates  $p^o$  and  $V^o$ , the normal velocity, is constant over the area  $A$ . The mechanical impedance  $Z_M$  is obtained if the normal velocity is constant

$$v^{o*} Z_M v^o = + \int_A \vec{Q}_{av} \cdot d\vec{a} = v^{o*} \int_A p^o da \quad (121)$$

where the righthand integral is the total force reacting on  $Q$ . The dual acoustical impedance  $Z_A$  is obtained if the pressure is constant

$$p^\circ Z_A^* p^{\circ*} = + \int_a \vec{J}_{av} \cdot d\vec{a} = p \int_a \vec{v}^{\circ*} \cdot d\vec{a} \quad (122)$$

where the righthand integral is the total volume velocity passing through  $Q$ . The equivalent relationship for the definition of the electrical impedance is slightly more complicated and has been treated in detail by Foldy and Primakoff<sup>1</sup>. The result of course must be

$$I Z_e I = - \int \vec{J} \cdot d\vec{a} = I V \quad (123)$$

if no extra power is radiated at the electrical terminals. Here  $V$  is the voltage drop between the terminals.

---

<sup>1</sup>Primakoff, H. and Foldy, L. L., op. cit., Part II, Jour. Acous. Soc. Am., v. 19, p. 50.

## APPENDIX II

### 1. Expansion of the $\Psi_n$ in Terms of Derivatives of the Directivity Pattern $\Psi_0$

First let us expand  $\Psi_n$  in a series of Legendre polynomials  $P_m(x)$

$$\Psi_n = \sum_{m=0}^{\infty} \Psi_{nm} P_m(x) \quad (1)$$

where  $x = \cos \theta$  and the  $\Psi_{nm}$  are constants independent of  $r$  and  $\theta$ . Application of the operator  $L_x( )$  gives the series

$$L_x(\Psi_n) = \frac{\partial}{\partial x} \left[ (1-x^2) \frac{\partial \Psi_n}{\partial x} \right] = - \sum_{m=0}^{\infty} m(m+1) \Psi_{nm} P_m(x) \quad (2)$$

Equation (2) may be substituted into the recurrence relation (3.6) yielding

$$\sum_{m=0}^{\infty} \left[ 2(n+1) \Psi_{n+1,m} + \{n(n+1) - m(m+1)\} \Psi_{nm} \right] P_m(x) = 0 \quad (3)$$

and since the summation must vanish for all  $x$ , one has the  $m$  equations

$$2(n+1) \Psi_{n+1,m} + (n-m)(n+m+1) \Psi_{nm} = 0 \quad (4)$$

It can easily be demonstrated that

$$\psi_{nm} = \frac{(m+n)!}{(m-n)!} \frac{\psi_{om}}{2^n n!} = P_m^{(n)}(1) \psi_{om} \quad (5)$$

will satisfy all the equations (4). Here the notation  $P_m^{(n)}(1)$  indicates that  $P_m(x)$  has been differentiated  $n$  times with respect to  $x$  and has been evaluated at  $x = 1$ .

Let us attempt to express the  $\psi_n$  in terms of derivatives of the directivity pattern. At  $x = 1$  the directivity pattern is

$$\psi_0(1) = \sum_{m=0}^{\infty} \psi_{om} P_m(1) = \sum_{m=0}^{\infty} \psi_{om} \quad (6)$$

and the  $n^{\text{th}}$  derivative of  $\psi_0$  evaluated at  $x = 1$  is

$$\psi_0^{(n)}(1) = \sum_{m=0}^{\infty} \psi_{om} P_m^{(n)}(1) \quad (7)$$

but by (5) this is just equal to a summation of  $\psi_{nm}$  over  $m$ . Thus

$$\psi_n(1) = \sum_{m=0}^{\infty} \psi_{nm} = \psi_0^{(n)}(1) \quad (8)$$

Similar manipulations at  $x = -1$  will show that

$$\psi_n(-1) = (-1)^n \psi_0^{(n)}(-1) \quad (9)$$

To evaluate  $\Psi_n$  for arbitrary  $x$  is more difficult. Let us first expand  $\Psi_0(x)$  in terms of its derivatives evaluated at  $x = 0$

$$\Psi_0(x) = \sum_{\nu=0}^{\infty} \Psi_0^{(\nu)}(0) \frac{x^\nu}{\nu!} \quad (10)$$

where  $\Psi_0^{(\nu)}(0)$  is the  $\nu^{\text{th}}$  derivative of the directivity pattern evaluated at  $x = 0$ . The powers of  $x$  may be expanded in a series of Legendre polynomials.<sup>1</sup>

$$\begin{aligned} \frac{x^\nu}{\nu!} &= \sum_{m=0}^{m=\nu} (2m+1) \frac{\sqrt{\pi} z^{-(\nu+1)} P_m(x) \cos^2 \pi \left(\frac{\nu+m}{2}\right)}{\left(\frac{\nu+m}{2} + \frac{1}{2}\right)! \left(\frac{\nu-m}{2}\right)!} \\ &= \sum_{m=0}^{m=\nu} (2m+1) P_m^{-\nu-1}(0) P_m(x) \cos^2 \pi \left(\frac{\nu+m}{2}\right) \end{aligned} \quad (11)$$

If (11) is substituted into (10) in place of the powers of  $x$  and the result substituted into the recurrence relation (3.6), it is possible to write

$$\Psi_n(x) = \sum_{\nu=0}^{\infty} B_{n\nu}(x) \Psi_0^{(\nu)}(0) \quad (12)$$

where

---

<sup>1</sup>Byerly, W.E., Fourier's Series and Spherical Harmonics, Ginn and Co., Boston, p. 178, 1893.

$$B_{nv}(x) = \sum_{m=0}^{m=v} (2m+1) P^{-v-1}(0) P_m^{(n)}(1) \cos^2 \pi \left( \frac{v+m}{2} \right) P_m(x) \quad (13)$$

The lowest non-zero values of  $B_{nv}$  may be found without much difficulty:

$$B_{nn}(x) = P_n(x) \quad (14)$$

$$B_{n,n+1}(x) = P_{n+1}(x) \quad (15)$$

$$B_{n,n+2}(x) = \frac{P_n(x) + (2n+2)P_{n+2}(x)}{2(2n+3)} \quad (16)$$

For other terms the recurrence relation

$$2(n+1)B_{n+1,v} + B_{n,v-2} = [v(v+1) - n(n+1)]B_{nv} \quad (17)$$

may be used. This relation may be proved by direct substitution of the  $B_{nv}(x)$  from (13). The first few  $B_{nv}$  have been computed and are shown in Table 1.

TABLE 1.  
 (APPENDIX II)  
 Values of  $B_{nv}(x)$  - See (13)

$n \backslash v$	0	1	2	3	4
0	$P_0$	$P_1(x)$	$\frac{P_0}{6} + \frac{P_2(x)}{3}$	$\frac{P_0(x)}{10} + \frac{P_3(x)}{15}$	$\frac{P_0}{120} + \frac{P_2(x)}{42} + \frac{P_4(x)}{105}$
1	0	$P_1(x)$	$P_2(x)$	$\frac{P_1(x)}{10} + \frac{2P_3(x)}{5}$	$\frac{P_2(x)}{14} + \frac{2P_4(x)}{21}$
2	0	0	$P_2(x)$	$P_3(x)$	$\frac{P_2(x)}{14} + \frac{3P_4(x)}{7}$
3	0	0	0	$P_3(x)$	$P_4(x)$
4	0	0	0	0	$P_4(x)$



After a little experimentation it is possible to guess a general form for the  $B_{n\nu}$  evaluated at  $x = 0$

$$B_{n\nu}(0) = \frac{(-1)^{\nu/2} n! \cos^2 \frac{\pi}{2} \nu}{2^n \frac{\nu}{2}! (n - \frac{\nu}{2})! (\nu - n)!} \quad (18)$$

Substitution of (18) into the recurrence relation (17) will prove that this is the correct choice. Note that at  $x = 0$  the  $B_{n\nu}$  exist for even values of the integer  $\nu$  only.

## 2. The Near Field of a Piston in an Infinite Baffle

The piston in an infinite baffle is equivalent to a thin pill box pulsating outward on both sides and therefore may be treated by the theory developed in Chapter III and the previous section of this appendix. The results check a simpler formulation for  $x = 1$  and yield a new result for  $x = 0$ .

The directivity pattern of a piston in an infinite baffle is

$$\psi_0 = \frac{2J_1(z_1 \sin \theta)}{z_1 \sin \theta} = \sum_{\nu=0}^{\infty} \left(\frac{J_2 z_1}{2}\right)^{2\nu} \frac{(\sin \theta)^{2\nu}}{\nu! (\nu+1)!} \quad (19)$$

where  $z_1 = kr_1$  and  $r_1$  is the radius of the piston. The  $\sin \theta$  terms may be expanded about  $x = 1$

$$(\sin \theta)^{2\nu} = (1-x^2)^\nu = \sum_{\mu=0}^{\mu=\nu} 2^{\nu-\mu} \binom{\nu}{\mu} (-1)^\mu (1-x)^{\mu+\nu} \quad (20)$$

where  $\binom{\nu}{\mu}$  indicates the binomial coefficients. Collecting terms for  $n = \mu + \nu$ , it is possible to write for the  $n^{\text{th}}$  derivative of the directivity pattern

$$\Psi_n(l) = \Psi_0^{(n)}(l) = \frac{n!}{2^n} \sum_{\nu=0}^{\nu=n} \binom{\nu}{n-\nu} \frac{\bar{z}_1^{2\nu}}{\nu!(\nu+1)!} \quad (21)$$

which will be the coefficient of the  $(j\bar{z})^{-n}$  term of the expansion of  $\Psi$  on the axis in front of a piston in an infinite baffle. An expression for  $\Psi$  in closed form can be obtained by direct integration of the source distribution.<sup>1</sup>

$$\Psi = 2j \frac{\bar{z}}{\bar{z}_1^2} \left[ \exp j(\bar{z} - \sqrt{\bar{z}^2 + \bar{z}_1^2}) - 1 \right] \quad (22)$$

Term by term expansion of this function shows that at least the first half dozen terms are identical with (21).

It is possible to evaluate the pressure in the near field of a piston source in the equatorial plane ( $x = 0$ ). The  $\nu^{\text{th}}$  derivative of the directivity pattern evaluated in this plane can be shown to be

---

<sup>1</sup>Stewart, G.W., and Lindsay, R.B., Acoustics, Van Nostrand, New York, p. 251, 1930.

$$\psi_0^{(\nu)}(0) = \frac{\nu!}{2^{\nu/2} \frac{\nu!}{2}} 2 \bar{z}_1^{\frac{\nu}{2}-1} J_{\frac{\nu}{2}+1}(\bar{z}_1) \quad (23)$$

for even  $\nu$  and is zero for odd  $\nu$ . Equations (18) and (23) can be substituted into (12) to yield a series expression for the coefficient of the  $(j \bar{z})^{-n}$  term in the expansion of  $\psi$  for this source.

### 3. Calculation of the Acoustic Center for a Spherical Source

The pressure in front of a general axially symmetrical spherical source of radius  $r_1$  is

$$p(r, \theta) = \rho c \sum_{m=0}^{\infty} \frac{V_m P_m(x)}{j h'_m(\bar{z}_1)} h_m(\bar{z}) \quad (24)$$

where  $V_m$  is the velocity amplitude of the  $m^{\text{th}}$  mode of vibration of the surface of the sphere, and as usual  $\bar{z} = kr$  and  $\bar{z}_1 = kr_1$ . The prime on the spherical Hankel function  $h_m$  indicates differentiation with respect to the argument. At low frequencies only the zero order term remains

$$\begin{aligned} p(r, \theta) &= \rho c \frac{V_0 h_0(\bar{z})}{j h'_0(\bar{z}_1)} = j \rho c \bar{z}_1^2 \frac{V_0 e^{-j(\bar{z}-\bar{z}_1)}}{\bar{z}} \\ &= J(r) [4 \pi r_1^2 V_0 e^{j\bar{z}_1}] \end{aligned} \quad (25)$$

where the term in the brackets must be the volume velocity emitted by the sphere.

At large distances

$$p(r, \theta) = \rho c \frac{e^{-j\bar{z}}}{\bar{z}} \sum_{m=0}^{\infty} \frac{V_m P_m(x)}{h'_m(\bar{z})} e^{jm\frac{\pi}{2}} \quad (26)$$

gives the expression for the far field pressure. Here the spherical Hankel functions of the second kind are used so that (26) will represent an outgoing wave for a positive  $j\omega t$  time dependence. If (26) is normalized by the pressure on the polar axis, one obtains the directivity pattern

$$\psi_0 = \frac{p(r, \theta)}{p(r, 0)} = \frac{\sum_{m=0}^{\infty} V_m P_m(x) e^{jm\frac{\pi}{2}} (h'_m)^{-1}}{\sum_{m=0}^{\infty} V_m e^{jm\frac{\pi}{2}} (h'_m)^{-1}} \quad (27)$$

The acoustic center  $\underline{a}$  as defined in (3.13) is given by

$$\bar{z}_a = ka = \frac{1}{2} \int_m \left[ \frac{\sum_{m=0}^{\infty} V_m m(m+1) e^{jm\frac{\pi}{2}} (h'_m)^{-1}}{\sum_{m=0}^{\infty} V_m e^{jm\frac{\pi}{2}} (h'_m)^{-1}} \right] \quad (28)$$

The mode velocities  $V_m$  for a point source are

$$V_m = (2m+1)V_0 \quad (29)$$

and for a piston that subtends the angle  $2\theta_0$  at the origin the  $V_m$  are

$$V_m = [P_{m-1}(x_0) - P_{m+1}(x_0)] \frac{V_0}{1-x_0} \quad (30)$$

where  $x_0 = \cos \theta_0$ .

Substituting the  $V_m$  for a piston into the expression for the acoustic center and evaluating the result at low frequencies, one finds that the important term is

$$\bar{z}_a = \frac{V_i}{V_0} \int_m \left[ j \frac{h'_0}{h_i} \right] = \frac{1}{2} \frac{P_0 - P_2}{1-x_0} \bar{z}_1 = \frac{3}{4} (1+x_0) \bar{z}_1 \quad (31)$$

This low frequency result and the general expression obtained by inserting either (29) or (30) into (28) were used in the numerical calculations leading to Fig. 3.3. The tables prepared by Morse, Feshbach and Lax<sup>1</sup> were found to be very useful.

---

<sup>1</sup>Morse, P.M., Feshbach, H. and Lax, M., "Scattering and Radiation from Circular Cylinders and Spheres", OSRD Report No. 62.1R, 1945.

#### 4. Radiation from a Point on a Sphere at High Frequencies

The expression for the acoustic center becomes rather hard to evaluate directly at high frequencies. The spherical Hankel functions have almost constant magnitude up to the term in which the order equals the argument. Thus if  $kr_1 = 20$ , one expects about twenty terms of equal magnitude before the series will show any signs of converging. Above the 20<sup>th</sup> term the magnitude of the  $h'_m$  increases very rapidly and the series practically breaks off. The phases of the terms below  $m = 20$  rotate rapidly, resulting in small differences of large numbers.

An integral approximation to the summation seemed to be the obvious method of circumventing the difficulties outlined above. The starting point for such an integral over  $m$  must be  $m = -\frac{1}{2}$  since the  $\frac{e^{jm\frac{\pi}{2}}}{h'_m}$  are even functions of  $m + \frac{1}{2}$

$$\frac{e^{jm\frac{\pi}{2}}}{h'_m} = \frac{e^{-j(m+1)\frac{\pi}{2}}}{h'_{-(m+1)}} \quad (32)$$

Let us assume that the coefficient of the  $h'_m$  term can be written as a series with terms of the form  $(m + \frac{1}{2})^n$ . Consider the general sum

$$\sum_n = \sum_{m=0}^{\infty} (m + \frac{1}{2})^n \frac{e^{jm\frac{\pi}{2}}}{h'_m} \rightarrow \int_0^{\infty} v^n \frac{e^{j\frac{\pi}{2}(v-\frac{1}{2})}}{h'_{v-\frac{1}{2}}} dv \quad (33)$$

where the continuous variable  $\nu = m + \frac{1}{2}$  is substituted under the integral.

Watson<sup>1</sup> gives an asymptotic form for the Bessel functions that is valid over the path of integration. Changing his notation slightly and avoiding explicit reference to higher order terms in  $\frac{1}{\gamma}$  one may write

$$h_{\nu-\frac{1}{2}} e^{-j\frac{\pi}{2}(\nu-\frac{1}{2})} = j \frac{e^{-j\gamma(\cosh\gamma - \gamma\sinh\gamma)}}{\gamma\sqrt{\cosh\gamma}} \left(1 + O\left(\frac{1}{\gamma}\right)\right) \quad (34)$$

where  $\frac{\nu}{\gamma} = j\sinh\gamma$  in contrast to Watson's notation.

This expression may be differentiated with respect to the argument of the spherical Hankel function

$$h'_{\nu-\frac{1}{2}} e^{-j\frac{\pi}{2}(\nu-\frac{1}{2})} = \frac{1}{\gamma} \sqrt{\cosh\gamma} e^{-j\gamma(\cosh\gamma - \gamma\sinh\gamma)} \left(1 + O\left(\frac{1}{\gamma}\right)\right) \quad (35)$$

where higher order terms have again been included in  $O\left(\frac{1}{\gamma}\right)$ .

The expression (35) is of the form usually used in saddle-point integration. The exponent will contribute a rapidly rotating phase at high frequencies along the present

-----  
<sup>1</sup>Watson, G.N., Theory of Bessel Functions, reprinted by McMillan, New York, pp. 260-267, 1948.

path of integration. However, deforming the contour so that it leaves the saddle point at  $\nu = 0$  on the path of steepest descent will cause the main contribution to the integral to occur at the origin. The path chosen will leave the origin at  $45^\circ$  and then proceed to infinity in the first quadrant. Consulting Watson's figure<sup>1</sup> giving the regions of validity of the expression (34) tells us that this path is satisfactory.

By the usual methods of saddle-point integration, it is possible to obtain

$$\sum_n = \left(\frac{n-1}{2}\right)! (2jz_0)^{\frac{n+1}{2}} \frac{z_0}{2j} e^{jz_0} \quad (36)$$

In order to compute the far-field pressure produced by a point source on a sphere at high frequencies, one should multiply (36) by  $2V_0 \rho c \frac{e^{-jz}}{z}$  and select  $n = 1$ . The pressure becomes

$$p(r, 0) = 2V_0 \rho c \frac{e^{-jz}}{z} \sum_n = 2V_0 \rho c \frac{e^{-j(z-z_0)}}{z} \cdot z_0^2 \quad (37)$$

$\begin{matrix} k \rightarrow \infty \\ r \rightarrow \infty \end{matrix}$

which appears to be right, since the pressure has been doubled and the phase changes by  $-\frac{\pi}{2}$  over the low frequency case (25).

Noting that only the highest power of  $m$  need be considered in evaluating any series at high frequencies, the

<sup>1</sup>Watson, G.N., op. cit., p. 265.



expression for the acoustic center may be approximated by

$$z_a = \frac{1}{2} \lim_{k \rightarrow \infty} \left[ \frac{\sum_3}{\sum_1} \right] = z_1 \quad (38)$$

The general term in the expansion of the pressure in inverse powers of  $r$  in front of this source may be evaluated at high frequencies by means of (36). The pressure turns out to be just twice that radiated by a simple source with the same volume velocity located at  $r = r_1$ . This should not be surprising, since this is what the geometrical optics approximation would predict.

#### 5. Pressure on the Axis from a Point Source on a Sphere

On the polar axis the pressure radiated by a point source on a sphere is

$$p(r, 0) = \rho c \sum_{m=0}^{\infty} \frac{(2m+1)V_0}{j h'_m(z_1)} h_m(z) \quad (39)$$

This expression was used to calculate the curves of Fig. 3.4. Most of the points for  $kr_1 = 1.0$  have been calculated by Stenzel<sup>1</sup>, and his data were used. At low frequencies it is possible to derive a simplified expression, since

$$\frac{h_m(z)}{h'_m(z_1)} = - \frac{z_1^{m+2}}{(m+1) z_1^{m+1}} \quad (40)$$

$k \rightarrow 0$

---

<sup>1</sup>Stenzel, H., "Guide for the Calculation of Sound Processes", Translated for Bureau of Ships, Navy Dept. Washington, D.C., p. 154, 1947.

the pressure becomes

$$p(r, 0) = j\rho c V_0 \frac{\bar{x}_1^2}{\bar{z}} \sum_{m=0}^{\infty} \left[ 2 \left( \frac{\bar{x}_1}{\bar{z}} \right)^m - \frac{1}{m+1} \left( \frac{\bar{x}_1}{\bar{z}} \right)^{m+1} \right] \quad (41)$$

$\kappa \rightarrow 0$

which may be put into closed form

$$p(r, 0) = j\rho c V_0 \frac{\bar{x}_1^2}{\bar{z}} \left[ \frac{2}{1 - \frac{r}{\bar{z}}} + \frac{r}{\bar{z}} \ln \left( 1 - \frac{r}{\bar{z}} \right) \right] \quad (42)$$

$\kappa \rightarrow 0$

This last expression makes the calculation of the pressure for the curve of Fig. 4.5 quite simple and accurate.

## BIOGRAPHICAL SKETCH

Jerome R. Cox, Jr. was born in Washington, D.C., on May 24, 1925. Six years later his parents left the East and settled in South Bend, Indiana, where he attended James Madison Grammar School and James Whitcomb Riley High School. He returned to the East to attend MIT, but in a few months was called into the service.

After serving in the infantry for a year in the United States and Italy, he was discharged and re-entered MIT. During June of 1947 he was awarded a Bachelor of Science degree in Electrical Engineering and in September, 1949, a Master of Science degree in Electrical Engineering. He was president of his social fraternity, Lambda Chi Alpha, an editor of the MIT humor magazine, Voo Doo, and a member of Tau Beta Pi, Eta Kappa Nu, and Sigma Xi. He continued his graduate study in the MIT Acoustics Laboratory and in September, 1951, was married to Miss Barbara Jane Lueders of Englewood, New Jersey. To her must go a large share of the credit for his continued study toward a distant goal. In June, 1952, he accepted a position at the Liberty Mutual Insurance Company. This work has been concerned with industrial noise control and the study of industrial deafness. On January 22, 1953, he became the father of an exceptional baby girl, Nancy Jane.

## BIBLIOGRAPHY

Periodicals

1. Aldridge, A.J., "Calibration of Wente Condenser Transmitter", Jour. Post Office Elec. Eng., v. 21, p. 223, 1928.
2. "Application de la Methode Electrostatique d'Etalonnage Absolu a Certains Types de Microphones," Note - 152, Centre de Recherches Scientifiques Industrielles and Maritimes, Marseille, 1947.
3. Arnold, H.D. and Crandall, I.B., "The Thermophone as a Precision Source of Sound", Phys. Rev., v. 10, p. 22, 1917.
4. Ballantine, S., "Effect of Diffraction Around the Microphone in Sound Measurement", Phys. Rev., v. 32, p. 988, 1928.
5. Ballantine, S., "Reciprocity in Electromagnetic, Mechanical, Acoustical, and Interconnected Systems", Proc. Inst. Radio Eng., v. 17, p. 929, 1929.
6. Ballantine, S., "Effect of Cavity Resonance on the Frequency Response Characteristics of the Condenser Microphone", Proc. Inst. Radio Eng., v. 18, p. 1206, 1930.
7. Ballantine, S., "Technique of Microphone Calibration", Jour. Acous. Soc. Am., v. 3, p. 319, 1932.
8. Barnes, E.J., "Discussion of a Paper by R.S. Cohen," Proc. Inst. Elec. Eng., v. 66, p. 195, 1928.
9. Bauer, B. "Transformer Analogs of Diaphragms," Jour. Acous. Soc. Am., v. 23, p. 680, 1951.
10. Carstensen, E.L., "Self-Reciprocity Calibration of Electroacoustic Transducers," Jour. Acous. Soc. Am., v. 19, p. 961, 1947.
11. Cook, R.K., "Absolute Pressure Calibration of Microphones", Jour. Acous. Soc. Am., v. 12, p. 415, 1941.

Periodicals, cont.

12. Cook, R.K., "Measurement of Electromotive Force of a Microphone", Jour. Acous. Soc. Am., v. 19, p. 503, 1947.
13. Cox, J.R., "Free Field Calibration with Closely Spaced Microphones", Jour. Acous. Soc. Am., v. 23, p. 622, 1951.
13. Cox, J.R., "Nonlinear Analysis of the Condenser Microphone," Quarterly Progress Report of the MIT Acous. Lab., p. 4, Oct.-Dec., 1951.
14. Crout, P.D., "An Extension of Lagrange's Equations to Electromagnetic Field Problems," Jour. of App. Phys. v. 19, p. 1007, 1948.
15. Foldy, L.L. and Primakoff, H., "General Theory of Passive Linear Electroacoustic Transducers and the Electroacoustic Reciprocity Theorem I and II", Jour. Acous. Soc. Am., v. 17, p. 109, 1945.
16. Foldy, L.L., "Theory of Passive Linear Electroacoustic Transducers with Fixed Velocity Distribution", Jour. Acous. Soc. Am., v. 21, p. 595, 1949.
17. Glover, J. and Baumzweiger, B., "A Moving Coil Pistonphone for Measurement of Sound Field Pressure", Jour. Acous. Soc. Am., v. 10, p. 200, 1939.
18. Hawley, M.S., "Substitution Method of Measuring the Open Circuit Voltage Generated by a Microphone," Jour. Acous. Soc. Am., v. 21, p. 183, 1949.
19. Hawley, M.S., "Reciprocity Pressure Response Formula which Includes the Effect of the Chamber Load on the Motion of the Transducer Diaphragms", Jour. Acous. Soc. Am., v. 22, p. 56, 1950.
20. Helmholtz, H. von, "Theorie der Luftschwingungen in Rohren mit offenen Enden," Crelles Journal, v. 57, p. 1, 1859.
21. Kennedy, W.J. and Bowar, C.P., "Absolute Pressure Generator and its Application to the Free-field Calibration of a Microphone", Jour. Acous. Soc. Am., v. 14, p. 19, 1942.

Periodicals, cont.

22. Lamb, H., "On Reciprocal Theorems in Dynamics", Proc. London Math. Soc., v. 19, 1888.
23. MacLean, W.R., "Absolute Measurement of Sound without a Primary Standard", Jour. Acous. Soc. Am., v. 12, p. 140, 1940.
24. Massa, F., "Working Standard for Sound Pressure Measurements", Jour. Acous. Soc. Am., v. 17, p. 29, 1945.
25. MacMillan, E.M., "Violation of the Reciprocity Theorem in Linear Passive Electromechanical Systems," Jour. Acous. Soc. Am., v. 18, p. 344, 1946.
26. MacMillan, E.M., "Further Remarks on Reciprocity", Jour. Acous. Soc. Am., v. 19, p. 922, 1947.
27. Oliver, D.A., "An Improved Condenser Microphone for Sound Pressure Measurements," Jour. Scientific Inst., v. 7, p. 113, 1930.
28. Rayleigh, Lord, "Some General Theorems Relating to Vibrations", Proc. London Math. Soc., v. 4, 1873.
29. Rayleigh, Lord, "On an Instrument Capable of Measuring the Intensity of Aerial Vibrations," Phil. Mag. v. 14, p. 186, 1882.
30. Rudnick, I. and Stein, M.N., "Reciprocity Free-field Calibration of Microphones to 100 kc in Air", Jour. Acous. Soc. Am., v. 20, p. 818, 1948.
31. Schottky, W., "Das Gesetz des Tiefempfangs in der Akustik und Elektroakustik", Zeits. f. Physik, v. 36, p. 689, 1926.
32. Simmonds, B.D. and Vrick, R.I., "The Plane Wave Reciprocity Parameter and its Application to the Calibration of Electroacoustic Transducers at Close Distances", Jour. Acous. Soc. Am., v. 21, p. 633, 1949.
33. Terry, R.L. and Matson, R.B., "Pulse Technique for the Reciprocity Calibration of Microphones", Jour. Acous. Soc. Am. v. 23, p. 684, 1951.
34. Thompson, S.P., "Theoretical Aspects of the Reciprocity Calibration of Electromechanical Transducers", Jour. Acous. Soc. Am., v. 21, p. 538, 1949.

Periodicals, cont.

35. Watters, B.G., "Sound Sources for Microphone Calibration," MIT Masters Thesis, 1953.
36. Wathen-Dunn, W., "On the Reciprocity Free-Field Calibration of Microphones," Jour. Acous. Soc. Am., v. 21,
37. Wente, E.C., "The Thermophone", Phys. Rev., v. 19, p. 333, 1922.
38. West, W., "Pressure on the Diaphragm of a Condenser Transmitter," Proc. Inst. Elec. Eng., v. 5, p. 145, 1930.
39. White, J.E., "Motional Impedance Analysis", Jour. Acous. Soc. Am., v. 18, p. 155, 1946.
40. Wiener, F.M., "Phase Distortion in Electroacoustic Systems", Jour. Acous. Soc. Am., v. 13, p. 115, 1941.
41. Wiener, F.M. and Mattia, A.L.D., "On the Absolute Pressure Calibration of Condenser Microphones by the Reciprocity Method", Jour. Acous. Soc. Am., v. 18, p. 341, 1946.

Books

1. Beranek, L.L. Acoustic Measurements, John Wiley, New York, 1949.
2. Bode, H.W., Network Analysis and Feedback Amplifier Design, D. Van Nostrand, Co., New York, p. 128, 1945.
3. Byerly, W.E., Fourier's Series and Spherical Harmonics, Ginn and Co., Boston, p. 178, 1893.
4. Guillemin, E.A., Communication Networks, Vol. II, John Wiley and Sons, Inc., New York, p. 137, 1935.
5. Morse, P.M., Vibration and Sound, McGraw-Hill, New York, p. 319, 1948.
6. Morse, P.M. and Feshbach, H., Methods of Theoretical Physics, McGraw-Hill Co., New York, p. 287, 1953.

Books, cont.

7. Morse, P.M., and Feshbach, H., and Lax, M., Scattering and Radiation from Circular Cylinders and Spheres, OSRD Report No. 62.1R, 1945.
8. Rayleigh, Lord, Theory of Sound, Vol. I, p. 154, Dover, New York, 1945.
9. Skilling, H.H., Fundamentals of Electric Waves, John Wiley, New York, 1948.
10. Slater, J.C. and Frank, N.H., Mechanics, McGraw-Hill Co., New York, p. 74, 1947.
11. Stenzel, H., Guide for the Calculation of Sound Processes, Translated for Bureau of Ships, Navy, Dept. Washington, D.C., p. 154, 1947.
12. Stewart, G.W., and Lindsay, R.B., Acoustics, Van Nostrand, New York, p. 251, 1930.
13. Watson, G.N., Theory of Bessel Functions, Reprinted by McMillan, New York, pp. 260-267, 1948.